8-2008

Zero DC offset active RC filter designs.

Kresimir Odorcic 1973-
University of Louisville

ZERO DC OFFSET ACTIVE RC FILTER DESIGNS

By

Kresimir Odorcic
B.S., California University of Pennsylvania, 1995
M.S., University of Louisville, 2002

A Dissertation
Submitted to the Faculty of the
Graduate School of the University of Louisville
in Partial Fulfillment of the Requirements
for the Degree of

Doctor of Philosophy

Department of Electrical and Computer Engineering
University of Louisville
Louisville, Kentucky

August 2008

ZERO DC OFFSET ACTIVE RC FILTER DESIGNS

By

Kresimir Odorcic
B.S., California University of Pennsylvania, 1995
M.S., University of Louisville, 2002

A Dissertation Approved on

May 20, 2008

by the following Dissertation Committee:

Dr. Peter Aronhime Dissertation Director

Dr. Jacek Zurada

Dr. Joseph Cole

Dr. Peter Quesada

Dr. Wei-Bin Zeng

ACKNOWLEDGEMENTS

I would like to thank my Dissertation Director and Academic Advisor Dr. Peter B. Aronhime for his assistance and guidance throughout my academic studies at the University of Louisville. I would also like to thank other committee members; Dr. Joseph Cole, Dr. Jacek Zurada, Dr. Wei-Bin Zeng, and Dr. Peter Quesada. Your comments and advice were truly invaluable, and your encouragement and support are much appreciated.

ABSTRACT

ZERO DC OFFSET ACTIVE RC FILTER DESIGNS

Kresimir Odorcic

May 20, 2008

A class of RC active filters is presented in which the DC offset of the operational amplifier (op-amp) is completely absent from the filter output [1]. Individual filter configurations (Low Pass, High Pass, Band Pass, Band Stop, All Pass) are discussed and corresponding transfer functions are defined. The effects of op-amp gain bandwidth product on filter responses are accounted for and presented in a table.

In order to understand the upper limit of dynamic responses, the maximum signal magnitude and corresponding frequency of maximum magnitude are calculated. The effects of noise generating components are defined and included, thus establishing the lower limit of dynamic responses for all filter configurations.

Step-by-step design procedures are given for most common filter configurations. Sample filters are designed based on chosen values for critical frequency ω_0 and filter quality factor Q. Filter schematics are captured and their frequency responses are simulated using circuit simulation software. Sample filters are built and their frequency responses are confirmed using a network analyzer. Extension to higher order filters is discussed and demonstrated.

TABLE OF CONTENTS

LIST OF TABLES

LIST OF FIGURES

CHAPTER I

INTRODUCTION

Active resistor capacitor (RC) filters have become a mainstay of analog filter design since the 1970s. They offer many advantages, especially at lower frequencies: design flexibility, requiring less weight, and occupying less space as compared to passive filter designs. Active RC filters can be miniaturized into very small packages using integrated circuit techniques, resulting in inexpensive mass production processes [2], [3].

The majority of modern active RC filters designs are based upon the KHN (Kerwin, Huelsmann, Newcomb), the Tow-Thomas, or the Akerberg-Mossberg second order filters, called "sections" when used to create higher order filters [4]-[7]. Higher order filters are implemented by cascading multiple sections. Desired filter functions are obtained by taking a signal from the output of a respective op-amp stage. The fact that a desired filter function is obtained directly at the output of an op-amp does present one drawback. Op-amp direct current (DC) offsets create a resulting DC output signal that is added to the desired signal. This DC output signal component can have adverse effects in some applications, such as in instrumentation. Filters used in high-precision instrumentation often require the use of circuits having low DC offset to provide an accurate output signal for interpretation [8], [9].

A circuit configuration has been proposed [1] which can be used to realize second order active RC filters, which offer three advantages:

(1) The active filters do not have any DC offset present in the filtered output signal.

(2) The active filters have zero clock feedthrough, since no clock is used.

(3) The active filters do not have any switching transients, since no switches are employed.

The primary advantage is the absence of DC parasitic signals at the outputs of these filters, even for higher order designs.

The circuit configuration is developed into specific filter functions. Resulting filter functions are mathematically characterized and discussed. Transfer functions and normalized transfer functions are presented, including the gain-bandwidth effects. Dynamic range analysis and noise analysis are performed as well, defining the upper and lower limits of applied input signal.

Specific design procedures for all filter configurations are outlined to aid in component selection during the filter design and the development process. A sample design procedure is carried out for all filter configurations following specific design procedures previously outlined. Designed filters are captured and their frequency response is simulated using Circuit Maker 2000 schematic capture and simulation software. Representative filter configurations are built on the bread board, and their frequency response is confirmed using a network analyzer.

A universal filter concept is developed by adding the switching and control circuits to the filter configuration. The universal filter is a software reconfigurable second order filter circuit, capable of performing the low pass (LP), band pass (BP), high pass (HP), and band stop (BS) filtering functions. Sample LP, BP, HP and BS filters are obtained based upon the universal filter design, and their frequency response is validated using Circuit Maker 2000 schematic capture and simulation software.

Extension to higher order filters is discussed, while maintaining the advantage of the absence of DC parasitic signals. The BP1 and HP2 filter configurations are extended into higher order filters, and their response is simulated via the simulation software.

The primary contributions of this work are:

(1) Clarifying the research in this area.

(2) Correcting the pre-existing errors.

(3) Extending the second order filter design into higher order filters.

(4) Developing design procedures for second and higher order filters (simulations of filter designs are provided and laboratory results are given).

(5) Proposing a universal programmable filter concept circuit.

CHAPTER II

SECOND ORDER FILTER TRANSFER FUNCTIONS

Providing a filter with no DC offset due to the op-amp presence requires that no DC transmission paths exist from the op-amp offset sources to the filter output port. Yet there must be a path for DC current to flow from the output of the op-amp to its inverting input so that negative feedback at DC can be established around the op-amp. In addition, DC current must be allowed to flow into or out of the non-inverting input [10]-[12]. The method used to ensure these conditions are achieved is based on taking the output of the filter at a port that is different from the output of the op-amp, and isolating the filter output from the op-amp output by capacitors which block DC parasitic signals.

Figure 1 depicts the configuration used to establish a general form for filter sections whose output signal is not taken directly from the output of the op-amp [1]. The block denoted as N_1 is a passive RC network. The block denoted as n_2 can be a passive or even an active RC network. Voltage sources V_A, V_B and V_C represent input signal sources applied individually or in combination, depending upon the desired filter configuration. Output V_{o1} represents the op-amp output, while V_O represents the filter output.

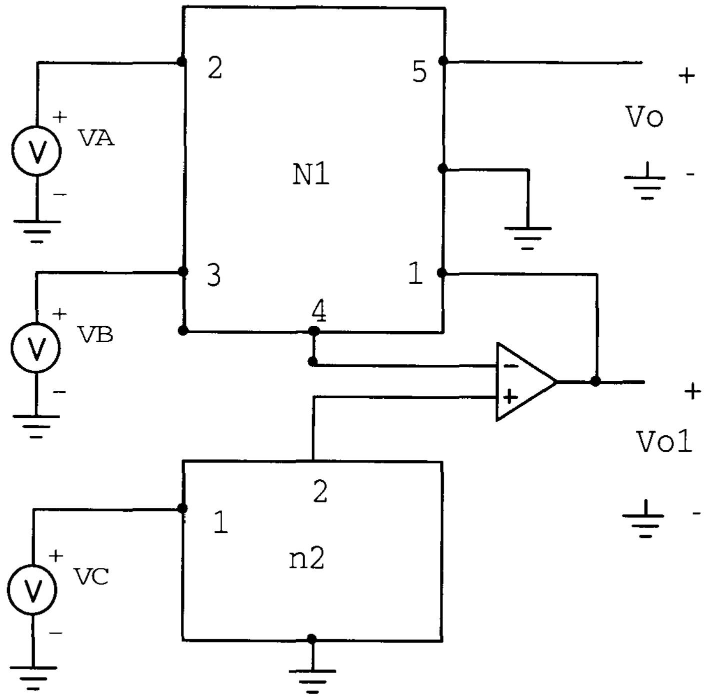

Figure 1. General configuration using passive RC networks N_1 and n_2

A. Input to Op-Amp Output

A non-ideal op-amp model with a finite open loop gain A(s) is applied for the development of the following transfer functions. The op-amp output voltage transfer functions with respect to input signal sources V_A, V_B and V_C are given by:

$$G_{A1} = \frac{V_{o1}}{V_A} = \frac{t_{42}(s)}{\frac{1}{A(s)} - t_{41}(s)} \tag{1}$$

$$G_{B1} = \frac{V_{o1}}{V_B} = \frac{t_{43}(s)}{\frac{1}{A(s)} - t_{41}(s)} \tag{2}$$

$$G_{C1} = \frac{V_{o1}}{V_C} = \frac{T_2(s)}{t_{41} - \frac{1}{A(s)}} \tag{3}$$

where $T_2(s)$ is the open-circuit voltage transfer function of network n_2, and t_{4i} are the open circuit voltage transfer functions of network N_1 from port i (i=1,2,3) to port 4 with other terminals of network N_1(except terminal 5) connected to the reference node [13]-[15].

B. Input to Filter Output

The same conditions previously specified for the op-amp output voltage transfer functions are applied for the filter output transfer functions. The filter output transfer functions with respect to each of the input signal sources V_A, V_B, and V_C are given by:

$$G_A(s) = \frac{V_o}{V_A} = \frac{t_{42}(s)t_{51}(s) - t_{41}(s)t_{52}(s) + \frac{t_{52}(s)}{A(s)}}{\frac{1}{A(s)} - t_{41}(s)} \tag{4}$$

$$G_B(s)=\frac{V_o}{V_B}=\frac{t_{43}(s)t_{51}(s)-t_{41}(s)t_{53}(s)+\dfrac{t_{53}(s)}{A(s)}}{\dfrac{1}{A(s)}-t_{41}(s)} \tag{5}$$

$$G_C(s)=\frac{V_o}{V_C}=\frac{T_2(s)t_{51}(s)}{t_{41}(s)-\dfrac{1}{A(s)}} \tag{6}$$

where t_{5i} are the open circuit voltage transfer functions of network N_1 from port i (i=1,2,3) to port 5, with other terminals of network N_1 connected to the reference node [13]-[15].

If |A(s)| approaches infinity in the op-amp model, then the filter voltage transfer functions become:

$$G_A(s)=\frac{t_{41}(s)t_{52}(s)-t_{42}(s)t_{51}(s)}{t_{41}(s)} \tag{7}$$

$$G_B(s)=\frac{t_{41}(s)t_{53}(s)-t_{43}(s)t_{51}(s)}{t_{41}(s)} \tag{8}$$

$$G_C(s)=\frac{T_2(s)t_{51}(s)}{t_{41}(s)} \tag{9}$$

The open circuit voltage transfer functions of network N_1 can be expressed as the ratios of two polynomials:

$$t_{ij}(s)=\frac{N_{ij}(s)}{D_C(s)} \tag{10}$$

where $D_C(s)$ is the characteristic polynomial of RC network N_1 and has roots only on the negative real axis. Applying equation (10), equations (4), (5), and (6) can be re-written as:

$$G_A(s) = \frac{\dfrac{N_{42}(s)N_{51}(s) - N_{41}(s)N_{52}(s)}{D_C(s)} + \dfrac{N_{52}(s)}{A(s)}}{\dfrac{D_C(s)}{A(s)} - N_{41}(s)} \tag{11}$$

$$G_B(s) = \frac{\dfrac{N_{43}(s)N_{51}(s) - N_{41}(s)N_{53}(s)}{D_C(s)} + \dfrac{N_{53}(s)}{A(s)}}{\dfrac{D_C(s)}{A(s)} - N_{41}(s)} \tag{12}$$

$$G_C(s) = \frac{T_2(s)N_{51}(s)}{N_{41}(s) - \dfrac{D_C(s)}{A(s)}} \tag{13}$$

respectively. For the ideal op-amp model case with infinitely large open loop gain ($|A(s)| = \infty$), expressions (7), (8), and (9) become:

$$G_A(s) = \frac{N_{41}(s)N_{52}(s) - N_{42}(s)N_{51}(s)}{D_C(s)N_{41}(s)} \tag{14}$$

$$G_B(s) = \frac{N_{41}(s)N_{53}(s) - N_{43}(s)N_{51}(s)}{D_C(s)N_{41}(s)} \tag{15}$$

$$G_C(s) = \frac{T_2(s)N_{51}(s)}{N_{41}(s)} \tag{16}$$

For the finite open loop gain op-amp model, analysis of the expressions for the numerators of $G_A(s)$ and $G_B(s)$ reveals some unique properties. The difference of the numerator products of N_1 are divided by the common characteristic polynomial of N_1. It can be demonstrated that these numerator products (in $G_A(s)$ and $G_B(s)$) have the characteristic polynomial $D_C(s)$ as a factor. Thus, when the op-amp is assumed to be ideal with infinitely large open loop gain, the characteristic polynomial of $G_A(s)$ and $G_B(s)$ becomes $D_C(s)N_{41}$. The characteristic polynomial of $G_C(s)$ reduces to N_{41}.

CHAPTER III

SECOND ORDER FILTER REALIZATION

The following expressions are widely used throughout this text. They are applicable to all transfer functions and all filter configurations. The purpose of these expressions is to reduce the size of transfer function equations, thus enabling a more concise presentation and easier tabulation of the results. Note that variables β, k_0, R_K, τ_A, τ_K, D(s) are introduced, while variables R_1, R_2, R_A, R_B, C_1, C_2 represent actual physical components used in filter designs.

$$\beta = \frac{R_2}{R_B} \tag{17}$$

$$k_0 = 1 + \beta \tag{18}$$

$$R_K = k_0 R_1 + R_2 \tag{19}$$

$$\tau_A = (C_1 + C_2) R_A \tag{20}$$

$$\tau_K = C_1 R_K \tag{21}$$

$$D(s) = s^2 C_1 C_2 R_A R_K + s(C_1 + C_2) R_A + 1 \tag{22}$$

The following expressions are applicable to specific transfer functions and filter configurations. Again, the purpose of these expressions is to reduce the physical size of transfer function expressions thus enabling a more concise presentation and easier tabulation of the results. Note that k_1 represents the network n_1 transfer function for the BS1 and BS2 configurations only, while k_2 represents the network n_2 transfer function specifically for HP1 and BS1. In the AP1 configuration, the transfer functions for both networks n_1 and n_2 must be equal in magnitude and are defined as $k_{12} = k_1 = k_2$. Expression $C_{n2}R_{n2}$ is applicable to the BP2, HP2, BS2, and AP2 configurations only.

$$k_1 = \frac{\dfrac{R_A}{1-k_1}}{\dfrac{R_A}{k_1} + \dfrac{R_A}{1-k_1}} \qquad \text{(BS1 and BS2 only)} \qquad (23)$$

$$k_2 = \frac{\beta C_2}{(C_1 + k_0 C_2)} \qquad \text{(HP1 and BS1 only)} \qquad (24)$$

$$k_{12} = k_1 = k_2 = \frac{\beta C_2}{2C_1 + (2+\beta)C_2} \qquad \text{(AP1 only)} \qquad (25)$$

$$C_{n2}R_{n2} = \frac{C_1 C_2 R_K}{(C_1 + k_0 C_2)} \qquad \text{(BP2, HP2, BS2 and AP2 only)} \qquad (26)$$

$$\frac{R_2}{R_B} = 1 + \frac{C_1}{C_2} \qquad \text{(AP2 only)} \qquad (27)$$

Figure 2 shows the general circuit configuration applicable to the second order filters. Note that network N_1 is realized as an RC network consisting of C_1, C_2, R_1, R_2, R_B and a purely resistive network n_1. For this specific circuit configuration, the previously defined transfer functions from filter output V_O to respective input signals V_A, V_B, and V_C are as follows:

$$G_A(s) = \frac{1 - \dfrac{(sC_1R_K + k_0)}{A(s)}}{D_A(s)} \qquad (28)$$

$$G_B(s) = \frac{-R_A\beta(sC_2 + \dfrac{sC_1}{A(s)})}{D_A(s)} \qquad (29)$$

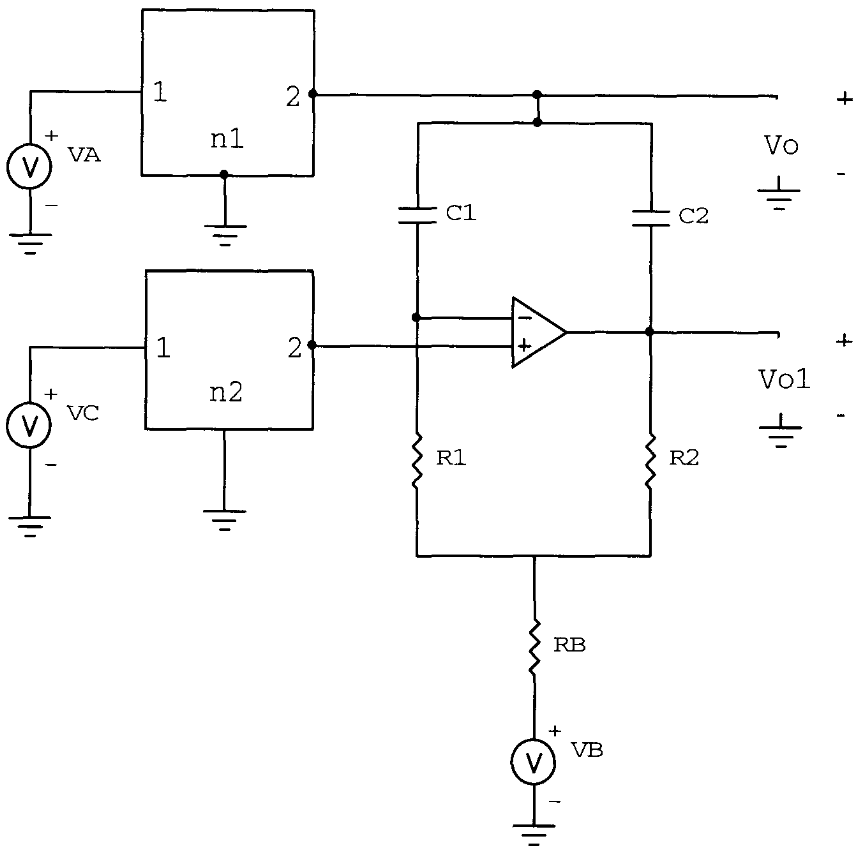

Figure 2. Circuit for second order sections

$$G_C(s) = \frac{T_2(s)R_A\left[s^2C_1C_2R_K + s(C_1 + k_0C_2)\right]}{D_A(s)} \tag{30}$$

Expression $D_A(s)$ represents the characteristic third order denominator polynomial for the above-mentioned transfer functions, assuming a non-ideal op-amp model with finite gain A(s). Applying the ideal op-amp model with infinite gain A(s) reduces the third order polynomial $D_A(s)$ to the second order polynomial D(s).

$$D_A(s) = D(s) - \frac{s^2C_1C_2R_AR_K + s\left[C_1R_K + (C_1 + C_2)k_0R_A\right] + k_0}{A(s)} \tag{31}$$

Assuming an ideal op-amp model with an infinite open loop gain A(s), transfer functions (28), (29), and (30) become:

$$G_A(s) = \frac{1}{D(s)} \tag{32}$$

$$G_B(s) = \frac{-sC_2R_A\beta}{D(s)} \tag{33}$$

$$G_C(s) = \frac{T_2(s)R_A\left[s^2C_1C_2R_K + s(C_1 + k_0C_2)\right]}{D(s)} \tag{34}$$

Note that the denominator polynomial has been reduced from $D_A(s)$ to D(s). Expressing the characteristic second order polynomial [16], [17] as:

$$\begin{aligned} D(s) &= HD_S(s) = H[s^2 + s(\frac{\omega_0}{Q}) + \omega_0^2] = s^2C_1C_2R_AR_K + s(C_1 + C_2)R_A + 1 \\ D(s) &= HD_S(s) = C_1C_2R_AR_K[s^2 + s\frac{(C_1 + C_2)R_A}{C_1C_2R_AR_K} + \frac{1}{C_1C_2R_AR_K}] \end{aligned} \tag{35}$$

then ω_0 and Q are given by:

$$\omega_0^2 = \frac{1}{C_1C_2R_AR_K} = \frac{1}{[(C_1+C_2)^2R_A^2Q^2]} \tag{36}$$

$$Q = \frac{\sqrt{\dfrac{C_1C_2R_K}{R_A}}}{(C_1+C_2)} \tag{37}$$

Tables 1 and 2 define the conditions required to implement each of the different filter types (LP, BP, HP, BS, AP). The characteristic polynomial D(s) for all filters listed in Table 2 is given by equations (22) and (35). The suffixes used for the BP, HP, BS, and AP filters differentiate between pole-zero relationships for filter configurations as defined by the structure of network n_2. If network n_2 is purely resistive (yielding a no-pole network), the corresponding filter configurations have 1 as a suffix. A suffix of 1 indicates that a zero of N_{51} is not cancelled by a pole of network n_2. If network n_2 is designed as an RC circuit (yielding a network with a pole at $-1/R_{n2}C_{n2}$), the corresponding filter configurations have 2 as a suffix. A suffix of 2 indicates that pole-zero cancellation between N_{51} and n_2 does occur.

An explanation of the organization of Tables 1 and 2 contributes to a better understanding of the transfer functions forms and the circuit configurations necessary to realize specific filter functions. In Table 1, columns 1 and 5, list different filter functions realizable with the circuit diagram in Figure 2. Table 1, columns 2 and 3, depict the required configurations for network n_1 and network n_2, respectively. Table 1, column 4, identifies the nodes where input signal V_i is applied to realize the desired filter response. It is important to note that unused input nodes ($V_{A,B,C} = 0$) must be properly terminated by connecting them to ground.

Table 1. Network and Signal Configurations for Second Order Filters

<table>
<tr><th>Filter</th><th>Network n_1</th><th>Network n_2</th><th>Input Signal</th><th>Filter</th></tr>
<tr><td>LP</td><td rowspan="3">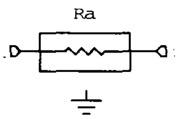</td><td rowspan="2">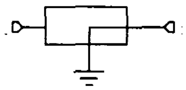</td><td>$V_A = V_i$
$V_B = 0$
$V_C = 0$</td><td>LP</td></tr>
<tr><td>BP1</td><td>$V_A = 0$
$V_B = V_i$
$V_C = 0$</td><td>BP1</td></tr>
<tr><td>HP1</td><td rowspan="3">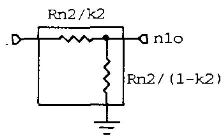</td><td>$V_A = 0$
$V_B = V_i$
$V_C = V_i$</td><td>HP1</td></tr>
<tr><td>BS1</td><td rowspan="2">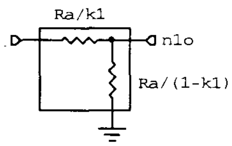</td><td>$V_A = V_i$
$V_B = V_i$
$V_C = V_i$</td><td>BS1</td></tr>
<tr><td>AP1</td><td>$V_A = V_i$
$V_B = V_i$
$V_C = V_i$</td><td>AP1</td></tr>
<tr><td>BP2</td><td rowspan="2">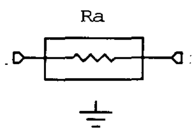</td><td>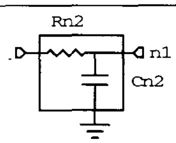</td><td>$V_A = 0$
$V_B = 0$
$V_C = V_i$</td><td>BP2</td></tr>
<tr><td>HP2</td><td rowspan="3">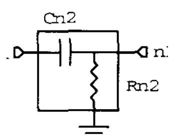</td><td>$V_A = 0$
$V_B = 0$
$V_C = V_i$</td><td>HP2</td></tr>
<tr><td>BS2</td><td>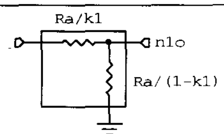</td><td>$V_A = V_i$
$V_B = 0$
$V_C = V_i$</td><td>BS2</td></tr>
<tr><td>AP2</td><td>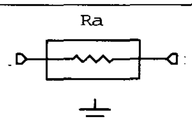</td><td>$V_A = V_i$
$V_B = V_i$
$V_C = V_i$</td><td>AP2</td></tr>
</table>

Table 2. Transfer Functions for Second Order Filters

Filter	Transfer Function $\frac{V_o}{V_i}$	Notes 1
LP	$\frac{1}{D(s)}$	No special requirements needed
BP1	$\frac{-sC_2R_A\beta}{D(s)}$	
HP1	$\frac{k_2(s^2C_1C_2R_AR_K)}{D(s)}$	$k_2 = \frac{\beta C_2}{(C_1 + k_0C_2)}$ $k_1 < 1$
BS1	$\frac{k_2(s^2C_1C_2R_AR_K) + k_1}{D(s)}$	
AP1	$\frac{k_{12}[s^2C_1C_2R_AR_K - s(C_1 + C_2)R_A + 1]}{D(s)}$	$k_1 = k_2 = k_{12} = \frac{\beta C_2}{2C_1 + (2+\beta)C_2}$
BP2	$\frac{s(C_1 + k_0C_2)R_A}{D(s)}$	$C_{n2}R_{n2} = \frac{C_1C_2R_K}{(C_1 + k_0C_2)}$
HP2	$\frac{s^2C_1C_2R_AR_K}{D(s)}$	$C_{n2}R_{n2} = \frac{C_1C_2R_K}{(C_1 + k_0C_2)}$ $k_1 < 1$
BS2	$\frac{s^2C_1C_2R_AR_K + k_1}{D(s)}$	
AP2	$\frac{s^2C_1C_2R_AR_K - s(C_1 + C_2)R_A + 1}{D(s)}$	$\frac{R_2}{R_B} = 1 + \frac{C_1}{C_2}$, $C_{n2}R_{n2} = \frac{C_1C_2R_K}{(C_1 + k_0C_2)}$
$\beta = \frac{R_2}{R_B}$	$k_0 = 1 + \beta$	$R_K = k_0R_1 + R_2$

Table 2, column 2, lists transfer functions for specific filter configurations. Table 2, column 3, defines equations and expressions applicable only to adjacent filter transfer functions. The bottom row in Table 2 denotes equations and expressions applicable to all filter configurations and corresponding transfer functions.

The transfer function associated with the LP configuration is recognized as being an all pole transfer function without finite zeros in the s-plane, i.e., both zeros are located at infinity. The resulting mathematical function exhibits low pass response in the frequency domain [18]-[21]. The gain in the pass band remains relatively constant for lower values of Q. Beyond undamped natural frequency ω_0 the gain decreases at the rate of 40 dB/decade or 12 dB/octave.

The BP1 and BP2 transfer functions are recognized as having one real zero located at the origin and the other zero located at infinity of the s-plane. In the frequency domain the resulting functions exhibit band pass response [18]-[21], with filter gain steadily increasing from DC to undamped natural frequency, and then steadily decreasing beyond the undamped natural frequency at the common rate of 20 dB/decade or 6 dB/octave. Undamped natural frequency ω_0 is also the "center" frequency of the pass band.

The transfer functions having two real zeros located at the origin of the s-plane are associated with the HP1 and HP2 filter configurations. These transfer functions exhibit high pass response in the frequency domain [18]-[21], with filter gain steadily increasing inside the stop band from DC to undamped natural frequency at the rate of 40 dB/decade or 12 dB/octave. Beyond undamped natural frequency the gain remains relatively constant inside the pass band for small values of Q.

The transfer functions associated with the BS1 and BS2 configurations are recognized as having two purely imaginary zeros located on the $j\omega$ axis of the s-plane. In the frequency domain these mathematical functions exhibit the band stop or "notch" response [18]-[21]. For the band stop response the filter gain remains relatively constant inside the pass band. The gain is steadily decreasing in the stop band as the "notch" frequency is approached from either zero frequency or high frequency.

The quality factor Q affects the frequency response of the LP, BP, HP and BS configurations in the vicinity of the undamped natural frequency. For the LP, BP, and HP filters the gain near the undamped natural frequency is dependent on quality factor Q. Larger Q values result in more pronounced "peaking", yielding higher gain and vice-versa. For the LP and HP filter configurations the Q values equal or smaller than 0.707 result in maximally flat pass band responses. The quality factor Q affects the sharpness of the BP and BS magnitude responses. Larger Q values result in steeper rates of gain change in the transition region, yielding narrower pass bands or stop bands for the BP and BS configurations respectively. Consequently, smaller Q values yield more gradual rates of gain change in the transition region, resulting in wider pass bands or stop bands for the BP and BS filters respectively.

The numerators of the AP1 and AP2 transfer functions are recognized as having the ability to produce two complex-conjugate zeros. In order to achieve the AP response, the complex-conjugate zeros on the right half side of the s-plane must be an exact reflection of the corresponding poles in the left half side of the s-plane with respect to the $j\omega$ axis. This achieves uniform gain magnitude across the frequency spectrum [18]-[21].

However, the phase response is frequency dependent, and it varies from 0 to -360 degrees.

Variable k_1 appears in the BS1 and BS2 transfer functions only. As mentioned earlier, k_1 represents the transfer function of network n_1. The value of k_1 is independent and is used to adjust the position of the zeros for the afore-mentioned configurations. For the BS1 and BS2 functions, network n_1 is implemented as a resistive voltage divider network; therefore, the magnitude of gain k_1 is always constant and less or equal to unity ($k_1 \leq 1$). In these instances, the Thevenin resistance of network n_1 must be equal to R_A. For other filter configurations where zero magnitude adjustment is not applicable, network n_1 reduces to resistor R_A. This yields the magnitude of gain k_1 equal to unity ($k_1 = 1$).

Variable k_2 appears in the HP1 and BS1 transfer functions only. As mentioned earlier, k_2 represents the transfer function of network n_2 when n_2 is implemented as a purely resistive voltage divider for the HP1 and BS1 filter functions, as shown in Table 1. In these instances, the magnitude of gain k_2 is always constant and less or equal to unity ($k_2 \leq 1$). In the AP1 configuration only, k_1 and k_2 are jointly referred to as k_{12} because the magnitude of k_1 must be equal to the magnitude of k_2 yielding $k_1 = k_2 = k_{12}$ as defined in Table 2.

As an example, it is desired to design a BS1 filter configuration with the magnitude of the zeros equal to the magnitude of the poles. Investigation of the BS1 voltage transfer function reveals that condition $k_1 = k_2$ must be satisfied in order to fulfill this design requirement. Therefore network n_1 is designed in such a way that one resistor connected between nodes 1 and 2 has the value R_A / k_1, and the other resistor connected between node 2 and ground has the value $R_A /(1 - k_1)$. If $k_1 = 1/2$ then both resistors have equal values. If $C_1 = C_2$ then the resistors needed to realize k_1 and k_2 transfer functions have equal values only if $R_2 = 2R_B$. For the AP1 filter in order to have equal valued resistors for the voltage dividers that realize transfer functions $k_1 = k_2 = 1/2$, it is required that $R_2 = 4R_B$.

The resistors realizing $k_1 = 1/2$ are equal in value, and the resistors realizing $k_2 = 1/2$ are equal in value; but the resistors realizing k_1 do not have to be equal in value to the resistors realizing k_2 in order to achieve $k_1 = k_2$.

CHAPTER IV

GAIN-BANDWIDTH EFFECTS

Table 2 lists V_O / V_i transfer functions for all filter configurations assuming an ideal op-amp model with infinite gain bandwidth product (GB). Practical op-amps have finite gain-bandwidth product, and so this limitation needs to be discussed and addressed [22]-[29].

Table 3 lists transfer functions V_O / V_i for all filter configurations assuming an op-amp model possessing finite gain-bandwidth product. The op-amp gain is denoted as A(s), and the op-amp is taken to be ideal for other considerations.

Normalized transfer functions for all filter configurations are given in Table 4. It is important to note that the open loop gain of the op-amp is defined as $A(s) = -1/s\tau$, where parameter τ is termed the op-amp "time constant" and $\tau = 1/GB$ [22]. Other expressions and assumption used for filter normalization are as follows:

$$s_n = \frac{s}{\omega_0} \tag{38}$$

$$\tau_n = \tau\omega_0 \tag{39}$$

$$C_1 = C_2 = C \tag{40}$$

$$\omega_0^2 = \frac{1}{C^2 R_A R_K} = \frac{1}{4Q^2 C^2 R_A^2} \tag{41}$$

Table 3. Voltage Transfer Functions Including the Effects of Finite GB

Filter Type	Normalized $\frac{V_o}{V_i}$ including Effects of Finite GB	Notes
LP	$\frac{1-\frac{(s\tau_K+k_0)}{A(s)}}{D_A(s)}$	$\beta=\frac{R_2}{R_B}$ $k_0=1+\beta$ $R_K=k_0R_1+R_2$ $\tau_K=C_1R_K$ $\tau_A=(C_1+C_2)R_A$ $k_2=\frac{\beta C_2}{(C_1+k_0C_2)}$ (HP1 and BS1 only) $k_1=k_2=k_{12}=\frac{\beta C_2}{2C_1+(2+\beta)C_2}$ (AP1 only) $k_1\le 1$ (BS1, BS2 only)
BP1	$\frac{-s\beta R_A(C_2+\frac{C_1}{A(s)})}{D_A(s)}$	
HP1	$\frac{s^2k_2C_1C_2R_AR_K-\frac{s\beta C_1R_A}{A(s)}}{D_A(s)}$	
BS1	$\frac{s^2k_2C_1C_2R_AR_K+k_1-\frac{[sC_1(k_1R_K+\beta R_A)+k_0k_1]}{A(s)}}{D_A(s)}$	
AP1	$\frac{k_{12}(s^2C_1C_2R_AR_K-s\tau_A+1)-\frac{[sC_1(k_{12}R_K+\beta R_A)+k_0k_{12}]}{A(s)}}{D_A(s)}$	
BP2	$\frac{sR_A(C_1+k_0C_2)}{D_A(s)}$	
HP2	$\frac{s^2C_1C_2R_AR_K}{D_A(s)}$	
BS2	$\frac{s^2C_1C_2R_AR_K+k_1-\frac{[k_1(s\tau_K+k_0)]}{A(s)}}{D_A(s)}$	
AP2	$\frac{s^2C_1C_2R_AR_K-s\tau_A+1-\frac{[sC_1(R_K+\beta R_A)+k_0]}{A(s)}}{D_A(s)}$	

Table 4. Normalized Voltage Transfer Functions Including the Effects of Finite GB

<table>
<tr><th>Filter Type</th><th>Normalized $\frac{V_o}{V_i}$ including Effects of Finite GB</th><th>Notes</th></tr>
<tr><td>LP</td><td>$\frac{1+s_n\tau_n[s_n(2Q)+k_0]}{D_A(s_n)}$</td><td rowspan="9">$D_A(s_n)=D(s_n)+s_n\tau_n D_1(s_n)$
$D(s_n)=s_n^2+\frac{s_n}{Q}+1$
$D_1(s_n)=s_n^2+s_n(2Q+\frac{k_0}{Q})+k_0$
$\beta=\frac{R_2}{R_B}$
$k_0=1+\beta$
$Q=\sqrt{\frac{R_K}{4R_A}}$
$R_K=k_0R_1+R_2$
$s_n=\frac{s}{\omega_0}$
$\tau_n=\tau\omega_0$
$k_2=\frac{\beta C_2}{(C_1+k_0C_2)}$
(HP1 and BS1 only)
$k_1=k_2=k_{12}=\frac{\beta C_2}{2C_1+(2+\beta)C_2}$
(AP1 only)
$k_1\le 1$ (BS1, BS2 only)</td></tr>
<tr><td>BP1</td><td>$\frac{\frac{s_n\beta}{2Q}(s_n\tau_n-1)}{D_A(s_n)}$</td></tr>
<tr><td>HP1</td><td>$\frac{s_n^2(k_2+\frac{\beta\tau_n}{2Q})}{D_A(s_n)}$</td></tr>
<tr><td>BS1</td><td>$\frac{s_n^2k_2+k_1+s_n\tau_n[s_n(2Qk_1+\frac{\beta}{2Q})+k_0k_1]}{D_A(s_n)}$</td></tr>
<tr><td>AP1</td><td>$\frac{k_{12}(s_n^2-\frac{s_n}{Q}+1)+s_n\tau_n[s_n(2Qk_{12}+\frac{\beta}{2Q})+k_0k_{12}]}{D_A(s_n)}$</td></tr>
<tr><td>BP2</td><td>$\frac{\frac{s_n}{2Q}(1+k_0)}{D_A(s_n)}$</td></tr>
<tr><td>HP2</td><td>$\frac{s_n^2}{D_A(s_n)}$</td></tr>
<tr><td>BS2</td><td>$\frac{s_n^2+k_1+s_n\tau_nk_1[s_n(2Q)+k_0]}{D_A(s_n)}$</td></tr>
<tr><td>AP2</td><td>$\frac{s_n^2-\frac{s_n}{Q}+1+s_n\tau_n[s_n(2Q+\frac{\beta}{2Q})+k_0]}{D_A(s_n)}$</td></tr>
</table>

$$Q = \sqrt{\frac{R_K}{4R_A}} \tag{42}$$

It can be seen from Table 4 that finite GB product has no effect on the BP2 and HP2 filter zeros; it only affects the gain constant of the HP1 filter. Setting capacitor values equal to each other $C_1 = C_2 = C$ places some limitations; at the same time it provides some simplifications in the component selection process.

Regarding AP1 filter design, setting $R_2 = 4R_B$ results in $k_1 = k_2 = k_{12} = 0.5$; this enables the use of equal valued resistors to realize the networks n_1 and n_2. For BS1 and AP2 filter designs, setting $R_2 = 2R_B$ also results in $k_1 = k_2 = 0.5$. This also enables the use of equal valued resistors to realize the networks n_1 and n_2 for BS1 filter design, and the network n_1 for AP2 filter design.

CHAPTER V

DYNAMIC RANGE

The dynamic range of Figure 2 filter configurations are carefully examined since the output of the filter configurations do not coincide with the output of the operational amplifiers used in the filter designs. Therefore, a new set of transfer functions is developed, which define the relationship between signal input and op-amp output. These transfer functions permit a user to determine the maximum signal level that can be maintained at the filter output V_O while avoiding clipping at the output of the op-amp V_{o1}. They are necessary for the calculation of dynamic range.

For each filter configuration three expressions are defined and presented: (1) voltage transfer function from signal input to op-amp output V_{o1} / V_i, (2) the frequency at which the magnitude of the voltage transfer function V_{o1} / V_i is maximum, and (3) the value of the maximum magnitude for the V_{o1} / V_i voltage transfer function.

Close approximations for the frequency of maximum magnitude and the value of maximum magnitude for V_{o1} / V_i are given as well. It is worth noting that the frequency of maximum magnitude for V_{o1} / V_i is either ω_0, or can be approximated as ω_0 for high values of quality factor Q [16].

Table 5 lists the V_{ol} / V_i voltage transfer functions for all the filter configurations defined in Table 2. Specific conditions and restrictions given in Table 2 are also applicable to the corresponding transfer functions in Table 5.

Table 6 lists the exact frequency of maximum magnitude and the exact value of maximum magnitude for V_{ol} / V_i transfer functions of LP, BP1, HP1, BS1, and AP1 filter configurations. For all entries in Table 6 it is assumed that $C = C_1 = C_2$.

Table 7 lists approximations for the frequency of maximum magnitude and the value of maximum magnitude for the filter configurations. The assumption $C = C_1 = C_2$ is applicable for all entries in Table 7. For the first half of Table 7 the expressions for the frequency of maximum magnitude and the value of maximum magnitude are obtained by applying the common approximation techniques on related expressions listed in Table 6.

For the second half of Table 7 additional restrictions are imposed on the BP2, HP2, BS2, and AP2 expressions for an approximate frequency of maximum magnitude and an approximate value of maximum magnitude. These restrictions are desired in order to simplify the filter design procedure and to reduce the algebraic complexity of presented expressions. Regarding the BP2, HP2, and BS2 filter expressions for an approximate frequency of maximum magnitude and an approximate value of maximum magnitude, it is assumed that $R_2 = R_B$. These assumptions yield the following parametric values for the respective filter configurations: $\beta = 1$, $k_0 = 2$, and $C_{n2}R_{n2} = CR_K / 3$. Regarding the AP2 filter expressions for an approximate frequency of maximum magnitude and an approximate value of maximum magnitude, it is assumed

Table 5. Op-Amp Output Voltage Transfer Functions of Second Order Filters

Filter Type	Op-Amp Output Voltage Transfer Function $\frac{V_{o1}}{Vi}$	Notes
LP	$\frac{-s\tau_K}{D(s)}$	$\beta = \frac{R_2}{R_B}$
BP1	$\frac{-\beta(s\tau_A + 1)}{D(s)}$	$k_0 = 1 + \beta$
HP1	$\frac{s^2 k_2 C_1 C_2 R_A R_K + s(k_2 \tau_K + K\tau_A) + K}{D(s)}$	$K = 1 + k_0(k_2 - 1)$
BS1	$\frac{s^2 k_2 C_1 C_2 R_A R_K + s[\tau_K(k_2 - k_1) + K\tau_A] + K}{D(s)}$	$\tau_A = (C_1 + C_2)R_A$ $\tau_K = C_1 R_K$
AP1	$\frac{s^2 k_{12} C_1 C_2 R_A R_K + sK\tau_A + K}{D(s)}$	$\omega_0^2 = \frac{1}{C_1 C_2 R_A R_K}$
BP2	$\frac{s^2 C_1 C_2 R_A R_K + s(\tau_K + k_0 \tau_A) + k_0}{(sC_{n2}R_{n2} + 1) \cdot D(s)}$	$Q = \frac{\sqrt{\frac{C_1 C_2 R_K}{R_A}}}{(C_1 + C_2)}$
HP2	$\frac{sC_{n2}R_{n2}[s^2 C_1 C_2 R_A R_K + s(\tau_K + k_0 \tau_A) + k_0]}{(sC_{n2}R_{n2} + 1) \cdot D(s)}$	$k_2 = \frac{\beta C_2}{(C_1 + k_0 C_2)}$
BS2	$\frac{sC_{n2}R_{n2}\{s^2 C_1 C_2 R_A R_K + s[\tau_K(1 - k_1) + k_0 \tau_A] + k_0\} - s\tau_K k_1}{(sC_{n2}R_{n2} + 1) \cdot D(s)}$	(HP1 and BS1 only) $k_{12} = \frac{\beta C_2}{2C_1 + (2 + \beta)C_2}$
AP2	$\frac{sC_{n2}R_{n2}[s^2 C_1 C_2 R_A R_K + s\tau_A + 1] - s(\beta\tau_A + \tau_K) - \beta}{(sC_{n2}R_{n2} + 1) \cdot D(s)}$	(AP1 only) $k_1 \le 1$ (BS1, BS2 only)

Table 6. Exact Frequency of Peaking and Maximum Magnitude of V_{o1} / V_1

Filter Type	Frequency of Maximum Magnitude	Maximum Magnitude
LP	ω_0	$2Q^2$
BP1	$\omega_0\sqrt{Q\sqrt{(Q^2+2)}-Q^2}$	$\dfrac{\beta}{\sqrt{2Q^3\sqrt{(Q^2+2)}-2Q^4-2Q^2+1}}$
HP1	ω_0	$k_2\sqrt{1+4Q^4}$
BS1	ω_0	$k_2\sqrt{4Q^2+[2Q^2(1-\frac{k_1}{k_2})-1]^2}$
AP1	$\omega_0\sqrt{\dfrac{Q\sqrt{(3+4Q^2)}-Q^2}{Q^2+1}}$	$k_{12}\sqrt{\dfrac{2Q^3\sqrt{(3+4Q^2)}+4Q^4+15Q^2+9}{2Q^3\sqrt{(3+4Q^2)}-4Q^4-Q^2+1}}$

Table 7. Approximations of Frequency of Peaking and Maximum Magnitude V_{o1} / V_i

Filter Type	Approx. Frequency of Maximum Magnitude		Approximate Maximum Magnitude
LP	ω_0		$2Q^2$
BP1	ω_0		β
HP1	ω_0		$2k_2Q^2$
BS1	ω_0	$k_1 = k_2$	$k_2 \frac{8Q^2+1}{4Q}$
		$k_1 \neq k_2$	$2\lvert k_2 - k_1\rvert Q^2 + \frac{k_1k_2}{\lvert k_2 - k_1\rvert}$
AP1	$\omega_0\sqrt{1-\frac{1}{4Q^2}}$		$k_{12}\frac{32Q^2+1}{8Q}$
BP2	$\omega_0\sqrt{1-\frac{1}{4Q^2}}$		$\frac{96Q^2+9}{32Q}$
HP2	$\omega_0\sqrt{1-\frac{1}{4Q^2}}$		$\frac{32Q^2-1}{16}$
BS2	$\omega_0\sqrt{1-\frac{1}{4Q^2}}$		$\frac{32Q^2-21}{16Q}$
AP2	$\omega_0\sqrt{1-\frac{1}{4Q^2}}$		$\frac{16Q^2-3}{4Q}$

that $R_2 = 2R_B$ since $R_2 / R_B = 1 + C_1 / C_2$. These assumptions yield the following parametric values for AP2 filter configuration: $\beta = 2$, $k_0 = 3$, $C_{n2}R_{n2} = CR_K / 4$.

A quick glance at the V_{o1} / V_i transfer functions for BP2, HP2, BS2, and AP2 filter configurations reveals a characteristic third order denominator polynomial [30], [31]. This phenomenon is caused by the absence of pole-zero cancellations at the op-amp output; in these instances the pole-zero cancellation occurs at the filter output [8]. For these filter configurations only an approximation for the frequency of maximum magnitude and the value of maximum magnitude for V_{o1} / V_i are given in Table 7. All third order transfer functions V_{o1} / V_i have identical expressions for an approximate frequency of maximum magnitude. These expressions are derived assuming the poles and zeros are not close to each other and that the Q value of dominant poles is high (Q>5), yielding imaginary component of the complex poles being much larger as compared to real component of the complex poles. A graphical procedure is described [16], where initially the vectors are drawn from all poles and zeros to the $j\omega$ axis. As the frequency is swept from the origin along the $j\omega$ axis, the vector drawn from the upper half-plane complex pole to the $j\omega$ axis frequency point varies rapidly in length and angle. At the same time, the remaining vectors drawn from the other poles to the $j\omega$ axis stay relatively unchanged. This yields to a conclusion that the upper half-plane complex pole is a dominant pole. Filter transfer functions are modified accordingly; a dominant pole factor is left unchanged and all non-dominant poles (and all zeros) are replaced by the constant term K=f($j\omega$). The remainder of the procedure used to calculate the frequency of maximum magnitude is exactly the same as it is used for other second order filter transfer functions V_{o1} / V_i. Modified transfer functions are first converted to $|G(j\omega)|^2$ form. Taking the 1st derivative with respect to ω, setting the numerator equal to zero, solving resulting equation, and applying common approximation techniques yields the expression for an approximate frequency of maximum magnitude for the BP2, HP2, BS2, and AP2 filters.

The application of the expressions listed in Tables 6 and 7 is best demonstrated by an example. An HP1 filter configuration is to be designed to meet the following requirements and assumptions: the desired value of Q is 10, the op-amp used can generate a 20Vp-p signal without distortion, $C_1 = C_2$, and $R_2 = R_B$. The maximum input signal that can be applied at the filter input, without causing distortion at the op-amp output is given in Tables 6 and 7:

$$V_{i(max)} = \frac{60}{\sqrt{40001}} V_{p-p} \approx 0.3 V_{p-p} \tag{43}$$

As another example, an HP2 filter configuration is to be designed as well, using the same requirements and assumptions used in the HP1 filter design and the transfer function listed in Table 7. The maximum input signal that can be applied at the input of HP2 filter, without causing distortion at the op-amp output is given by:

$$V_{i(max)} \approx \frac{320}{3159} V_{p-p} \approx 0.1 V_{p-p} \tag{44}$$

Initial comparison of the calculated results would yield a premature conclusion that HP1 filter has better dynamic range. The fact that the filter output does not coincide with the op-amp output makes dynamic range analysis more complex. In the example above, it is important to note that the magnitude of the output signal of HP1 filter configuration is 1/3 the magnitude of the output signal of the HP2 filter configuration.

These results are based upon design assumptions and the transfer functions given in Table 2.

CHAPTER VI

NOISE PERFORMANCE OF FILTERS

The smallest magnitude signal that can be successfully filtered with an acceptable signal to-noise ratio (SNR) defines the maximum resolution of the filter circuit. This smallest magnitude signal is quantified and characterized via noise analysis. Also, noise analysis defines the lower limit of dynamic range analysis [32], [33].

Electrical noise is a random phenomenon and its instantaneous value is unpredictable. Therefore noise can be characterized and quantified only on a statistical basis. In many instances electrical noise has a Gaussian or normal distribution, and so it is possible to predict an instantaneous amplitude value in terms of probabilities and statistics.

A. Noise Source Summation

Another unique approach in noise analysis refers to the summation properties of the noise sources. Frequently in noise analysis and calculations the voltage noise sources appear in series and the current noise sources appear in parallel. If two voltage noise sources E_{n1} and E_{n2} are connected in series and uncorrelated, their equivalent rms values add up in Pythagorean fashion by taking the square root of the sum of the squared magnitudes of the individual sources:

$$E_{nSum} = \sqrt{E_{n1}^2 + E_{n2}^2} \tag{45}$$

The same rule applies to two uncorrelated current noise sources I_{n1} and I_{n2} connected in parallel:

$$I_{nSum} = \sqrt{I_{n1}^2 + I_{n2}^2} \qquad (46)$$

Equations (45) and (46) clearly indicate that in an instance of two noise sources of uneven strength, the noise minimization efforts should be directed towards the stronger, more dominant noise source [11].

B. Noise Spectrum and Power Density

Due to the random nature of electrical noise, noise power is spread over all parts of the frequency spectrum. Thus when referring to the rms value of equivalent noise, the relevant frequency band must be specified over which the measurements and calculations are performed. The rate of change of noise power with respect to frequency is called the noise power density. The two most common forms of noise densities are white noise and 1/f noise. White noise has a uniform spectral density, resulting in equivalent power of the white noise being proportional to the bandwidth regardless of the band's location in the frequency spectrum. The 1/f noise power density varies inversely with frequency. The power of 1/f noise is proportional to the natural logarithm ratio of the frequency band limits regardless of the band's location within the frequency spectrum [32].

The initial step in noise analysis is identification of the specific noise generating components within a circuit undergoing the noise analysis. For Figure 2 circuit configurations, the noise generating components are resistors and operational amplifiers. Note that capacitors do not generate electrical noise [11], [34], [35]. Once identified, appropriate noise models need to be created for the noise generating components.

C. Resistor Noise Model

Thermal noise, also referred to as Johnson noise, is present in all passive resistive elements and is caused by the random motion of electrons due to ambient temperature. The resistor noise model is constructed by connecting a thermal noise voltage source in series with an otherwise noiseless resistor. This thermal noise voltage source can be further modeled for resistors using the spectral density function denoted by e_R, or the power density function denoted by e_R^2. The spectral density function and the power density function for any given resistance R are defined respectively as:

$$e_R = \sqrt{4kTR} \qquad (\frac{V}{\sqrt{Hz}}) \tag{47}$$

$$e_R^2 = 4kTR \qquad (\frac{V^2}{Hz}) \tag{48}$$

In (47) and (48), T represents the absolute temperature in degrees K and k is Boltzmann's constant [11], [32]. Equations (47) and (48) indicate that the resistor thermal noise is of the white type with uniform spectral and power density.

D. Network n_2 Noise Model

Figure 3(a) shows the network n_2 noise equivalent circuit for the HP1, BS1, and AP1 filters. Figure 3(b) shows the network n_2 noise equivalent circuit for the BP2, HP2, BS2, and AP2 filters.

The circuit configuration in Figure 3(a) can be simplified to a single noise source with the following power density:

$$e_{Rn2}^2 = 8kTR_{n2} \qquad (\frac{V^2}{Hz}) \tag{49}$$

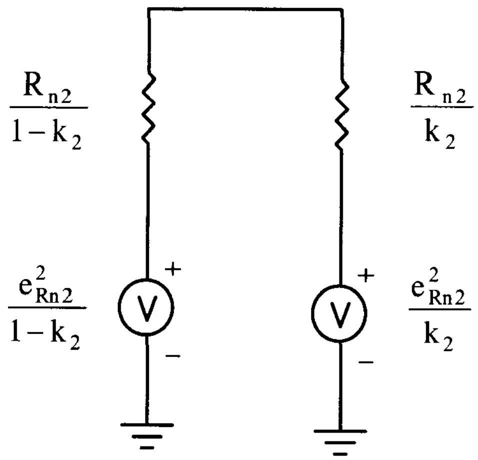

(a)

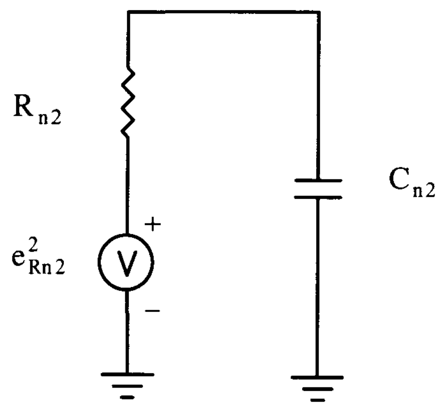

(b)

Figure 3. Thermal noise sources from resistors of network n_2

(a) Resistive voltage divider realizing k_2 ratio, used in HP1, BS1 and AP1.

(b) RC circuit used in BP2, HP2, BS2, and AP2.

Analysis of (49) reveals that the effective noise source of Figure 3(a) has twice as large a magnitude compared to resistor R_{n2}. The equivalent Thevenin resistance for the purely resistive network n_2 is the parallel combination of the two resistors comprising network n_2, which yields:

$$Z_{n2(RR)} = R_{n2} \tag{50}$$

The output noise power density for the circuit configuration in Figure 3(b) is defined as:

$$e_{Rn2}^2 = 4kTR_{n2}\left|\frac{1}{1+j\omega R_{n2}C_{n2}}\right|^2 \qquad (\frac{V^2}{Hz}) \tag{51}$$

The equivalent Thevenin impedance for the RC network n_2 is the parallel combination of the resistor R_{n2} and the impedance of the capacitor C_{n2}, which yields:

$$Z_{n2(RC)} = \frac{R_{n2}}{1+sR_{n2}C_{n2}} \tag{52}$$

Network n_2 noise, like resistor noise, is of the white type with uniform power density across the frequency spectrum.

E. Op-Amp Noise Model

Op-amp noise, like any integrated circuit noise, is a mixture of white noise and 1/f noise. Typical op-amp noise densities are shown in Figure 4. Analysis of Figure 4 reveals that at low frequencies 1/f noise dominates, while at high frequencies the noise is predominantly white. The boundary between the two regions is called the corner frequency f_c and can be determined by intersecting the 1/f noise asymptote and the white noise floor. The conclusion stemming from Figure 4 is that a more narrow frequency spectrum results in a smaller amount of equivalent noise present in the circuit. Thus in

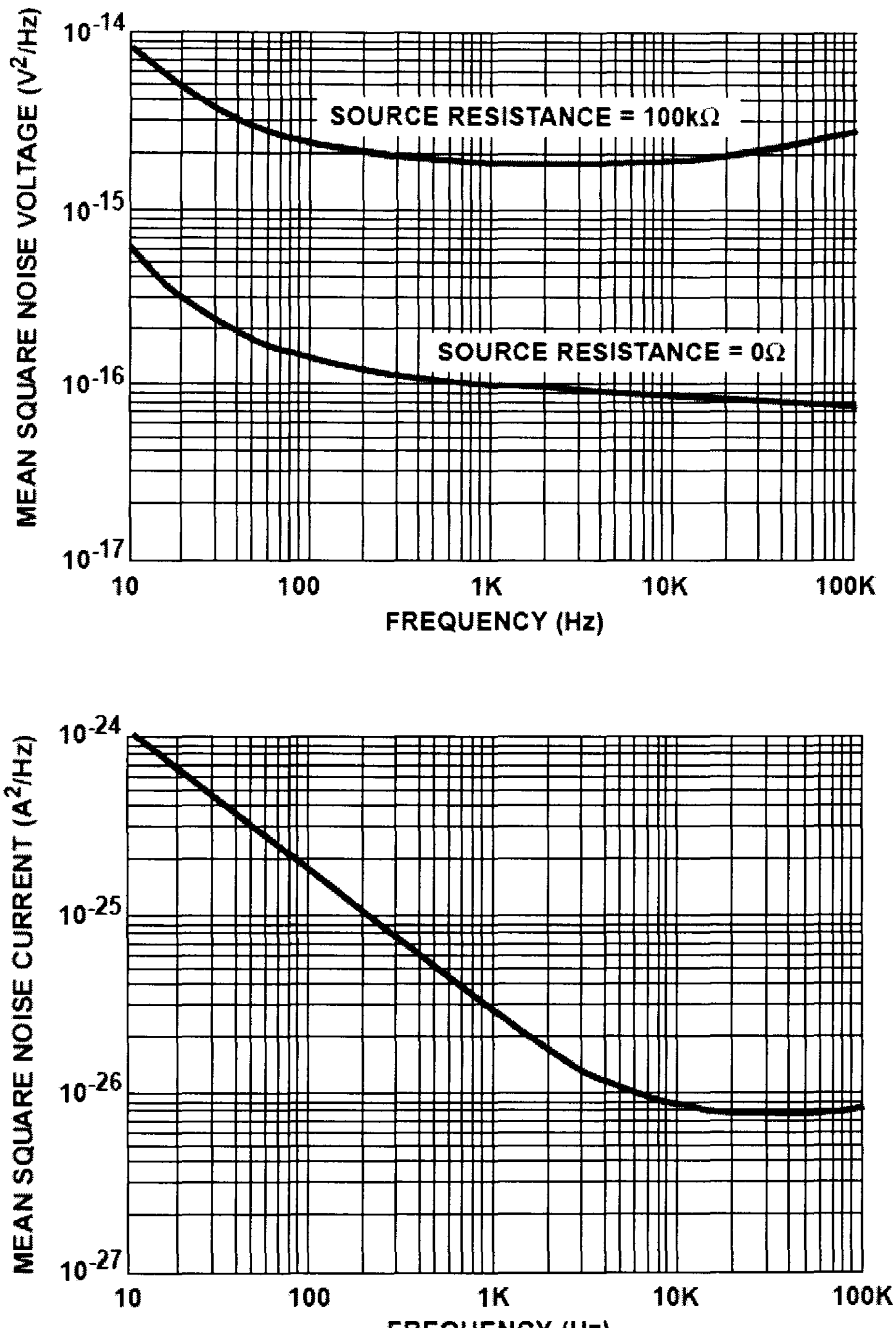

Figure 4. Example of op-amp noise curves

(Courtesy of Intersil Corporation)

low noise design it is recommended that one limit the operating bandwidth to a minimum.

A "noisy" op-amp is modeled by adding three input noise sources to the "noiseless" op-amp model. Two noise sources are current noise generators i_{nn} and i_{np} connected between each op-amp input and ground. The remaining noise source is a voltage noise generator e_n connected in series with one of the op-amp inputs, as shown in Figure 5 [11], [17]. The op-amp noise model bears striking similarity to the op-amp offset and bias model used to analyze the effects of input offset voltage and input bias currents. This comparison is valid since V_{OS} and I_B may be viewed as DC noise sources. Unlike V_{OS} and I_B, the magnitudes of the noise sources e_n and i_p are constantly changing due to the random nature of noise, so their contributions must be summed in rms fashion. In general, the noise signature contribution of the two current noise generators is negligible comparing to the voltage noise generator, especially if the magnitude of the impedance "seen" by each of the current sources is less than $100\,k\Omega$. This simplifies the analysis and calculation of the total noise signal present at the output of the amplifier.

F. Noise Transfer Functions

The next step in noise modeling is the development of the transfer functions from every noise source to the filter output. The transfer functions for each of the effective noise sources are presented in Table 8. It is important to note that all noise sources are assumed to be uncorrelated [11], [32], [33]. The transfer function associated with network n_2 entry is applicable to both network n_2 noise models previously defined.

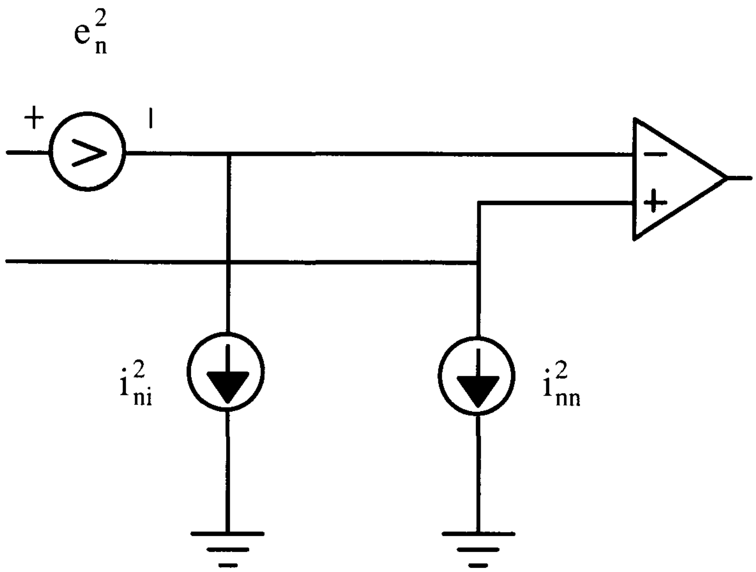

Figure 5. Noise model of an op-amp

Table 8. Transfer Functions of Noise Sources to Filter Output

Component / Source	Transfer Function
R_A	$\dfrac{1}{s^2C_1C_2R_AR_K + s(C_1+C_2)R_A + 1}$
R_B	$\dfrac{-s(\frac{C_2R_2R_A}{R_B})}{s^2C_1C_2R_AR_K + s(C_1+C_2)R_A + 1}$
R_1	$\dfrac{sC_2R_Ak_0}{s^2C_1C_2R_AR_K + s(C_1+C_2)R_A + 1}$
R_2	$\dfrac{sC_2R_A}{s^2C_1C_2R_AR_K + s(C_1+C_2)R_A + 1}$
R_{T2}	$\dfrac{s^2C_1C_2R_AR_K + s(C_1+k_0C_2)R_A}{s^2C_1C_2R_AR_K + s(C_1+C_2)R_A + 1}$
Op Amp e_n^2	$\dfrac{s^2C_1C_2R_AR_K + s(C_1+k_0C_2)R_A}{s^2C_1C_2R_AR_K + s(C_1+C_2)R_A + 1}$
Op Amp i_{n1}^2	$\dfrac{sC_2R_AR_K}{s^2C_1C_2R_AR_K + s(C_1+C_2)R_A + 1}$
Op Amp i_{n2}^2	$\dfrac{Z_{T2}[s^2C_1C_2R_AR_K + s(C_1+k_0C_2)R_A]}{s^2C_1C_2R_AR_K + s(C_1+C_2)R_A + 1}$

The noise signal at the output of n_2 network must be multiplied by the transfer function associated with network n_2 to determine the noise contribution of network n_2 to the filter output signal. The impedance Z_{n2} represents the equivalent impedance of network n_2 as "seen" by the op-amp current noise source i_{n2}.

G. Calculation of Total RMS Noise

A common task in noise analysis is determination of the total rms noise E_{no} present at the output of the circuit when: (1) the spectral noise density $e_{ni}(f)$ at the input of the circuit is known, and (2) the circuit's noise frequency characteristic $A_n(f)$ is known. Assuming a circuit with a single noise source $e_{ni}(f)$ and the noise frequency characteristics $A_n(f)$, the noise spectral density at the output is defined as:

$$e_{no}(f) = |A_n(f)| e_{ni}(f) \tag{53}$$

The total rms output noise E_{no} is calculated by integrating $e_{no}^2(f)$ over the entire frequency range of interest and then taking the square root of the result [11], yielding

$$E_{no} = \sqrt{\int_{f(\text{lower})}^{f(\text{upper})} |A_n(f)|^2 e_{ni}^2(f) df} \tag{54}$$

The values of $A_n(f)$ and $e_{ni}(f)$ are usually available in graphical form, so the expression in (54) cannot be evaluated analytically. In this instance E_{no} can be approximated via graphical integration techniques. The steps for calculating total rms noise E_{no} using graphical integration techniques are given below:

Step (1) - Obtain the graphs for $e_{ni}(f)$ and $G_n(f)$.

Step (2) - $G_n(f)$ is given as a Bode plot. To enable the integration process, its gain axis is linearized and converted from decibels to dimensionless unit, yielding $A_n(f)$.

Step (3) - Both graphs $e_{ni}(f)$ and $A_n(f)$ are analyzed and divided into appropriate frequency intervals enabling accurate curve characterization within each interval.

Step (4) - $e_{ni}(f)$ curve is characterized by developing a mathematical function $e_{ni}(f)$ for each frequency interval.

Step (5) - $A_n(f)$ curve is characterized by developing a mathematical function $A_n(f)$ for each frequency interval.

Step (6) - Integration process is carried out, yielding an equivalent rms noise source for each frequency interval.

Step (7) - The resulting interval rms noise sources are uncorrelated and can be added in Pythagorean fashion, yielding the total rms output noise E_{no}.

The calculation of total rms noise using the graphical integration technique is carried out for the LP filter, shown in Figure 6. The noise analysis results are given in Table 9.

H. Other Considerations

The ultimate goal in noise analysis is the determination of the total rms noise present at the input and output of the circuit knowing (a) the spectral noise density present at the input of the circuit, and (b) the circuit's frequency response. In a fixed gain amplifier design this process is somewhat simplified, since the circuit's frequency response remains relatively unchanged throughout the frequency spectrum of interest.

Table 9. Equivalent RMS Noise for Sample LP Filter Design

Component	Value/PN	$T_{AMBIENT}$	Bandwidth	RMS Noise	Total RMS Noise
R_A	4.02 kΩ	25 C (298 K)	10 Hz – 100 kHz	295.83 nV	**3.008 uV**
R_B	2.26 kΩ			490.63 nV	
R_1	10 kΩ			1.2655 uV	
R_2	10 kΩ			233.29 nV	
Op-Amp	LMV 721			2.6573 uV	

Unlike amplifiers, active RC filter noise analysis presents an additional set of challenges; not only do the noise densities vary, but the filter gain significantly varies across the same frequency spectrum as well. Noise, being an electrical signal, is subject to similar filtering properties when passing through a filter circuit. A concept of noise equivalent bandwidth (NEB) is introduced to simplify the noise analysis of filter circuits. The noise equivalent bandwidth represents the frequency span of a brickwall power gain response having the same area as the power gain response of the original circuit [11]. The noise equivalent bandwidth can be computed analytically, and it can be calculated by numerical integration or estimated via piecewise graphical integration.

The goal of low noise filter design is to reduce the noise effects on the performance of the filter so that the equivalent noise signals present at the filter input and output are minimized over the frequency spectrum of interest. From the noise models (48, 49, 51, Figs. 3 and 5) it is concluded that the noise signature in a given filter design can be minimized by:

(1) Limiting the circuit's operating bandwidth to a minimum resulting in the reduction of the noise equivalent bandwidth.

(2) Reducing the ohmic values of resistors to minimize the magnitude of their thermal noise voltage sources, especially equivalent resistances "seen" by the i_{nn} and i_{np} op-amp current noise sources.

(3) Reducing the ambient temperature to minimize the magnitude of resistor thermal noise voltage sources.

(4) Choosing the low noise op-amps with low e_n, i_n, and f_c values [36], [37].

There is a practical limit on reduction of resistor ohmic values. Excessively small ohmic values result in loading of the op-amp ports yielding op-amp operation outside desired and predictable states. Elevated ambient temperatures negatively affect the filter's noise performance by increasing the magnitude of resistor thermal noise sources. The ambient temperature is an independent factor; reducing the ambient temperature to desired levels is rarely feasible or practical, and so its effects on filter designs must be taken into consideration.

I. Noise Analysis of Higher Order Filters

Since higher order filters are created by cascading multiple first or second order filters, the noise analysis of higher order filters is an extension of the noise analysis of first or second order filters. The first step is the completion of noise analysis for individual first or second order filter sections. The next step is a definition of the noise equivalent bandwidth NEB for each filter section. For the noise analysis of multi stage filter circuits two important concepts must be kept in mind:

(1) The noise sources are uncorrelated and must be added in Pythagorean fashion.

(2) Noise is an electrical signal and is subject to same filtering properties when passing through a filter circuit.

Equivalent noise signals are calculated sequentially from the first filter section to the last filter section. The equivalent noise signal at the output of the first filter section is an rms sum of (a) the noise present in a signal to be filtered, and (b) the noise generated by the section itself. The equivalent noise signal at the output of the subsequent filter sections, including the last filter section, is an rms sum of (a) the noise internally generated by the section itself, and (b) the noise coupled from the previous sections subject to filtering characteristics of the section itself.

CHAPTER VII

SECOND ORDER FILTER SENSITIVITIES

Table 9 lists the sensitivities of ω_0 and Q with respect to each of the components comprising original network N_1. Analysis of the expressions listed in Table 9 indicates that the filter designs have very low values of Q and ω_0 sensitivities with respect to each of the filter components, which is a major advantage in any filter design [17], [38], [39].

The Q and ω_0 sensitivities with respect to R_A are independent from the other component values and are always equal to -0.5. The Q and ω_0 sensitivities with respect to resistors R_B, R_1, and R_2 are always in the range between -0.5 and 0.5, regardless of the chosen component ratio between resistors R_B, R_1, and R_2. This conclusion is based upon the observation that the denominator expressions for sensitivities in question consist of the sum of the numerator expressions and additional positive terms. For example, the expressions for sensitivities of Q and ω_0 with respect to R_1 and R_2 have denominators that contain complete numerator expressions plus either resistor value R_1 or R_2. Similarly, the expressions for sensitivities of Q and ω_0 with respect to R_B have denominators that contain a complete numerator expression plus resistor values R_2 and R_1. In both cases their ratio is always much smaller than unity for any reasonable values of resistor components. Taking into consideration the multiplying factors 0.5 or -0.5

Table 10. Sensitivities of ω_0 and Q

Component	ω_0 Sensitivity	Q Sensitivity
R_A	$-\frac{1}{2}$	$-\frac{1}{2}$
R_B	$\frac{1}{2}\left(\frac{\frac{R_1R_2}{R_B}}{R_1+R_2+\frac{R_1R_2}{R_B}}\right)$	$-\frac{1}{2}\left(\frac{\frac{R_1R_2}{R_B}}{R_1+R_2+\frac{R_1R_2}{R_B}}\right)$
R_1	$-\frac{1}{2}\left[\frac{R_1(1+\frac{R_2}{R_B})}{R_1+R_2+\frac{R_1R_2}{R_B}}\right]$	$\frac{1}{2}\left[\frac{R_1(1+\frac{R_2}{R_B})}{R_1+R_2+\frac{R_1R_2}{R_B}}\right]$
R_2	$-\frac{1}{2}\left[\frac{R_2(1+\frac{R_1}{R_B})}{R_1+R_2+\frac{R_1R_2}{R_B}}\right]$	$\frac{1}{2}\left[\frac{R_2(1+\frac{R_1}{R_B})}{R_1+R_2+\frac{R_1R_2}{R_B}}\right]$
C_1	$-\frac{1}{2}$	$\frac{1}{2}\left(\frac{C_2-C_1}{C_1+C_2}\right)$
C_2	$-\frac{1}{2}$	$\frac{1}{2}\left(\frac{C_1-C_2}{C_1+C_2}\right)$

yields the conclusion that the resulting range of sensitivities is always between these two values.

The ω_0 sensitivities with respect to C_1 and C_2 are independent from the other component values and are always equal for -0.5. It is interesting to note that the Q sensitivity to either capacitor C_1 or C_2 is equal to 0 if both capacitor values are set equal to each other, $C_1 = C_2$.

A comparison between Table 9 sensitivities and the Sallen and Key 2nd order filter sensitivities reveal that the Sallen and Key filter sensitivities can be much higher [17]. For positive gain Sallen and Key filters, the Q sensitivities with respect to some filter components are dependent on Q value and amplifier gain K value. This means that for large Q values, the Q sensitivities are much greater than unity. It is possible to reduce these undesirable high sensitivities by using a larger spread of component values, such as 10:1. Unfortunately, using a large spread of component values is not desirable for practical design.

The use of infinite gain or Rauch filters [40] somewhat reduces the sensitivity problem associated with the positive gain Sallen and Key filters. The infinite gain filters have root loci that do not cross into the right half of the s-plane for any reasonable value of Q ($Q \leq 10$). These filters are always stable regardless of gain, and their sensitivities are usually lower as compared to the positive gain Sallen and Key filters. Unfortunately, the infinite gain filters have several disadvantages: (a) they have complex design methods, (b) their element value spreads are large, and (c) they require large gain values which are more difficult to stabilize as compared to low gain values of positive gain Sallen and Key filters.

CHAPTER VIII

DESIGN PROCEDURE

The initial challenge in any filter design is the determination of the order of the specific filter function required to meet a set of filtering specifications. Filter specifications usually consist of the pass band specification set and the stop band specification set [41], [42]. Actual parameters are as follows:

Pass band parameters:

A_{P-MAX} - The maximum permissible variation or "ripple" of the filter's magnitude characteristic inside the pass band (specified in dB).

ω_P - Critical or boundary pass band frequency for which A_{P-MAX} condition must be satisfied (specified in rad/sec), or

f_P - Critical or boundary pass band frequency for which A_{P-MAX} condition must be satisfied (specified in Hz).

Stop band parameters:

A_{S-MIN} - The minimum attenuation required for the filter's magnitude characteristic inside the stop band (specified in dB).

ω_S - Critical or boundary stop band frequency for which A_{S-MIN} condition must be satisfied (specified in rad/sec), or

f_S - Critical or boundary stop band frequency for which A_{S-MIN} condition must be satisfied (specified in Hz).

Thus far, presented filtering functions are confined to 2^{nd} order systems only. Higher order filters are discussed in Chapter XII. For the purpose of developing a design procedure for the circuit configurations presented thus far, the design restriction to 2^{nd} order systems remains in effect. Therefore the burden is placed on the designer to verify that the applicable 2^{nd} order configuration satisfies both the pass band parameters and the stop band parameters. Once acceptability of a 2^{nd} order filter configuration is confirmed, the pass band and stop band parameters are converted to specific design parameters permitting circuit component value selections. In this specific case, the pass band and stop band parameters are converted into quality factor (Q), and undamped natural frequency (ω_0) filter parameters. Once Q and ω_0 are defined, component values are selected and calculated for desired filter configuration.

Design procedures are centered on a general design procedure that is applicable to all filter configurations. The general design procedure is presented first, followed by specific design procedures outlining network n_1 and n_2 configurations. It is recommended that the general design procedure be performed first, followed by specific design procedures for the networks n_1 and n_2 applicable to a respective filter configuration. Additional guidelines should be followed such as: using the same component values as often as possible, selecting capacitor values and calculating resistor values [43]-[49].

A. General Design Procedure

The purpose of this procedure is to calculate and select component values for $R_A, R_K, R_B, R_1, R_2, C_1, C_2$. In order to simplify the design procedure, capacitor values

C_1 and C_2 are set equal to each other yielding $C = C_1 = C_2$. Therefore, the undamped natural frequency ω_0 and quality factor Q are now defined respectively as:

$$\omega_0^2 = \frac{1}{C^2 R_A R_K} \quad \Rightarrow \quad \omega_0^2 = f(C, R_A, R_K) \tag{55}$$

$$\omega_0^2 = \frac{1}{4Q^2 R_A^2 C^2} \quad \Rightarrow \quad \omega_0^2 = f(Q, R_A, C) \tag{56}$$

$$Q = \sqrt{\frac{R_K}{4R_A}} \quad 4Q^2 = \frac{R_K}{R_A} \quad \Rightarrow \quad Q = f(R_A, R_K) \tag{57}$$

R_K is introduced as a variable and is defined in terms of actual circuit components and filter parameters as:

$$R_K = 4Q^2 R_A \quad \Rightarrow \quad R_K = f(Q, R_A) \tag{58}$$

$$R_K = \frac{R_1 R_B + R_2 R_B + R_1 R_2}{R_B} \quad \Rightarrow \quad R_K = f(R_1, R_2, R_B) \tag{59}$$

Step (1) - Given the Q specification, use (57) to calculate the ratio between resistors R_K and R_A. Note that higher values of Q yield larger R_K / R_A ratios and vice-versa. Using this ratio express resistor $R_K = f(Q, R_A)$, as shown in (58).

Step (2) - Pick a capacitor value C for capacitors C_1 and C_2. A good starting point is any standard capacitor value between 1nF and 0.1uF.

Step (3) - Substitute capacitor value C, undamped natural frequency value ω_0, and expression $R_K = f(Q, R_A)$ into (55). Calculate the value of resistor R_A. Alternatively, substitute capacitor value C, undamped natural frequency value ω_0, and the Q value into (56) to calculate the value of resistor R_A.

Step (4) – Using (58) calculate the value of resistor R_K.

Step (5) - Pick resistor values R_1 and R_2. A good starting point is any standard resistor value (or values) between $10\,k\Omega$ and $100\,k\Omega$. In order to simplify the remainder of the design procedure, the same resistor value can be used for both resistors.

Step (6) - Substitute the resistor values for R_1, R_2, and R_K into (59). Calculate the value of resistor R_B.

Step (7) - Ensure that all chosen and calculated resistor values are between $1\,k\Omega$ and $100\,k\Omega$. If not, repeat the general design procedure by selecting different resistor or capacitor values. Applying impedance scaling technique may be an alternate method to achieve desired value range. Resistor values R_A and R_K are multiplied by scaling factor k, while capacitor value C is divided by scaling factor k, or vice-versa. This ensures that undamped natural frequency ω_0 and quality factor Q remain unchanged after the impedance scaling procedure is completed.

B. Network n_2 Design Procedure for the HP1 and BS1 Filters

Step (1) – Replace network n_2 with a voltage divider network, consisting of two resistors R_{n2}/k_2 and $R_{n2}/(1-k_2)$. The transfer function of network n_2 is k_2. Table 2 defines variable k_2 for the HP1 and BS1 filters as:

$$k_2 = \frac{\beta C_2}{(C_1 + k_0 C_2)} \tag{60}$$

Assuming that capacitor $C_1 = C_2$, (60) simplifies to:

$$k_2 = \frac{R_2}{2R_B + R_2} \tag{61}$$

Calculate variable k_2 using previously determined values for resistors R_2 and R_B. The resistors R_2 and R_B are defined and calculated in the general design procedure, shown in section A.

Step (2) - Pick R_{n2} to be any resistance value between $10\,k\Omega$ and $100\,k\Omega$. Calculate the values for both resistors R_{n2}/k_2 and $R_{n2}/(1-k_2)$.

C. Network n_1 Design Procedure for BS1 Filter

Step (1) - Replace network n_1 with a voltage divider network, consisting of two resistors R_A/k_1 and $R_A/(1-k_1)$. The transfer function of network n_1 is k_1, and the equivalent Thevenin resistance of network n_1 remains R_A. Variable k_1 defines the placement of two purely imaginary zeros located on the $j\omega$ axis of the s-plane. A larger k_1 value yields greater zero magnitude and vice-versa. The value of k_1 is independent and can be set to any desired value with the limitation of $0<k_1<1$. A common practice in BS filter design is to set the magnitude of zeros equal to the magnitude of poles, resulting in variables $k_1 = k_2$ for the BS1 filter design. Table 2 defines variable k_2 as:

$$k_2 = \frac{\beta C_2}{(C_1 + k_0 C_2)} \tag{62}$$

Assuming that capacitor $C_1 = C_2$ and $k_1 = k_2$, (62) simplifies to:

$$k_1 = \frac{R_2}{2R_B + R_2} \tag{63}$$

Calculate variable k_1 using previously determined resistance values for R_2 and R_B.

Step (2) - The value of R_A is calculated in the general design procedure, given in section A. Calculate the values for both resistors R_A/k_1 and $R_A/(1-k_1)$.

D. Network n_1 Design Procedure for AP1 Filter

Step (1) – Replace network n_1 with a voltage divider network, consisting of two resistors R_A / k_1 and $R_A /(1-k_1)$. The transfer function of network n_1 is k_1, and the equivalent Thevenin resistance of network n_1 remains R_A. The variables k_1 and k_2 affect the placement of two complex zeros with respect to the complex poles in the s-plane. In order to achieve the AP filter response the complex zeros on the right half side of the s-plane must be an exact reflection of the corresponding poles on the left half side of the s-plane with respect to the $j\omega$ axis. This is accomplished by setting the variables $k_1 = k_2 = k_{12}$ for the AP1 filter design. Table 2 defines variable k_{12} as:

$$k_1 = k_2 = k_{12} = \frac{\beta C_2}{2C_1 + (2+\beta)C_2} \qquad (64)$$

Assuming that capacitor $C_1 = C_2$, (64) simplifies to:

$$k_1 = k_2 = k_{12} = \frac{\dfrac{R_2}{R_B}}{4 + \dfrac{R_2}{R_B}} \qquad (65)$$

Calculate variable k_{12} using previously determined resistance values for R_2 and R_B.

Step (2) - Calculate the values for both resistors R_A / k_{12} and $R_A /(1-k_{12})$.

E. Network n_2 Design Procedure for AP1 Filter

Step (1) – Replace network n_2 with a voltage divider network, consisting of two resistors R_{n2} / k_2 and $R_{n2} /(1-k_2)$. The transfer function of network n_2 is k_2. Apply the AP1 configuration requirement of $k_1 = k_2 = k_{12}$. Table 2 defines variable k_{12} as:

$$k_1 = k_2 = k_{12} = \frac{\beta C_2}{2C_1 + (2+\beta)C_2} \tag{66}$$

Assuming that capacitor $C_1 = C_2$, (66) simplifies to:

$$k_1 = k_2 = k_{12} = \frac{\frac{R_2}{R_B}}{4 + \frac{R_2}{R_B}} \tag{67}$$

Calculate variable k_{12} using previously determined resistance values for R_2 and R_B.

Step (2) - Pick R_{n2} to be any resistance value between $10\,\mathrm{k\Omega}$ and $100\,\mathrm{k\Omega}$. Calculate the values for both resistors R_{n2}/k_{12} and $R_{n2}/(1-k_{12})$.

F. Network n_2 Design Procedure for the BP2, HP2, BS2, and AP2 Filters

Step (1) - Replace network n_2 with a simple RC network, consisting of resistor R_{n2} and capacitor C_{n2}. Table 2 defines the time constant $C_{n2}R_{n2}$ as:

$$C_{n2}R_{n2} = \frac{C_1 C_2 R_K}{C_1 + k_0 C_2} \tag{68}$$

Assuming that capacitor $C_1 = C_2$, (68) simplifies to:

$$C_{n2}R_{n2} = \frac{CR_B R_K}{R_2 + 2R_B} \tag{69}$$

Pick a standard capacitor value for C_{n2}.

Step (2) - The values of R_B, R_K, and R_2 are defined in the general design procedure, shown in section A. Use (69) to calculate the value of R_{n2}.

G. LP Filter Design Procedure

The filter transfer function V_O / V_i is defined as:

$$\frac{V_O}{V_i} = \frac{1}{s^2C^2R_AR_K + s2CR_A + 1} \tag{70}$$

Step (1) - Follow the general design procedure by completing steps 1 through 7 in section A.

Step (2) - Replace network n_1 with resistor R_A.

Step (3) - Replace network n_2 with a $0\,\Omega$ jumper connected between n_2 output terminal and the DC ground. This effectively ties the non-inverting input of the op-amp to ground.

Step (4) - Apply the input signal in place of V_A. Properly remove the other signal sources ($V_B = V_C = 0$) by replacing them with $0\,\Omega$ impedance.

Step (5) - Using final component values re-calculate parameters Q and ω_0 to ensure design validity and accuracy.

H. BP1 Filter Design Procedure

The filter transfer function V_O / V_i is defined as:

$$\frac{V_O}{V_i} = \frac{-sCR_A\beta}{s^2C^2R_AR_K + s2CR_A + 1} \tag{71}$$

Step (1) - Follow the general design procedure by completing steps 1 through 7 given in section A.

Step (2) - Replace network n_1 with resistor R_A.

Step (3) - Replace network n_2 with a $0\,\Omega$ jumper connected between n_2 output terminal and the DC ground. This effectively ties the non-inverting input of the op-amp to ground.

Step (4) - Apply the input signal in place of V_B. Properly remove the other signal sources ($V_A = V_C = 0$) by replacing them with $0\,\Omega$ impedance.

Step (5) - Using final component values re-calculate parameters Q and ω_0 to ensure design validity and accuracy.

I. HP1 Filter Design Procedure

The filter transfer function V_O / V_i is defined as:

$$\frac{V_O}{V_i} = \frac{k_2(s^2C^2R_AR_K)}{s^2C^2R_AR_K + s2CR_A + 1} \tag{72}$$

Step (1) - Follow the general design procedure by completing steps 1 to 7 of section A.

Step (2) - Replace network n_1 with resistor R_A.

Step (3) - Follow the network n_2 design procedure for the HP1 and BS1 filters given in section B.

Step (4) - Apply the input signal in place of the V_B and V_C. Properly remove the remaining signal source ($V_A = 0$) by replacing it with a $0\,\Omega$ impedance.

Step (5) - Using final component values re-calculate parameters Q and ω_0 to ensure design validity and accuracy.

J. BS1 Filter Design Procedure

The filter transfer function V_O / V_i is defined as:

$$\frac{V_O}{V_i} = \frac{k_2(s^2C^2R_AR_K) + k_1}{s^2C^2R_AR_K + s2CR_A + 1} \tag{73}$$

Step (1) - Follow the general design procedure by completing steps 1 to 7 listed in section A.

Step (2) - Follow the network n_1 design procedure for BS1 filter given in section C.

Step (3) - Follow the network n_2 design procedure for the HP1 and BS1 filters outlined in section B.

Step (4) - Apply the input signal in place of the V_A, V_B and V_C.

Step (5) - Using final component values re-calculate parameters Q and ω_0 to ensure design validity and accuracy.

K. AP1 Filter Design Procedure

The filter transfer function V_O / V_i is defined as:

$$\frac{V_O}{V_i} = \frac{k_{12}(s^2C^2R_AR_K - s2CR_A + 1)}{s^2C^2R_AR_K + s2CR_A + 1} \tag{74}$$

Step (1) - Follow the general design procedure by completing section A steps 1 to 7.

Step (2) - Follow the network n_1 design procedure for AP1 filter specified in section D.

Step (3) - Follow the network n_2 design procedure for AP1 filter given in section E.

Step (4) - Apply the input signal in place of the V_A, V_B and V_C.

Step (5) - Using final component values re-calculate parameters Q and ω_0 to ensure design validity and accuracy.

L. BP2 Filter Design Procedure

The filter transfer function V_O / V_i is defined as:

$$\frac{V_O}{V_i} = \frac{sCR_A(2+\beta)}{s^2C^2R_AR_K + s2CR_A + 1} \tag{75}$$

Step (1) - Follow the general design procedure by completing steps 1 through 7 given in section A.

Step (2) - Replace network n_1 with resistor R_A.

Step (3) - Follow the network n_2 design procedure for the BP2, HP2, BS2, and AP2 filters outlined in section F.

Step (4) - Apply the input signal in place of V_C. Properly remove the other signal sources ($V_A = V_B = 0$) by replacing them with $0\,\Omega$ impedance.

Step (5) - Using final component values re-calculate parameters Q and ω_0 to ensure design validity and accuracy.

M. HP2 Filter Design Procedure

The filter transfer function V_O / V_i is defined as:

$$\frac{V_O}{V_i} = \frac{s^2C^2R_AR_K}{s^2C^2R_AR_K + s2CR_A + 1} \tag{76}$$

Step (1) - Follow the general design procedure by completing steps 1 to 7 specified in section A.

Step (2) - Replace network n_1 with resistor R_A.

Step (3) - Follow the network n_2 design procedure for the BP2, HP2, BS2, and AP2 filters given in section F.

Step (4) - Apply the input signal in place of V_C. Properly remove the other signal sources ($V_A = V_B = 0$) by replacing them with $0\,\Omega$ impedance.

Step (5) - Using final component values re-calculate parameters Q and ω_0 to ensure design validity and accuracy.

N. BS2 Filter Design Procedure

The filter transfer function V_O / V_i is defined as:

$$\frac{V_O}{V_i} = \frac{s^2C^2R_AR_K + k_1}{s^2C^2R_AR_K + s2CR_A + 1} \tag{77}$$

Step (1) - Follow the general design procedure by completing steps 1 through 7 of section A.

Step (2) - Replace network n_1 with resistor R_A.

Step (3) - Follow the network n_2 design procedure for the BP2, HP2, BS2, and AP2 filters outlined in section F.

Step (4) - Apply the input signal in place of the V_C and V_A. Properly remove the remaining signal source ($V_B = 0$) by replacing it with a $0\,\Omega$ impedance.

Step (5) - Using final component values re-calculate parameters Q and ω_0 to ensure design validity and accuracy.

O. AP2 Filter Design Procedure

The filter transfer function V_O / V_i is defined as:

$$\frac{V_O}{V_i} = \frac{s^2C^2R_AR_K - s2CR_A + 1}{s^2C^2R_AR_K + s2CR_A + 1} \tag{78}$$

Step (1) - For this particular filter configuration modify the general design procedure to accommodate the following AP2 design requirement listed in Table 2:

$$\frac{R_2}{R_B} = 1 + \frac{C_1}{C_2} \tag{79}$$

Assuming that capacitor $C_1 = C_2$, (79) simplifies to:

$$\frac{R_2}{R_B} = 2 \tag{80}$$

As a consequence of limitations imposed by equations (79) and (80), the expression for resistor R_K reduces to:

$$R_K = 2R_B + 3R_1 \tag{81}$$

Follow the general design procedure by implementing above-mentioned requirements.

Step (2) - Replace network n_1 with resistor R_A.

Step (3) - Follow the network n_2 design procedure for the BP2, HP2, BS2, and AP2 filters given in section F.

Step (4) - Apply the input signal in place of the V_A, V_B and V_C.

Step (5) - Using final component values re-calculate parameters Q and ω_0 to ensure design validity and accuracy.

CHAPTER IX

DESIGN EXAMPLES AND SIMULATION RESULTS

The design procedures are carried out in their entirety for all filter configurations. Filters are designed to satisfy an established set of filter specifications: quality factor Q=2, and undamped natural frequency $\omega_0 = 2\Pi \cdot 1000$ rad/sec. The quality factor value is purposefully chosen to be larger than 0.707 to avoid the LP and HP filters having maximally flat response, and to ensure some "peaking" is present and observed in the vicinity of undamped natural frequency [50]-[53].

A. Design Assumptions and Recommendations

The following component values are selected from the standard resistor and capacitor values and are applied, as appropriate, in respective filter designs: $R_1 = R_2 = R_{n2} = 10k\Omega$, and $C_1 = C_2 = C_{n2} = 10nF$. The remaining component values are calculated by following the design procedures outlined in Chapter VIII:

Step (1) - Follow applicable general design example.

Step (2) - Replace network n_1 with resistor R_A, or follow applicable network n_1 design example.

Step (3) - Replace network n_2 with a $0\,\Omega$ impedance by tying the non-inverting op-amp input to ground, or follow applicable network n_2 design example.

Step (4) - Apply the input signal in place of appropriate source (or sources), replace remaining source (or sources) with a $0\,\Omega$ impedance. Filter schematic diagrams with final component values are shown in Figures 6-14.

Observe that calculated resistance values for R_A and R_B are replaced with the closest standard 1% resistor values. The application of 1% tolerance parts may yield an unacceptable variation in filter parameters from one filter to the next in mass production process. In this case a designer may opt to choose standard 0.1% tolerance resistor parts and smaller tolerance capacitor parts yielding an overall smaller variation of filter parameters between the mass-produced filter units.

Note that resistor R_K is an introduced variable and it does not translate directly into actual physical component. Therefore the calculated value for R_K is not replaced with the closest standard 1% resistor value; rather it is left "as is" in order to minimize the calculation error caused by the R_K value round-off.

B. Circuit Simulation Procedure

The SPICE-based circuit simulation software packages are commonly used to simulate circuit operation. They are capable of performing DC operating point analysis, transient analysis, and AC sweep analysis. In this particular instance Circuit Maker 2000 software is used to capture the filter schematics and draw the frequency response curves for each of the 2nd order filter configurations. Other SPICE-based circuit simulation software packages with equivalent capability can be used to accomplish the same task.

The schematic diagrams for each filter configuration are captured and created. Careful attention is devoted to appropriate SPICE model selection and implementation.

Selection of realistic op-amp models is important, such as general-purpose op-amp model that simulates electrical characteristics of 741 op-amp family. Regarding the input signal source, implementation of VAC source enables AC sweep analysis.

Upon capturing and re-creating schematic diagrams, DC operating point analysis is performed to ensure simulated DC operating point node voltages are in accordance with expected DC operating point values. If unusual or unexpected node voltages are generated during DC operating point analysis, schematic capture integrity and accuracy is re-checked and re-verified.

Upon successful completion of DC operating point analysis, transient analysis is performed as another tool to verify the circuit integrity. The goal of transient analysis is a confirmation that a sinusoidal waveform is generated by an input signal source, and that sinusoidal signal is propagated undistorted to the filter's output. If any signs of signal distortion are detected, schematic capture integrity and accuracy are re-checked and re-verified.

Successful completion of DC operating point and transient analysis are recommended pre-requisites prior to execution of AC sweep analysis. AC sweep analysis setup is activated. Start sweep frequency is set at 10 Hz. Stop sweep frequency is set at 100 kHz. Horizontal or frequency axis is set to logarithmic scale. Vertical gain axis is set for dB scale, and vertical phase axis is set for degrees scale. For maximum resolution either the largest number of evaluation points or the smallest step size is selected, whichever option is applicable. Filter undamped natural frequency ($\omega_0 \approx 2\Pi \cdot 1000$ rad/sec) is placed in the middle of the selected AC sweep range. This is done to permit the observation and analysis of the filter responses in both the pass band and the stop band.

The results of AC sweep analysis are presented in Figs. 6-14. For each filter configuration the schematic diagram is shown together with the resulting Bode plot. The simulation results obtained agree with the expected and anticipated results for magnitude and phase response.

Simulated frequency responses of the LP, HP1, and HP2 filters are shown in Figs. 6-8. In all three cases the gain in the pass band remains relatively constant. A slight "peaking" in magnitude response is observed in the vicinity of the undamped natural frequency $\omega_0 \approx 2\Pi \cdot 1000$ rad/sec, caused by the Q value being greater than 0.707 (Q=2). The gain in the stop band is decreasing at the rate of 40 dB/decade (12 dB/octave) for the LP filter, or increasing at the rate of 40 dB/decade (12 dB/octave) for the HP1 and HP2 filters. The phase shift is steadily decreasing from 0 to -180 degrees for the LP filter, from -180 to -360 degrees for the HP1 filter, and from +180 to 0 degrees for the HP2 filter. At undamped natural frequency ω_0, the phase shift is at the midpoint of the simulated phase shift range yielding -90, -270, and 90 degree phase shift values for the LP, HP1, and HP2 filters respectively.

Resulting frequency responses of BP1 and BP2 filters are shown in Figs. 9-10. In both cases the gain steadily increases at the rate of 20 dB/decade as the frequency is varied from the low frequency to the undamped natural frequency. Beyond the undamped natural frequency ω_0 to high frequency, the gain decreases at the rate of 20 dB/decade. Undamped natural frequency $\omega_0 \approx 2\Pi \cdot 1000$ rad/sec is also the "center" frequency of the pass band.

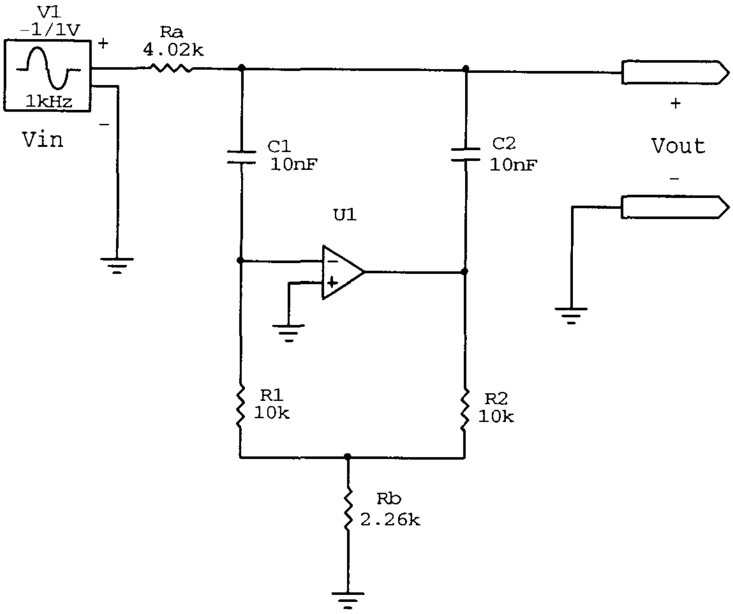

(a)

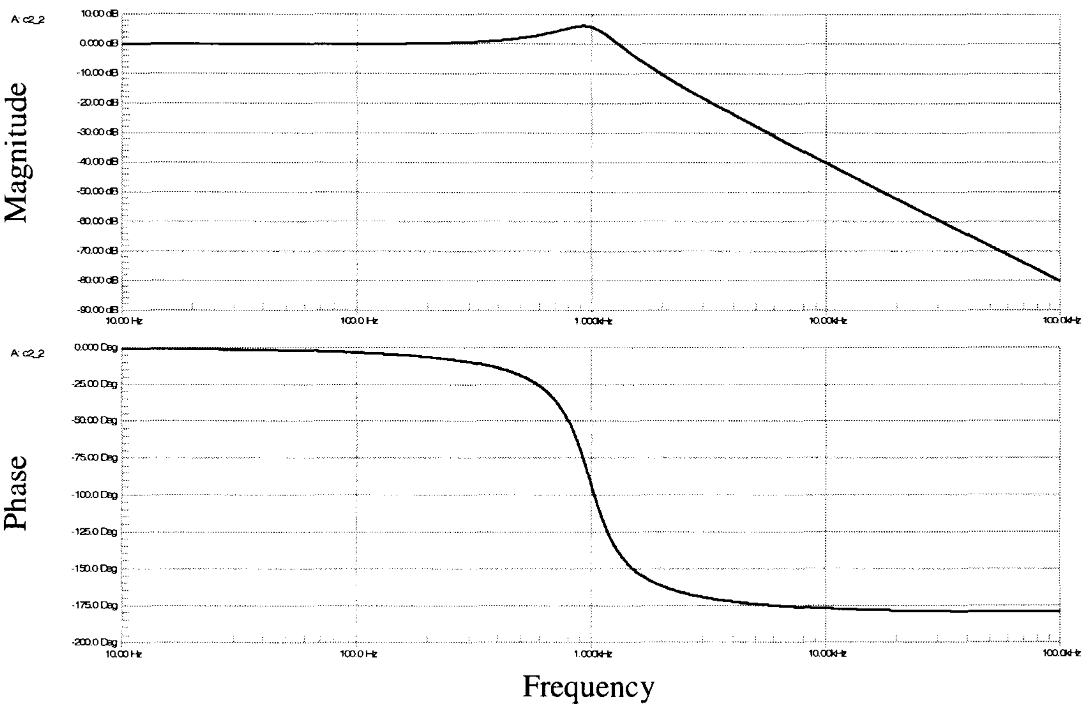

(b)

Figure 6. LP filter simulation results, $\omega_0 = 2\Pi \cdot 1000$ rad/sec, Q=2

(a) Schematic diagram and (b) magnitude and phase AC sweep response

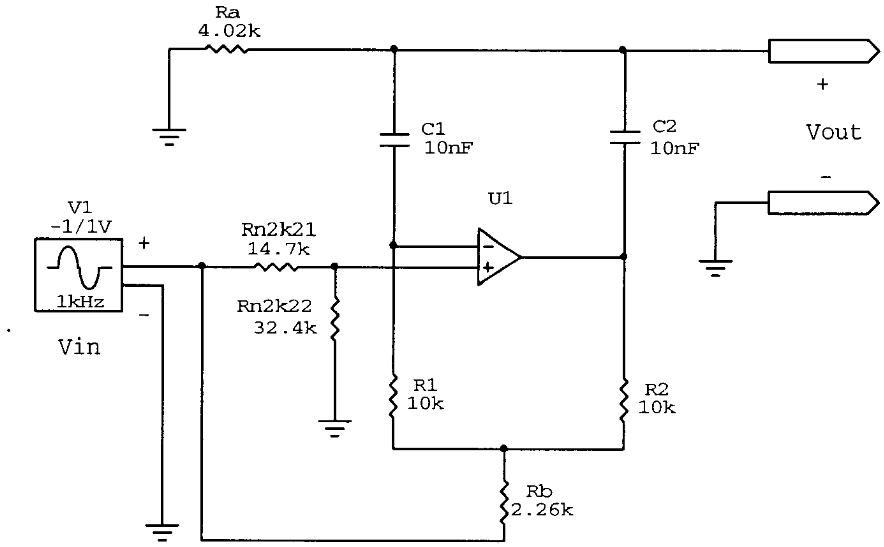

(a)

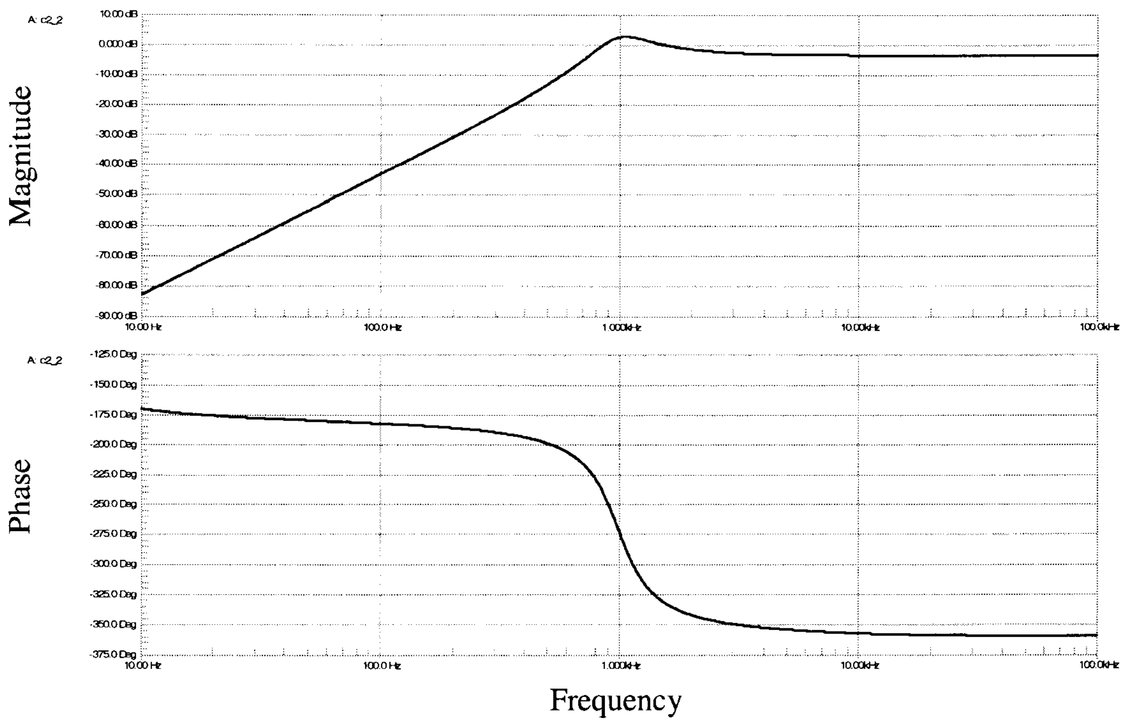

(b)

<u>Figure 7</u>. HP1 filter simulation results, $\omega_0 = 2\Pi \cdot 1000$ rad/sec, Q=2

(a) Schematic diagram and (b) magnitude and phase AC sweep response

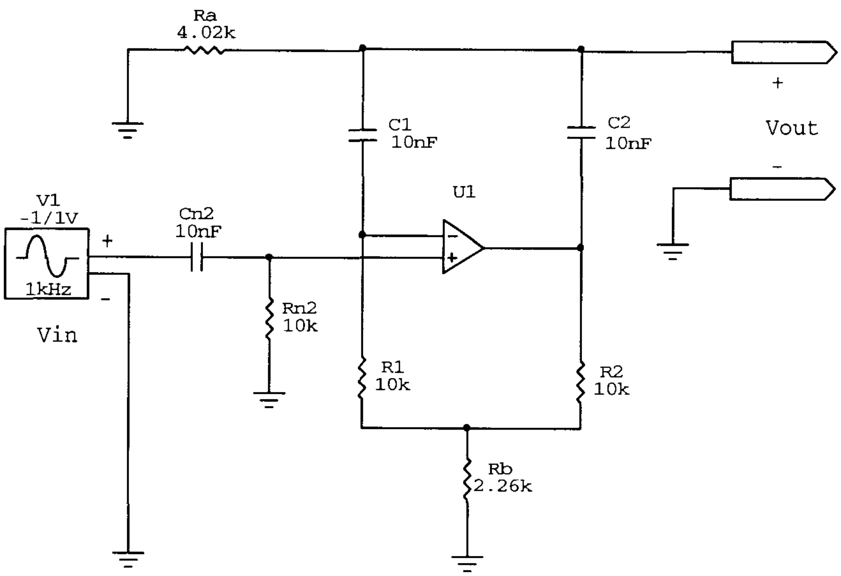

(a)

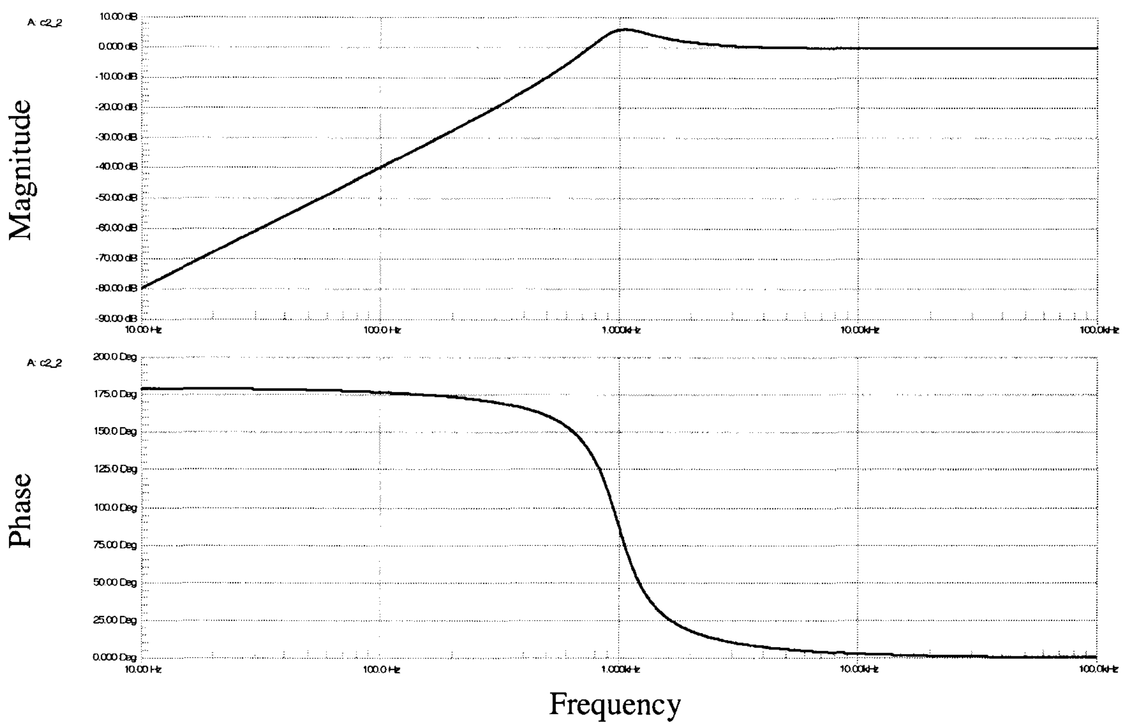

(b)

Figure 8. HP2 filter simulation results, $\omega_0 = 2\Pi \cdot 1000$ rad/sec, Q=2

(a) Schematic diagram and (b) magnitude and phase AC sweep response

The phase response of BP1 and BP2 filter configurations are not the same due to the difference in the network n_2 configuration. For the BP1 filter, the phase shift is steadily decreasing from -90 to -270 degrees, while for the BP2 filter, the phase shift is steadily decreasing from +90 to -90 degrees. The phase shift midpoint occurs at the undamped natural frequency ω_0, resulting in -180 and 0 degrees phase shift values for the BP1 and BP2 filters respectively.

Frequency responses of the BS1 and BS2 filter configurations are shown in Figs. 11-12. In both instances, the filter gain remains relatively constant in the pass band. The gain is sharply and steadily decreasing in the stop band as the "notch" frequency is approached either from low frequency or high frequency. The undamped natural frequency $\omega_0 \approx 2\Pi \cdot 1000$ rad/sec represents the center or "notch" frequency of the stop band. For both BS configurations, the phase shift remains relatively constant at 0 degrees inside the pass band. As the notch frequency is approached from low frequency, the phase shift initially decreases to approximately -90 degrees, and then it instantaneously changes to approximately +90 degrees just above the notch frequency. Beyond the notch frequency the phase shift decreases towards 0 degrees (or -360 degrees) as the sweep frequency moves away from the notch frequency toward high frequency.

An ideal BS filter response involves setting the magnitude of poles in the left half side of the s-plane equal to the magnitude of zeros located on the $j\omega$ axis. This results in a uniform gain magnitude in the pass band, both above and below the notch frequency. The modification of independent parameter k_1 yields an additional two unique responses observed in the BS filter configurations. They are referred to as: (1) the high pass notch

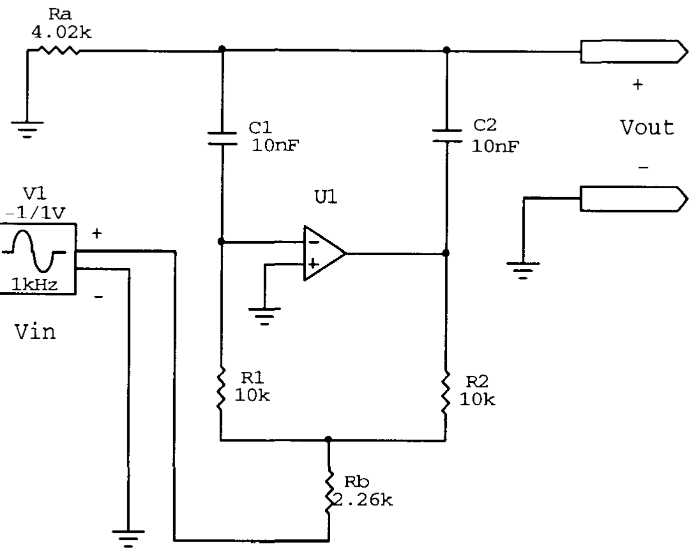

(a)

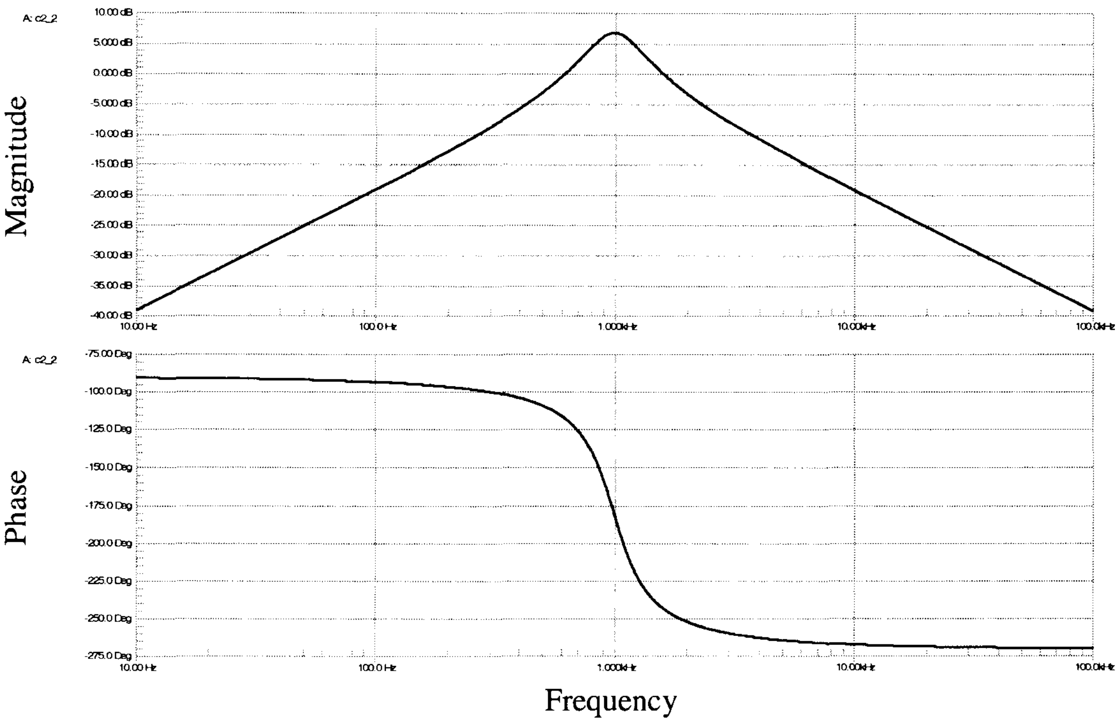

(b)

Figure 9. BP1 filter simulation results, $\omega_0 = 2\Pi \cdot 1000$ rad/sec, Q=2

(a) Schematic diagram and (b) magnitude and phase AC sweep response

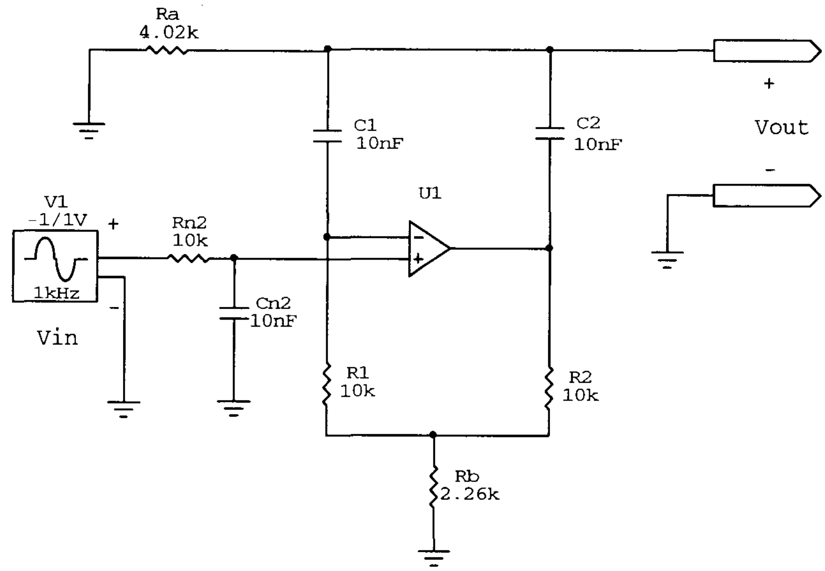

(a)

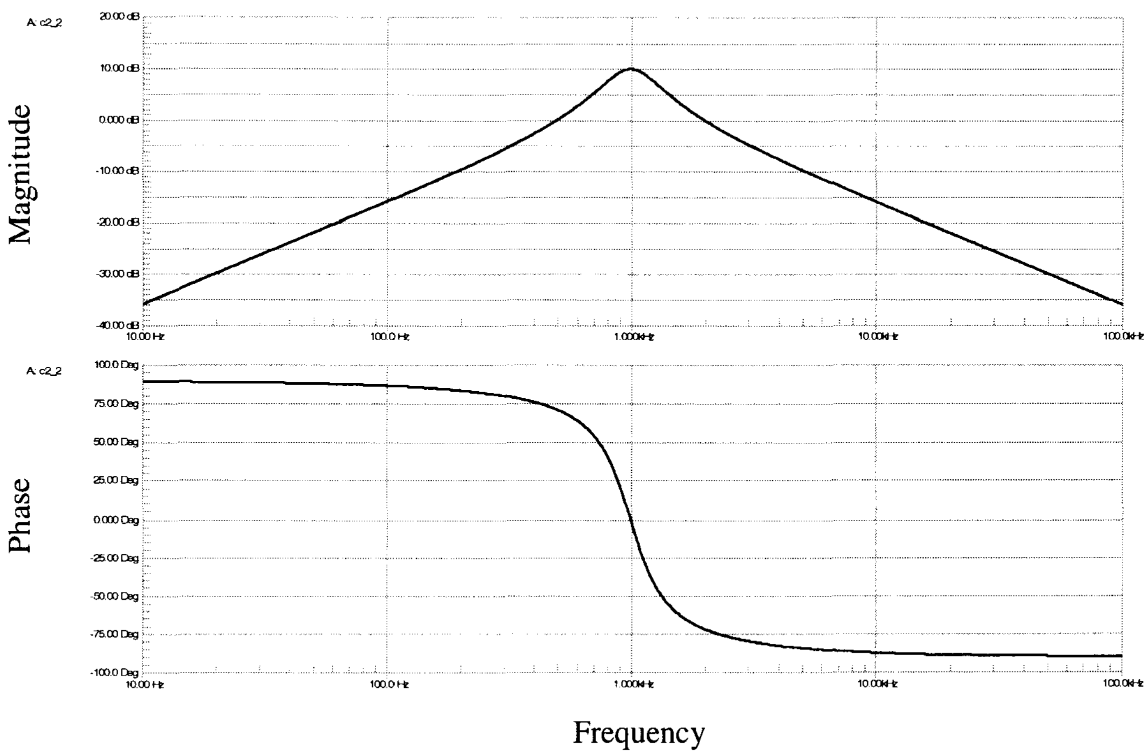

(b)

Figure 10. BP2 filter simulation results, $\omega_0 = 2\Pi \cdot 1000$ rad/sec, Q=2

(a) Schematic diagram and (b) magnitude and phase AC sweep response

response and (2) the low pass notch response; denoting the differences in the pass band gain magnitudes above and below the notch frequency.

For the HP notch response parameter k_1 is adjusted to be smaller than parameter k_2 in the BS1 filter design, or parameter k_1 is adjusted to be smaller than unity in the BS2 filter design. The net result is that the magnitude of zeros located on the $j\omega$ axis is smaller as compared to the magnitude of poles located in the left half side of the s-plane. A careful analysis of the resulting gain response reveals that the pass band gain below the notch frequency is lower as compared to the pass band gain above the notch frequency. The notch frequency is slightly shifted to a lower frequency. The phase response deviations around the notch frequency are observed as well. As the notch frequency is approached from low frequency, the phase shift does not fully decrease from 0 to -90 degrees, but then it suddenly increments beyond +90 degrees just above the notch frequency. Beyond the notch frequency the phase shift eventually returns to 0 degrees.

For the LP notch response parameter k_1 is adjusted to be larger than parameter k_2 in the BS1 filter design. The net result is that the magnitude of zeros located on the $j\omega$ axis is larger as compared to the magnitude of poles located in the left half side of the s-plane. The analysis of the resulting gain response shows that the pass band gain below the notch frequency is higher as compared to the pass band gain above the notch frequency. The notch frequency is slightly shifted to a higher frequency. The phase response anomalies around the notch frequency are noted as well. As the notch frequency is approached from low frequency, the phase shift decreases from 0 to -90 degrees and beyond, and then it jumps to slightly less than +90 degrees just above the

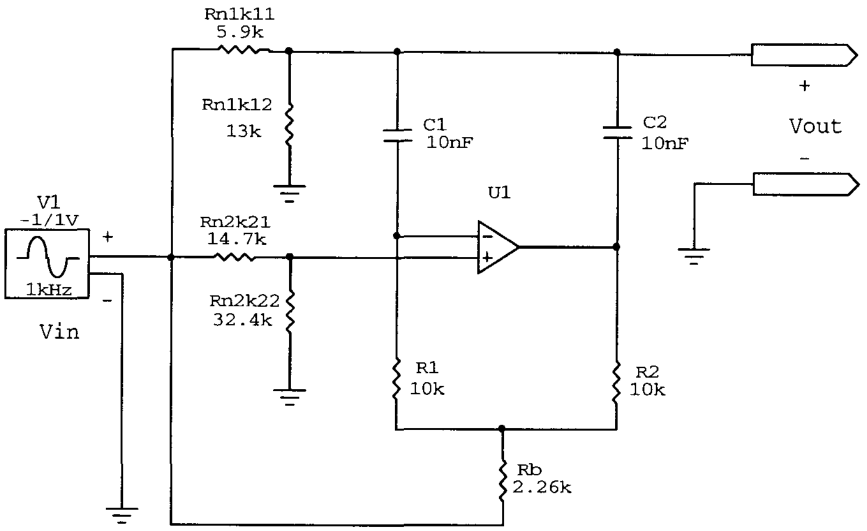

(a)

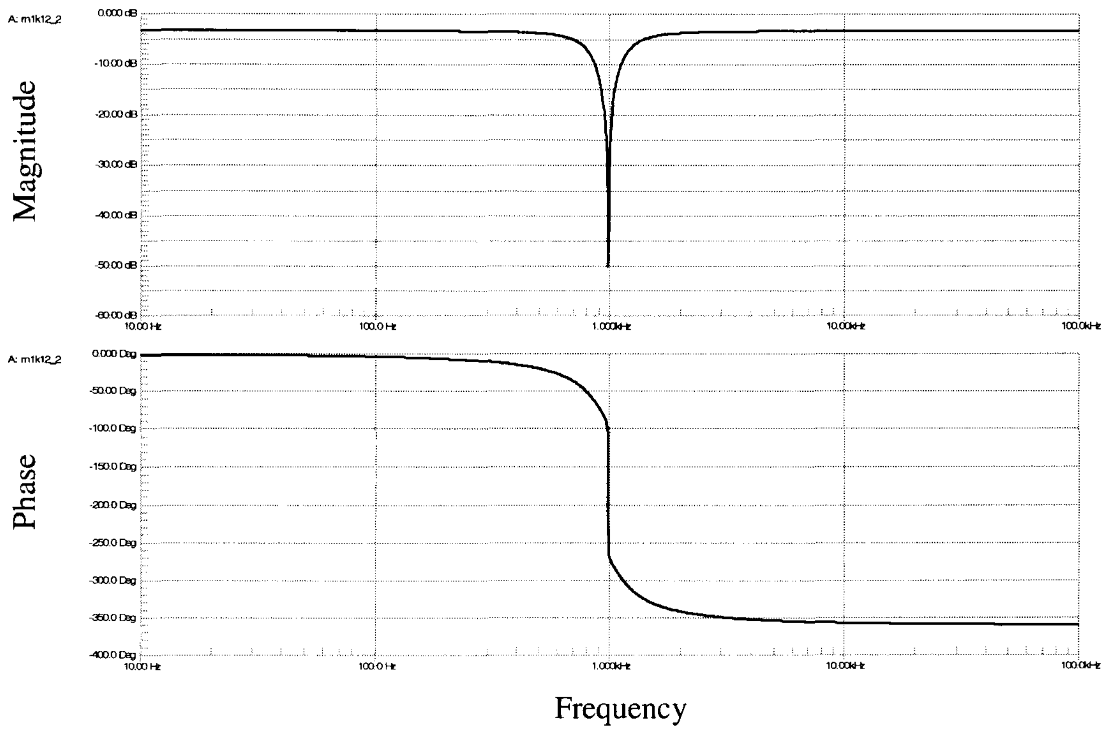

(b)

Figure 11. BS1 filter simulation results, $\omega_0 = 2\Pi \cdot 1000$ rad/sec, Q=2

(a) Schematic diagram and (b) magnitude and phase AC sweep response

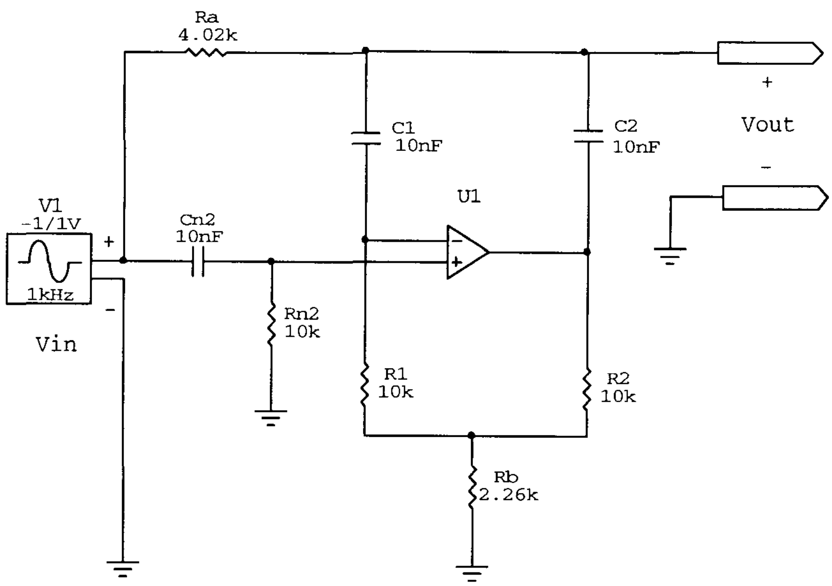

(a)

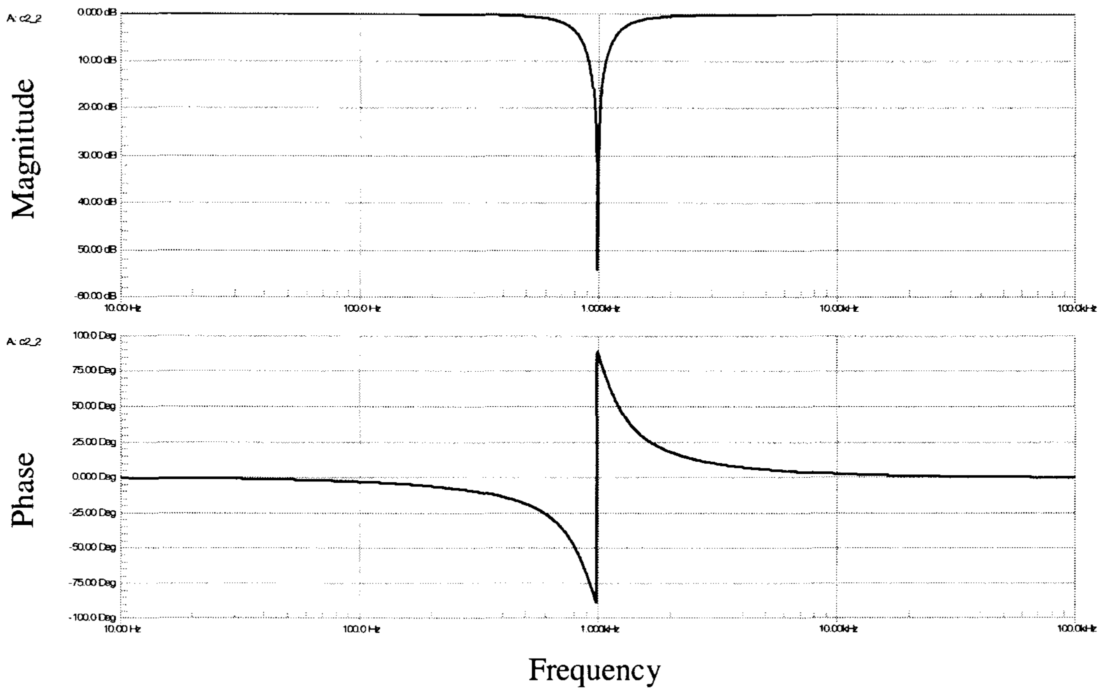

(b)

Figure 12. BS2 filter simulation results, $\omega_0 = 2\Pi \cdot 1000$ rad/sec, Q=2

(a) Schematic diagram and (b) magnitude and phase AC sweep response

notch frequency. Beyond the notch frequency the phase shift eventually returns to 0 degrees.

Simulated frequency responses of AP1 and AP2 filter configurations are shown in Figs. 13-14. The filter gain remains relatively constant across the swept frequency spectrum. The phase response is frequency dependent. As the frequency is swept from low frequency to high frequency, the phase shift steadily decreases from 0 degrees to -360 degrees (or 0 degrees). At undamped natural frequency $\omega_0 \approx 2\Pi \cdot 1000$ rad/sec the phase shift is approximately -180 degrees.

A magnified view of the AP1 and AP2 gain response graphs reveals two anomalies requiring further attention. A slight gain increase in the vicinity of the undamped natural frequency is observed for the AP1 response while a slight gain decrease is observed in the vicinity of the undamped natural frequency for the AP2 response. An ideal AP response is characterized by a perfectly flat magnitude response throughout the frequency spectrum. This is achieved by setting the magnitude of poles in the left hand side of the s-plane equal to the magnitude of zeros located in the right hand side of the s-plane. In addition, the poles and zeros must mirror each other with respect to the $j\omega$ axis of the s-plane.

If the magnitude of the zeros is greater than the magnitude of the poles, or the magnitude of the Q of the zeros is smaller than the Q of the poles - the filter exhibits a slight gain increase or swell in the magnitude response near the undamped natural frequency ω_0. Alternatively, if the magnitude of the zeros is smaller than the magnitude of the poles, or the magnitude of the Q of the zeros is greater than the Q of the poles - the filter exhibits a slight gain decrease or dip in its magnitude response near the undamped

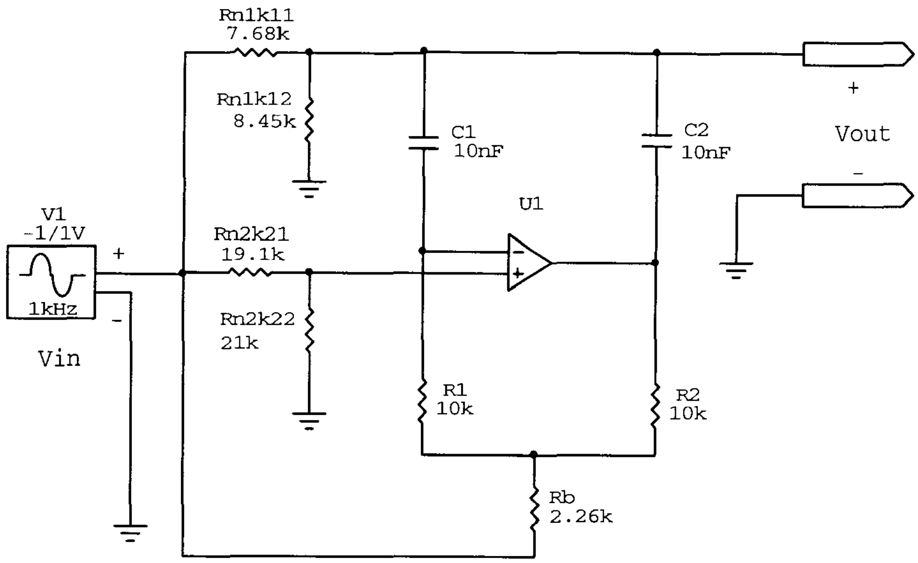

(a)

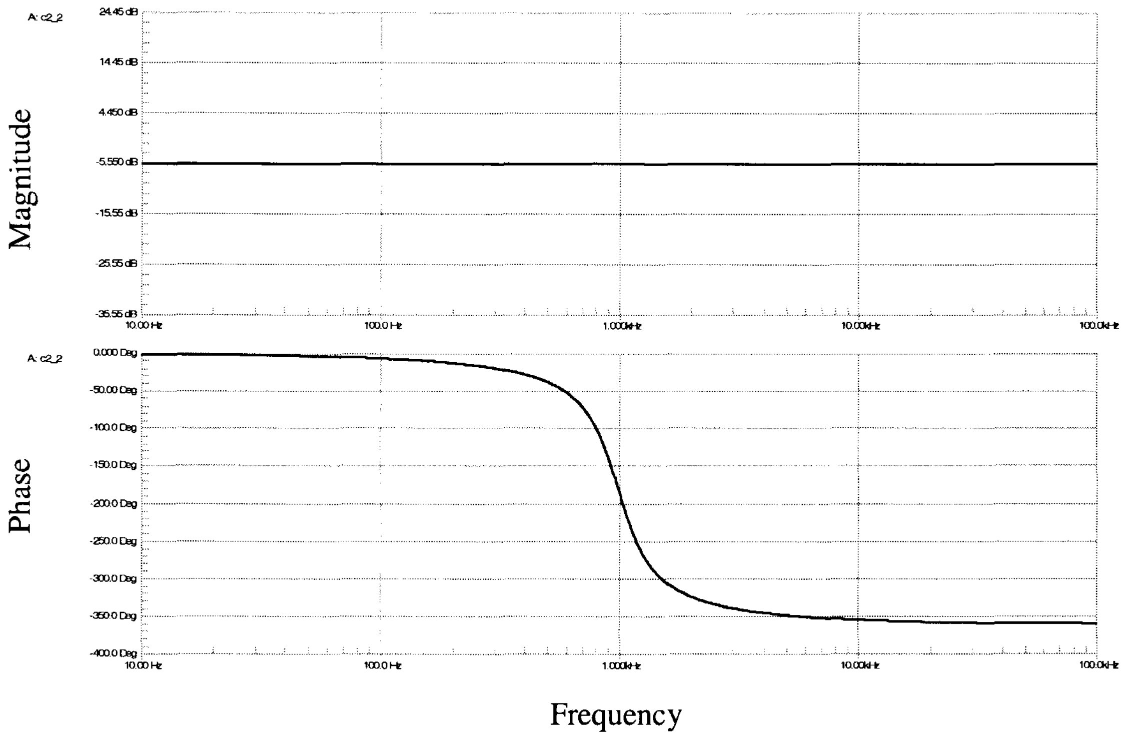

(b)

Figure 13. AP1 filter simulation results, $\omega_0 = 2\Pi \cdot 1000$ rad/sec, Q=2

(a) Schematic diagram and (b) magnitude and phase AC sweep response

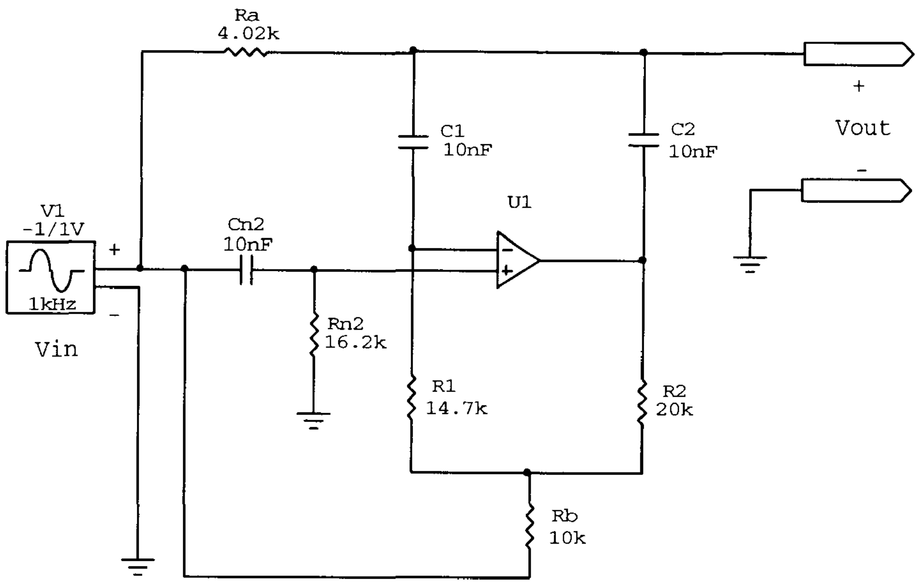

(a)

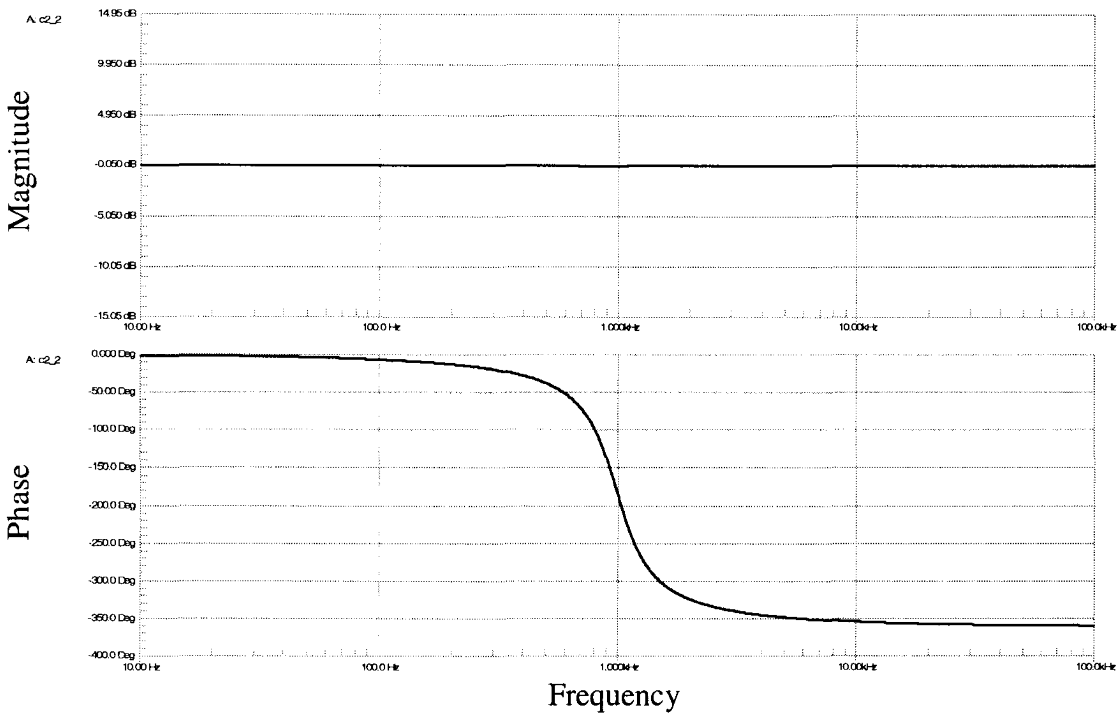

(b)

Figure 14. AP2 filter simulation results, $\omega_0 = 2\Pi \cdot 1000$ rad/sec, Q=2

(a) Schematic diagram and (b) magnitude and phase AC sweep response

natural frequency ω_0. These imperfections in AP magnitude responses, caused by non-ideal pole-zero relationships, result from rounding off calculated resistor values to the nearest standard 1% resistor values and using non-ideal op-amp models in circuit simulations.

CHAPTER X

LABORATORY MEASUREMENTS

Sample designs for the LP, BP1, HP1, BS1, and AP1 filters with undamped natural frequency $\omega_0 = 2\Pi \cdot 1000$ rad/sec and filter quality factor Q=2 are built on a breadboard. Any general-purpose, dual supply op-amp part numbers in DIP-8 package can be used as active elements for the breadboard assembly. In this instance LM741 general-purpose op-amp is selected as a primary amplifier of choice and several other higher performance op-amps are tested during the follow-up investigation and analysis. For passive components leaded resistors and capacitors must be used; smaller tolerance parts are preferred over larger tolerance parts to provide improved accuracy of the filter response and to enable stringent control of the resulting filter parameters. Standard 1% tolerance resistor components and standard 5% tolerance capacitor components are used in construction of all filter configurations.

During the breadboard assembly careful attention is devoted to ensure that all feedback loops are as short as possible. This is achieved by keeping the passive component leads as short as possible and connecting them close to their respective op-amp integrated circuit pins. Due to very high open loop gain of the modern op-amps, both power supply pins of each op-amp integrated circuit are bypassed using capacitors with respect to power supply ground. These high frequency bypass capacitors are placed close to the op-amp power supply pins +V and -V. Bypassing the op-amp power supply pins and maintaining electrically short feedback loops ensures the stability and predictability of the filter's responses and prevents undesired circuit oscillations.

Modern operational amplifiers have a variety of built-in-protection circuitry to protect the devices from overvoltage, overcurrent, and short circuit conditions. Regardless of these protection features some basic rules are followed to protect the op-amps from accidental damage. The filter circuits are always powered up with no input signal present. The input signal is only applied after ensuring the circuits have been properly energized. The input signal is always removed before the filter circuits are powered down. The goal is to prevent the signal presence at the op-amp inputs when respective op-amp is de-energized. This condition can cause a permanent damage to a respective op-amp integrated circuit.

The filters are powered up by Hewlett Packard dual programmable power supply E3630A. The supply is programmed to generate +15V and -15V with current limit set at 50 mA to protect the filter components in case of accidental short circuit conditions.

The network analyzer used to measure the frequency responses is Agilent 4395A. The analyzer is set up for the AC sweep measurement from 10 Hz to 100 kHz. The filter circuits are initially powered up before being connected to the network analyzer. The signal generating and input signal sensing probes of the analyzer are connected at the filter input, while the output signal sensing probe of the analyzer is connected at the filter output. Upon completion of the AC sweep the resulting magnitude and phase responses are viewed on the display, and can be stored on magnetic or flash drive media.

The frequency responses of the LP, BP1, HP1, BS1, and AP1 filters are shown in Figs. 15-19 respectively. The magnitude and phase responses are in overall agreement

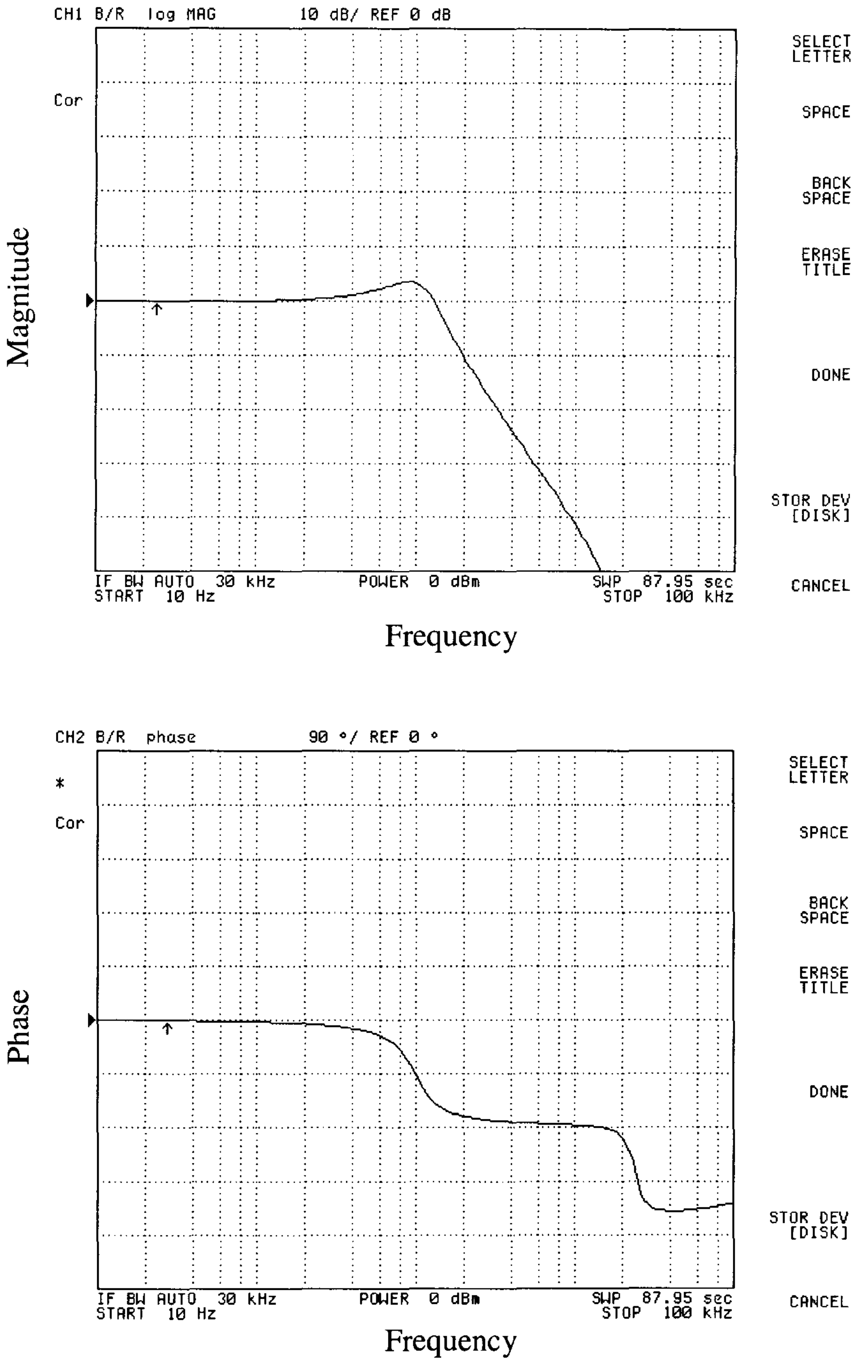

Figure 15. Measured frequency response of the LP filter

Magnitude and phase AC sweep response

with expected responses and simulation results. A few observed anomalies in the magnitude and phase responses are further investigated, analyzed, and discussed.

Regarding measured LP filter phase response shown in Figure 15, there is an additional phase shift of -140 degrees observed at approximately 20 kHz. When the LP filter magnitude response is re-scaled or zoomed out on the network analyzer display, it is apparent that the filter gain stops decreasing beyond approximately 20 kHz and remains relatively unchanged at higher frequencies. This phenomenon is contrary to expected and observed LP filter simulation results. A two step experiment is set up where: (a) LM741 op-amp in the LP filter design is replaced with a higher performance op-amps possessing higher gain bandwidth products, and (b) the resulting LP filter designs are characterized using the network analyzer.

The first part of the experiment involves utilization of the LF353P op-amp possessing a unity gain bandwidth of 3 MHz. LF353P based LP filter response is characterized using the network analyzer. The analysis of resulting LP filter phase response reveals that the observed phase anomaly is shifted to a higher frequency, with additional -140 degree phase shift occurring at 30 kHz. In the LP magnitude response, 30 kHz corresponds to a frequency beyond which the filter gain stops decreasing and remains relatively constant.

The second part of the experiment involves utilization of the MC33078P op-amp having a unity gain bandwidth of 16 MHz. MC33078 based LP filter response is also characterized using the network analyzer. The resulting LP phase response reveals that the phase anomaly is shifted even higher in the frequency spectrum, with additional -140

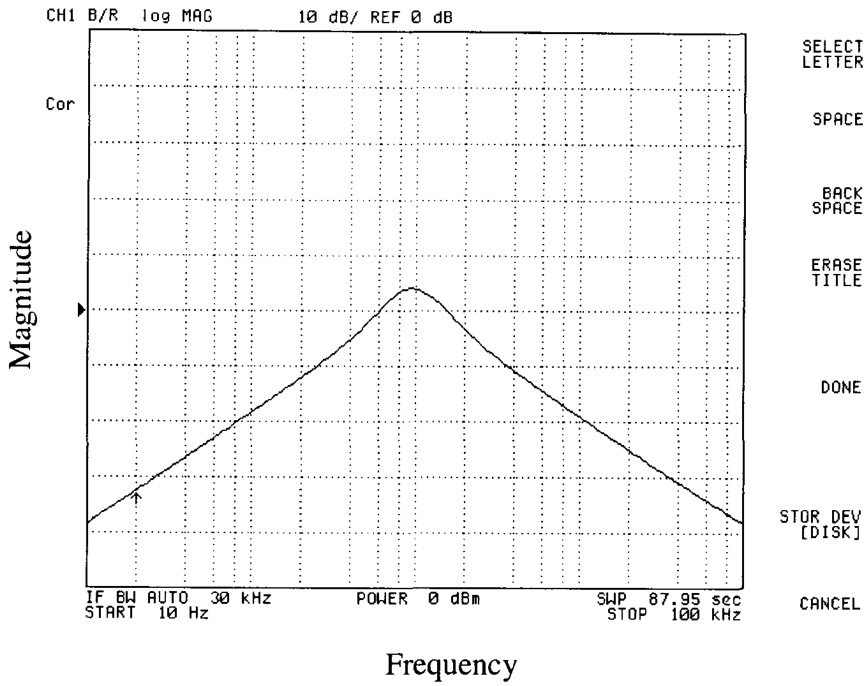

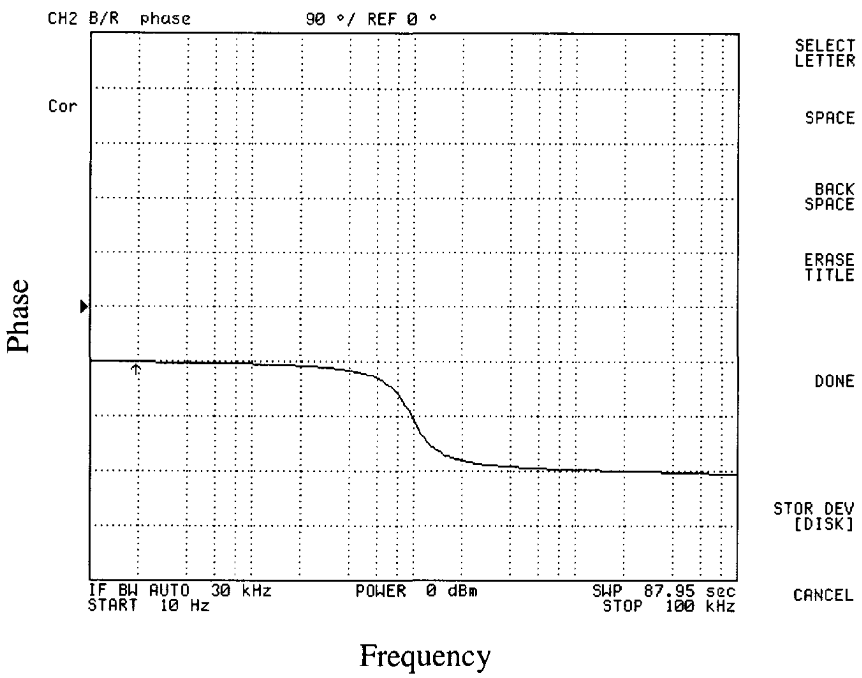

Figure 16. Measured frequency response of the BP1 filter

Magnitude and phase AC sweep response

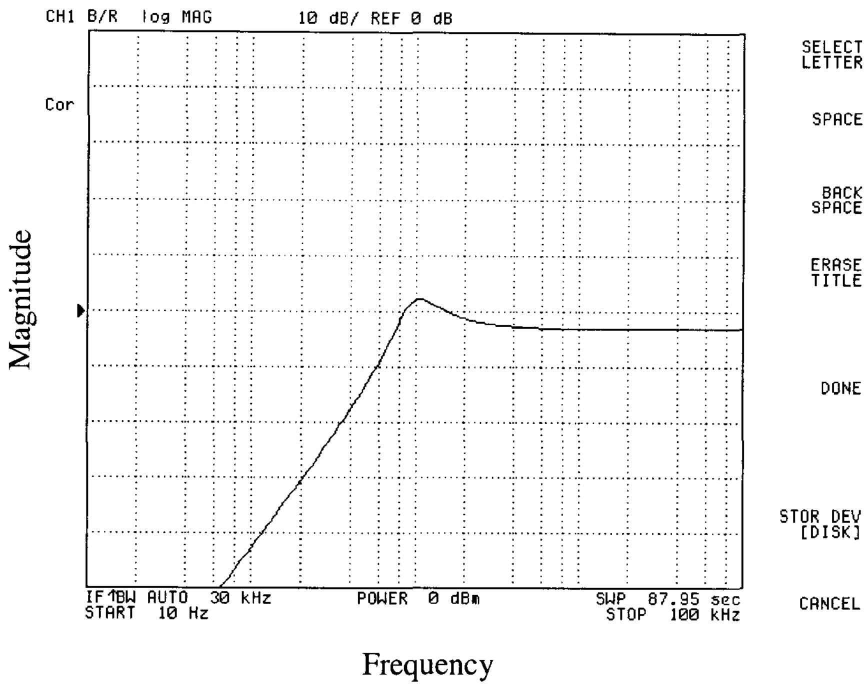

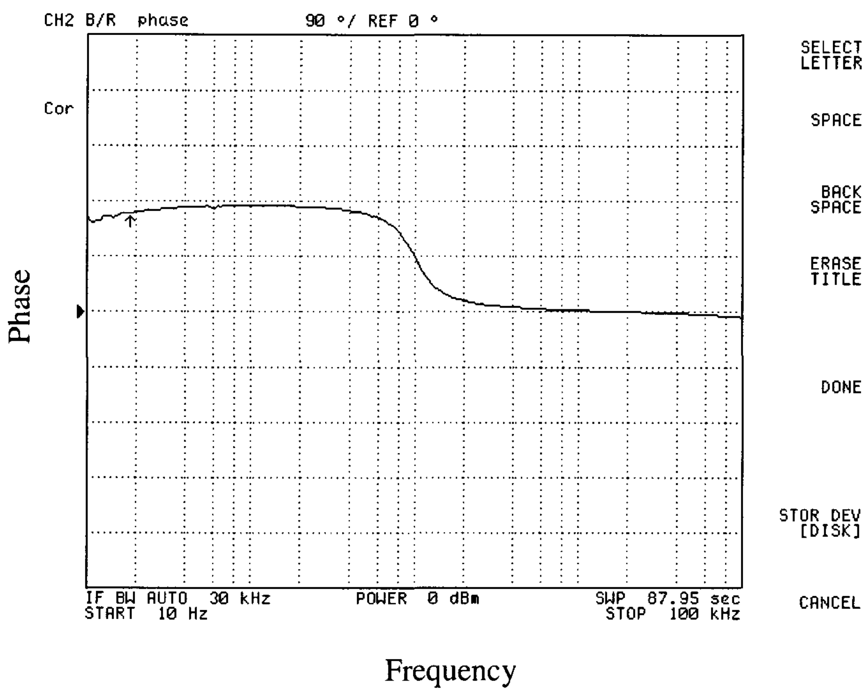

Figure 17. Measured frequency response of the HP1 filter

Magnitude and phase AC sweep response

degree phase shift occurring at 60 kHz. In the LP magnitude response, 60 kHz corresponds to a frequency beyond which the filter gain stops decreasing and remains relatively constant.

From repeated measurement results it is clear that the observed phenomenon is related to the op-amp gain bandwidth product. The larger the gain bandwidth product of the op-amp, the higher is the frequency where the observed gain and phase anomalies occur. The conclusion is that the observed phenomenon is caused by the op-amp inability to maintain the required gain at higher frequencies due to the op-amp gain bandwidth limitations.

For measured HP1 response shown in Figure 17, the phase shift appears to be increasing from +150 degrees to +180 degrees as the input signal frequency is swept from 10 Hz to 40 Hz. This is contrary to expected and simulated results for the HP1 filter showing phase shift remaining relatively unchanged at +180 degrees in this lower part of the frequency spectrum from 10 Hz to 40 Hz. The answer to this phenomenon is related to the test equipment limitation. The network analyzers in general are not very accurate in measuring and calculating the phase shift of very low frequency signals. This problem is compounded if the phase shift measurement includes small magnitude, low frequency signals, as is the case during the HP1 frequency characterization. Thus it is concluded that the observed phase shift anomaly in the HP1 frequency response is caused by the test equipment limitation to accurately measure and calculate the phase shift of small magnitude, low frequency signals.

Regarding the BS1 phase response, it appears that the phase shift does not decrease completely to -90 degrees and then increase completely to +90 degrees in

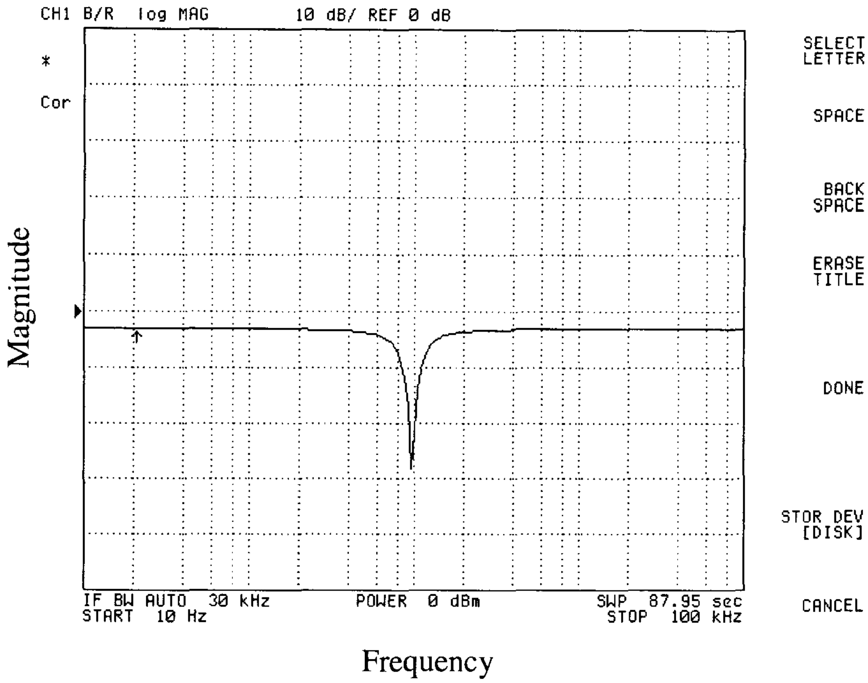

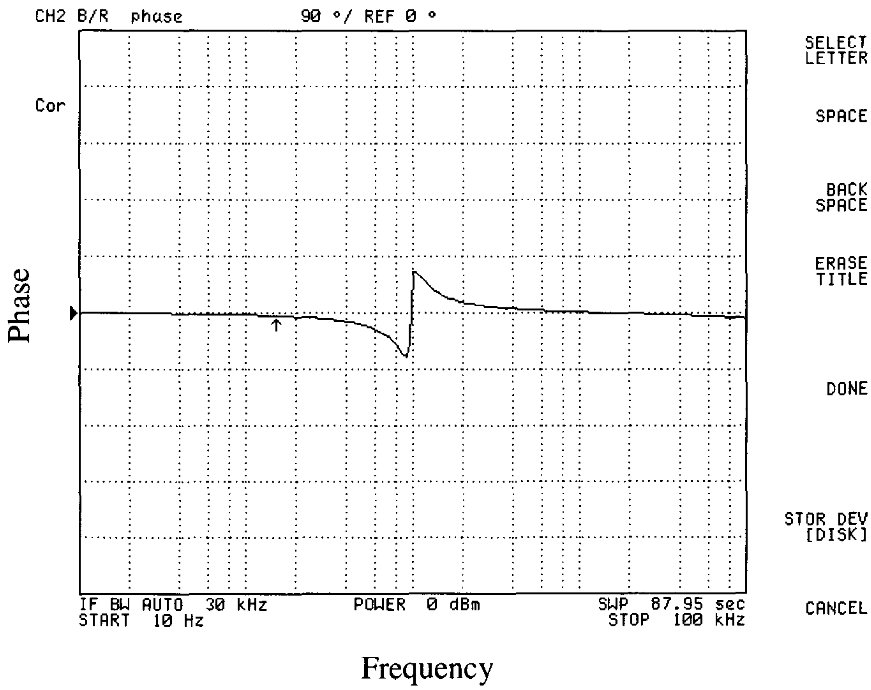

Figure 18. Measured frequency response of the BS1 filter

Magnitude and phase AC sweep response

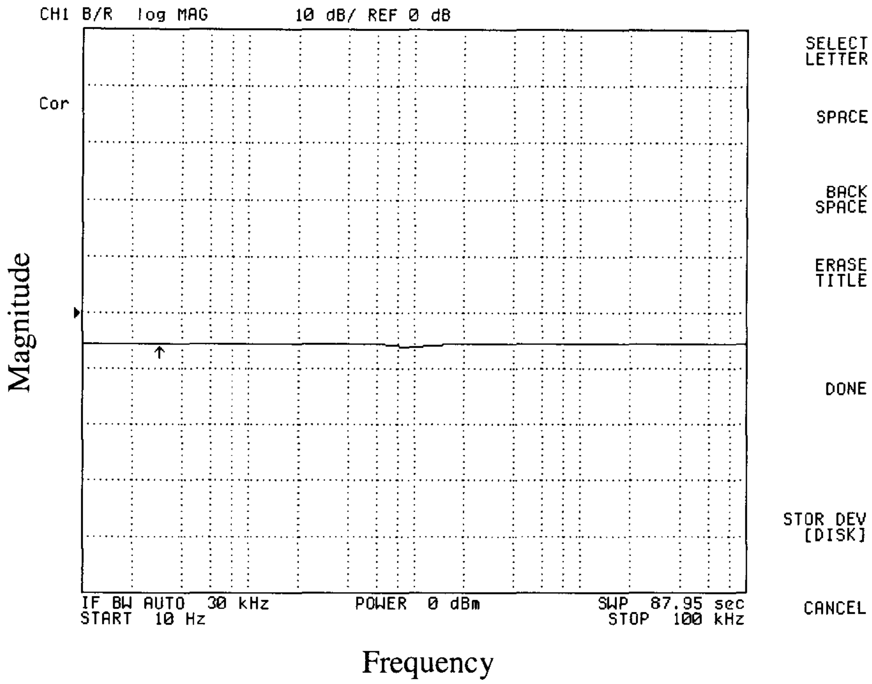

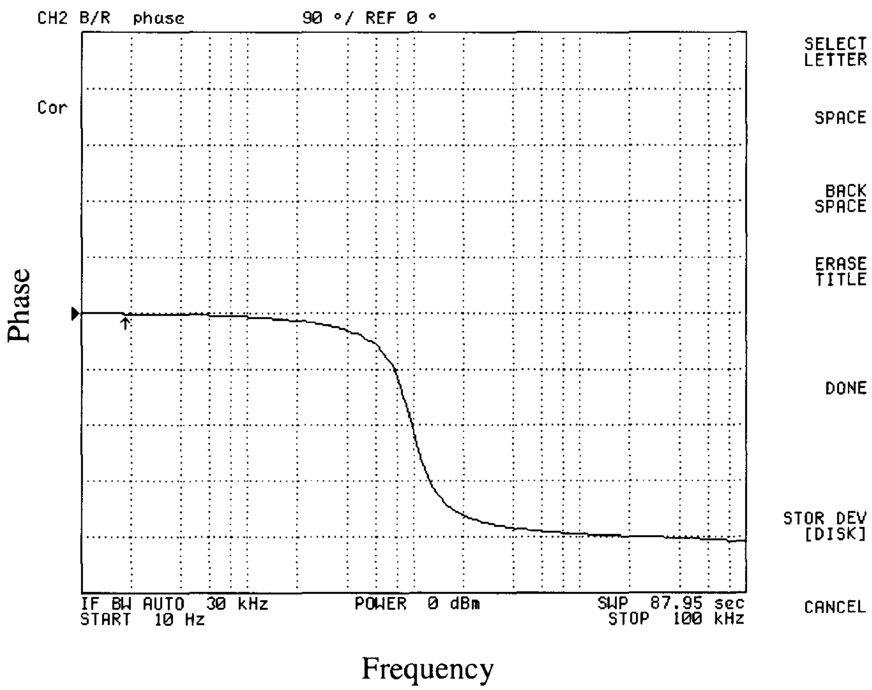

Figure 19. Measured frequency response of the AP1 filter

Magnitude and phase AC sweep response

the vicinity of the undamped natural frequency. The measured phase shift range appears to be limited between -70 and +70 degrees. At undamped natural frequency ω_0 the phase shift does not change instantaneously from one extreme to the other extreme phase shift value yielding a vertical slope in the phase shift response; as it is expected and confirmed by the BS1 filter simulation results. Rather, the measured phase shift response yields a non-vertical sloping line connecting the two extreme phase shift values of -70 and +70 degrees that passes through 0 degree phase shift point at undamped natural frequency ω_0. This phenomenon is characterized by the BS1 function zeros that are not purely imaginary and do not strictly lie on the $j\omega$ axis in the s-plane. These zeros have a small real component as well as dominant imaginary component, thus placing said zeros in the left half side of the s-plane very close to the $j\omega$ axis. The resulting BS1 function yields above-described phase response.

For measured AP1 magnitude response, shown in Figure 19, there is a slight gain decrease or magnitude dip observed near the undamped natural frequency. An ideal AP response is characterized by a perfectly flat magnitude response throughout the frequency spectrum. This is achieved by setting the magnitude of poles in the left hand side of the s-plane equal to the magnitude of zeros located in the right hand side of the s-plane. In addition, the poles and zeros must mirror each other with respect to the $j\omega$ axis of the s-plane. If the magnitude of the zeros is slightly smaller than the magnitude of the poles, or the magnitude of the Q of the zeros is slightly greater than the Q of the poles - the AP filter exhibits a gain decrease or dip in the vicinity of the undamped natural frequency as it is observed in Figure 19. This imperfection in the AP1 magnitude response, caused by non-ideal pole zero relationship, results from rounding off calculated resistor values to the nearest standard 1% resistor values; as well as the assumption of an ideal op-amp model in design equations for calculating passive component values.

CHAPTER XI

UNIVERSAL SECOND ORDER FILTER

The analysis of Figure 2, Table 1, equations (36) and (37) reveals some commonalities across various filter configurations. More specifically:

(1) Figure 2 reveals that the core of proposed circuit design, consisting of C_1, C_2, R_1, R_2, R_B and the op-amp is common and applicable to all filter configurations.

(2) Equations (36) and (37) demonstrate that the components defining the filter's undamped natural frequency ω_0 and quality factor Q are common across all filter configurations.

(3) Comparison of Table 1 entries shows that the differences between various filter configurations are based primarily on:

(a) The selection of input signal application nodes V_A, V_B, V_C, and

(b) The implementation and configuration of networks n_1 and n_2.

Presented similarities and commonalities across various filter configurations raise a question whether it is possible to design a universal second order filter, electronically programmable circuit, capable of re-configuring itself for desired filtering operation. Such circuit would consist of the following functional blocks:

(1) The filter nucleus sub-circuit, containing components C_1, C_2, R_1, R_2, R_B, and an op-amp. The nucleus sub-circuit should remain unchanged for all circuit configurations and selected filtering functions. The component selection of the filter nucleus sub-circuit

should define the undamped natural frequency and the quality factor for all filter configurations realizable by the proposed universal filter design.

(2) Programmable network sub-circuit, consisting of:

(a) Programmable network u_1 and input signal source V_A,

(b) Programmable network u_2 and input signal source V_C, and

(c) Programmable network u_3 and input signal source V_B.

These programmable networks should be fully electronically re-configurable in order to enable the implementation of desired filtering functions.

(3) Control sub-circuit, consisting of required structures of logic gates. This digital sub-circuit should enable the re-configuration of the networks u_1, u_2, and u_3 in response to control logic signals applied at its inputs.

A. Filter Nucleus Sub-circuit

The filter nucleus sub-circuit remains unchanged, as shown in Figure 2. It includes C_1, C_2, R_1, R_2, R_B, and an op-amp. Note that all components defining undamped natural frequency ω_0 and quality factor Q are contained within the filter nucleus sub-circuit, which is an advantage for proposed universal filter design. As this universal filter is re-programmed for different filtering functions, its response parameters (ω_0 and Q) remain unchanged. By carefully constructing the networks u_1, u_2, and u_3, the filter nucleus sub-circuit is able to realize the LP, BP1, HP1, and BS1 filter configurations.

B. Re-configurable Networks u_1, u_2, and u_3

The re-configurable or programmable networks u_1, u_2, and u_3 are realized as resistor networks whose configuration can be set and changed with an addition of electronic programmable switches. To reduce design complexity, the preferred electronic programmable switches should be of single-pole double-throw (SPDT) construction CMOS analog switches, such as MAX394 manufactured by MAXIM Semiconductors. The SPDT CMOS programmable switches operate as follows:

(a) The presence of logic LO (or logic "0") at the control input causes normally-closed (NC) and common (COM) terminals to be tied together.

(b) The presence of logic HI (or logic "1") at the control input causes normally-open (NO) and common (COM) terminals to be tied together.

The single-pole single-throw (SPST) type CMOS analog switches can be used as well, but the given design then requires twice as many SPST switches as compared to SPDT switches. An SPDT switch can be realized by using an inverter and two SPST switches. One terminal of each SPST switch must be tied together, forming a common (COM) terminal of the SPDT switch. The remaining two terminals constitute the normally-open (NO) and normally-closed (NC) terminals of the SPDT switch. The control signal for one SPST switch is an inverted version of the control signal for the other SPST switch, ensuring the closure of only one SPST switch at any given time. Either the normally-open (NO) terminal or normally-closed (NC) terminal, but not both, can be tied to the common (COM) terminal of such improvised SPDT switch.

Figure 20 shows the circuit configuration for network u_1. It consists of signal source V_A, the resistors R_A / k_1 and $R_A /(1-k_1)$, and the CMOS analog SPDT switches

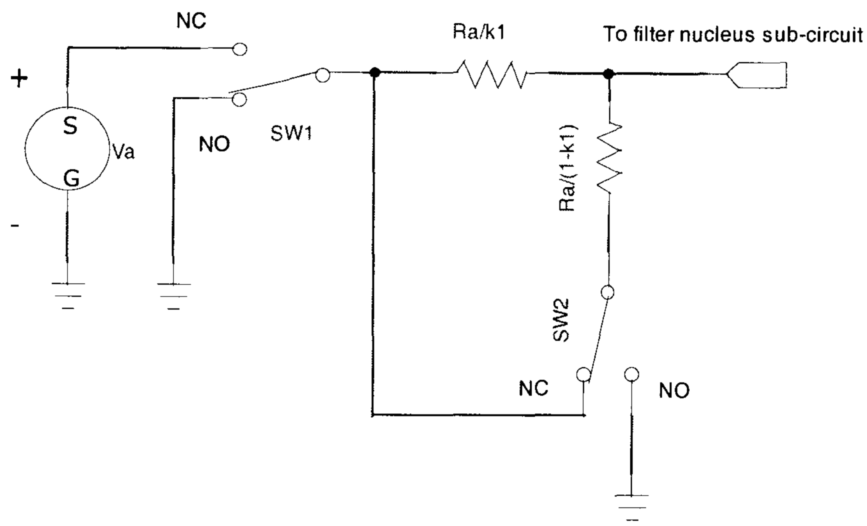

(a)

Filter Type	SW1 (active contacts)	SW2 (active contacts)
LP	NO	NC
BP1	NC	NC
HP1	NC	NC
BS1	NO	NO

(b)

Figure 20. Re-configurable network u_1

(a) Schematic diagram with switch states shown in default LP configuration,

(b) Required switch states necessary to realize different filter transfer functions.

SW1 and SW2. By placing the CMOS analog switches SW1 and SW2 in a specific state, it is possible to re-configure network u_1 to be:

(a) Equivalent to resistor R_A, with the transfer function $k_1 = 1$, connected to source V_A (for LP configuration).

(b) Equivalent to resistor R_A, disconnected from source V_A, and grounded (for the BP1 and HP1 configurations).

(c) Equivalent to a voltage divider network consisting of resistors R_A / k_1 and $R_A /(1 - k_1)$, with the transfer function $k_1 < 1$, connected to source V_A (for BS1 configuration).

Figure 21 shows the circuit configuration for network u_2. It consists of signal source V_C, the resistors R_{n2} / k_2 and $R_{n2} /(1 - k_2)$, and the CMOS analog SPDT switch SW3. By placing the CMOS analog switch SW3 in a specific state, it is possible to re-configure network u_2 to be:

(a) Equivalent to resistor R_{n2}, disconnected from source V_C, and grounded (for the LP and BP1 configurations).

(b) Equivalent to a voltage divider network consisting of the resistors R_{n2} / k_2 and $R_{n2} /(1 - k_2)$, with the transfer function $k_2 < 1$, connected to source V_C (for the HP1 and BS1 configurations).

Figure 22 shows the circuit configuration for network u_3. It consists of signal source V_B, resistor R_B, and the CMOS analog SPDT switch SW4. By placing the CMOS analog switch SW4 in a specific state, it is possible to re-configure network u_3 to be:

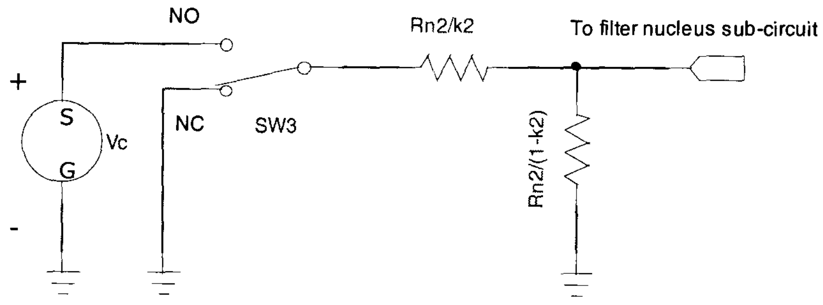

(a)

Filter Type	SW3 (active contacts)
LP	NC
BP1	NC
HP1	NO
BS1	NO

(b)

Figure 21. Re-configurable network u_2

(a) Schematic diagram with switch states shown in default LP configuration,

(b) Required switch states necessary to realize different filter transfer functions.

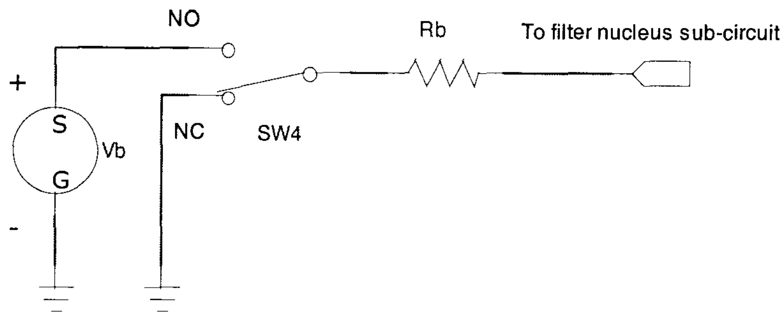

(a)

Filter Type	SW4 (active contacts)
LP	NC
BP1	NO
HP1	NO
BS1	NO

(b)

Figure 22. Re-configurable network u_3

(a) Schematic diagram with switch states shown in default LP configuration,

(b) Required switch states necessary to realize different filter transfer functions.

(a) Equivalent to resistor R_B, disconnected from source V_B, and grounded (for LP configuration).

(b) Equivalent to resistor R_B, and connected to source V_B (for the BP1, HP1, and BS1 configurations).

C. Control Sub-circuit

The control sub-circuit is a digital circuit, designed as a structure of logic gates. As stated previously, the control sub-circuit should enable the re-configuration of the networks u_1, u_2, and u_3, in response to control logic signals applied at its inputs. The goal of the control sub-circuit design is to be as simple as possible to maximize reliability, minimize the hardware complexity, maximize operational simplicity, and minimize required board or chip space. The simplicity is achieved by minimizing the number of required input and output control signals.

The control sub-circuit must be able to re-configure the universal second order filter into four unique configurations, corresponding to the LP, BP1, HP1, and BS1 filter configurations. Therefore the control sub-circuit must be able to resolve and distinguish between four unique commands applied at its inputs. Translating this requirement into binary number system, it yields that two input signal lines are required for the control sub-circuit to distinguish between four unique states. The unique states are defined as follows: 00, 01, 10, and 11.

The control sub-circuit must be able to control four different CMOS analog switches, named SW1, SW2, SW3, and SW4. The operation of these switches is independent from one another, and no two switches are to be controlled by the same circuit. Therefore the control sub-circuit must have four separate output lines, controlling four independent switches.

The next step is the development of the switch state tables and the truth tables for the control sub-circuit, based on the control sub-circuit requirements. Both tables presented aid in logic function definition, gate selection, and gate arrangement. To summarize, the control sub-circuit requires two input signal lines and four output control lines. Table 11 shows the switch states table, while Table 12 shows the equivalent logic truth table. For both tables column 1 lists specific filter configurations, while column 2 lists the corresponding input signals associated with each filter configuration. The remaining columns show either the switch states, or equivalent logic states associated with specific switch states. Note that four unique input commands have been assigned to four specific filter configurations.

The simplest way to design the control sub-circuit is to design a separate gate structure to control each CMOS analog switch. This breaks down the truth table shown in Table 11 into four smaller truth tables for each of the four gate structures. Each gate structure has two inputs (for command signal), and a single output (for switch control). Overall the control sub-circuit consists of four gate structures, each having an independent output line and sharing common input lines.

Figure 23 shows the gate structure for controlling the switch SW1 with corresponding truth table. The circuit was developed using Boolean algebra, by re-writing the truth table as the sum of products (sum of minterms). The resulting circuit consists of two NOT gates, two AND gates and a single OR gate. Presented truth table is

Table 11. Input Signals and Switch States for Control Sub-circuit

Filter type	Input signal	SW1 (active contacts)	SW2 (active contacts)	SW3 (active contacts)	SW4 (active contacts)
LP	00	NO	NC	NC	NC
BP1	01	NC	NC	NC	NO
HP1	10	NC	NC	NO	NO
BP1	11	NO	NO	NO	NO

Table 12. Input Signals and Switch Control Signals for Control Sub-circuit

Filter type	Input signal	SW1 control signal	SW2 control signal	SW3 control signal	SW4 control signal
LP	00	1	0	0	0
BP1	01	0	0	0	1
HP1	10	0	0	1	1
BP1	11	1	1	1	1

also recognized as equivalent to XNOR logic function, so proposed gate structure can be replaced with a single XNOR gate.

Figure 24 shows the gate structure for controlling the switch SW2. The presented truth table is recognized as the logic AND function, thus the resulting circuit consists of one AND gate.

Figure 25 shows the gate structure for controlling the switch SW3. As in the case of SW1 gate controlling structure, the circuit was developed by re-writing the truth table as the sum of products (or sum of minterms). The resulting circuit consists of one NOT gate, two AND gates, and one OR gate.

Figure 26 shows the gate structure for controlling the switch SW4. The presented truth table is recognized as equivalent to the logic OR function, thus the resulting circuit consists of one OR gate.

D. Universal Second Order Filter Simulations

Circuit Maker 2000 circuit simulation software is used to capture the universal filter schematics and draw the frequency response curves for each of the filter configurations. Other SPICE-based circuit simulation software packages could also be used to accomplish the same task. The filter parameters have been carried over from previous sections, resulting in universal 2^{nd} order filter design having the undamped natural frequency $\omega_0 = 2\Pi \cdot 1000$ rad/sec and the quality factor Q=2.

The schematic diagrams of universal filter configurations are captured and created. Careful attention is devoted to appropriate SPICE model selection and

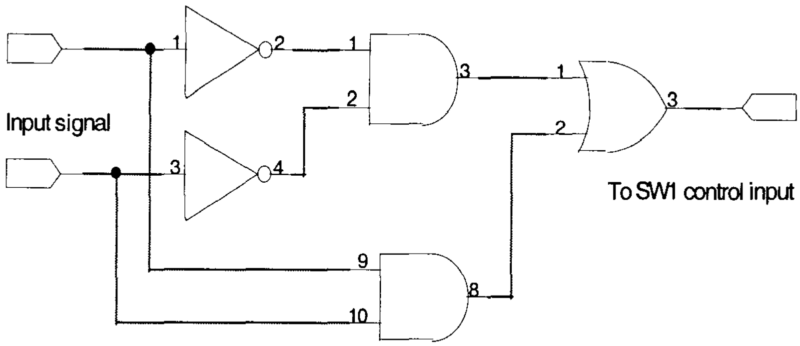

(a)

Filter Type	Input Signal	SW1 control input
LP	00	1
BP1	01	0
HP1	10	0
BS1	11	1

(b)

Figure 23. Control sub-circuit for SW1

(a) Schematic diagram,

(b) Truth table.

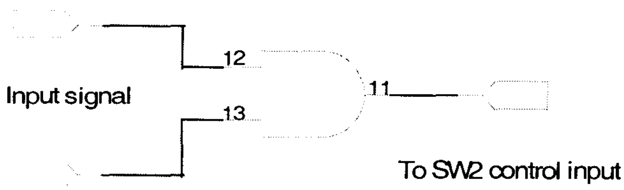

(a)

Filter Type	Input Signal	SW2 control input
LP	00	0
BP1	01	0
HP1	10	0
BS1	11	1

(b)

Figure 24. Control sub-circuit for SW2

(a) Schematic diagram,

(b) Truth table.

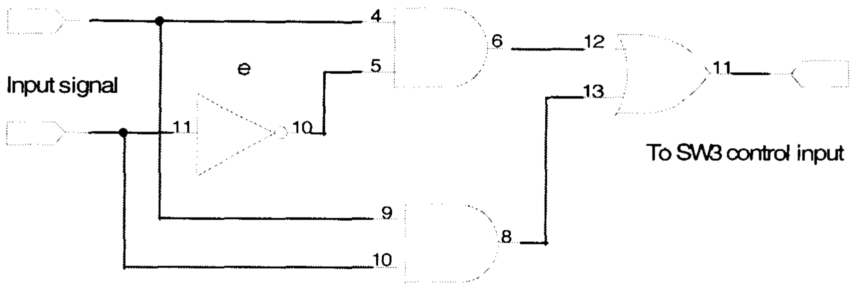

(a)

Filter Type	Input Signal	SW3 control input
LP	00	0
BP1	01	0
HP1	10	1
BS1	11	1

(b)

Figure 25. Control sub-circuit for SW3

(a) Schematic diagram,

(b) Truth table.

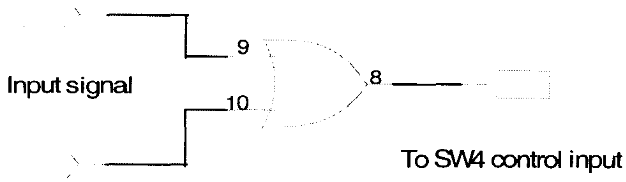

(a)

Filter Type	Input Signal	SW4 control input
LP	00	0
BP1	01	1
HP1	10	1
BS1	11	1

(b)

Figure 26. Control sub-circuit for SW4

(a) Schematic diagram,

(b) Truth table.

implementation. For the input signal source, the implementation of VAC source enables the AC sweep analysis. For the filter nucleus circuit, a general-purpose op-amp model is applied. Each CMOS analog SPDT switch is implemented by using two CMOS analog SPST switches, since the SPICE model of SPDT analog switch is not available within Circuit Maker 2000 simulation software. The SPDT switches have been constructed by tying in series two SPST switches, so that a common node forms common (COM) terminal of the SPDT switch. The remaining two terminals constitute normally open (NO) and normally closed (NC) terminals of the SPDT switch. The addition of a NOT gate at the control signal input for one SPST switch ensures that the control signals at both SPST switches are an inverted logic version of each other, resulting in closure of only one SPST switch at any given time.

Upon capturing and re-creating the schematic diagrams, it is recommended to perform the DC operating point analysis and transient analysis as additional tests to confirm design validity and circuit integrity. Following design confirmation enable the AC sweep analysis; set start sweep frequency at 10 Hz and stop sweep frequency at 100 kHz. Set the horizontal or frequency axis to logarithmic scale. Set the magnitude vertical axis for decibel scale, and the phase vertical axis for degree scale. For maximum resolution select either the largest number of evaluation points, or the smallest step size (whichever is applicable). Note that the filter undamped natural frequency ($\omega_0 = 2\Pi \cdot 1000$ rad/sec) is placed in the middle of selected AC sweep range. This is done to allow the observation and analysis of the filter responses in both the pass band and the stop band. The results of the AC sweep analysis are presented in Figures 27-30.

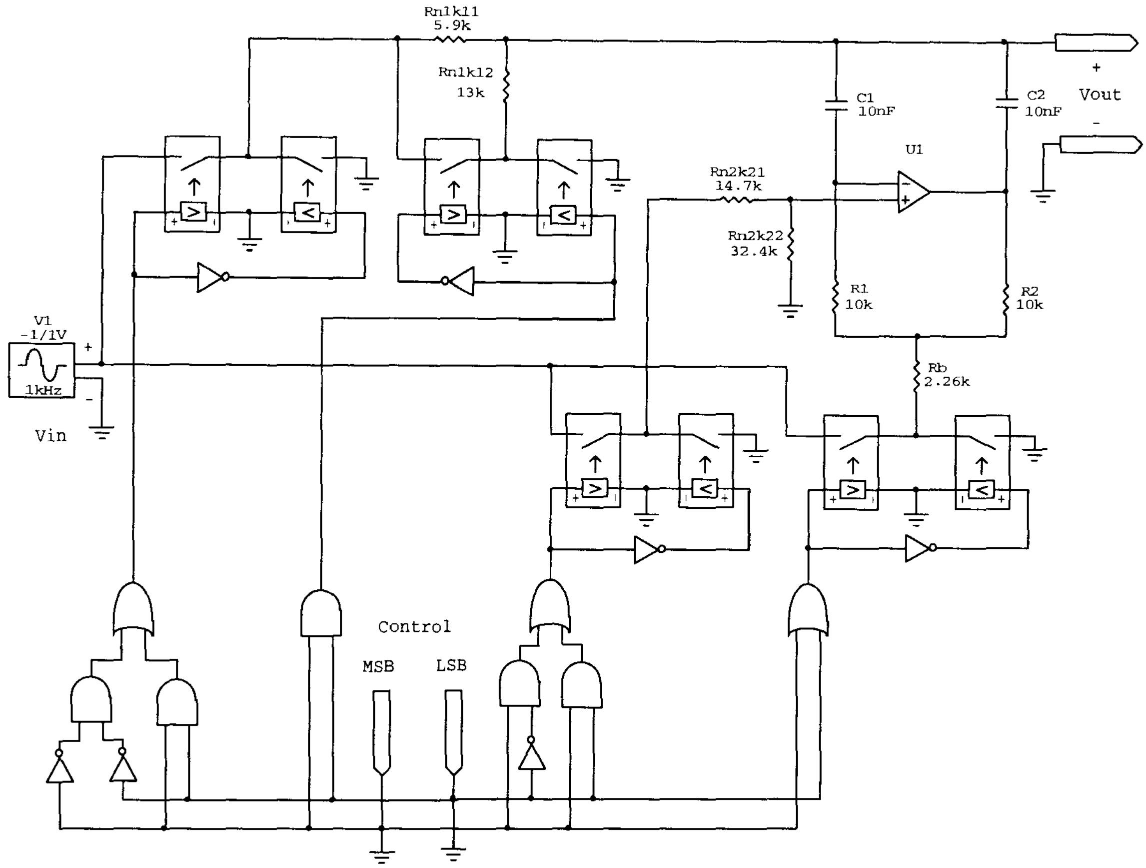

(a)

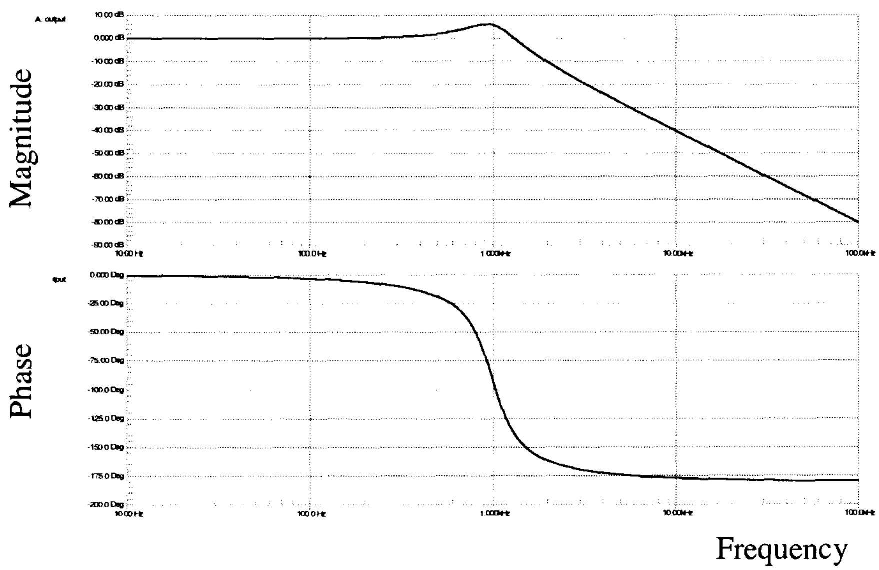

(b)

Figure 27. Universal filter set for LP configuration, $\omega_0 = 2\Pi \cdot 1000$ rad/sec, Q=2

(a) Schematic diagram, and (b) frequency response.

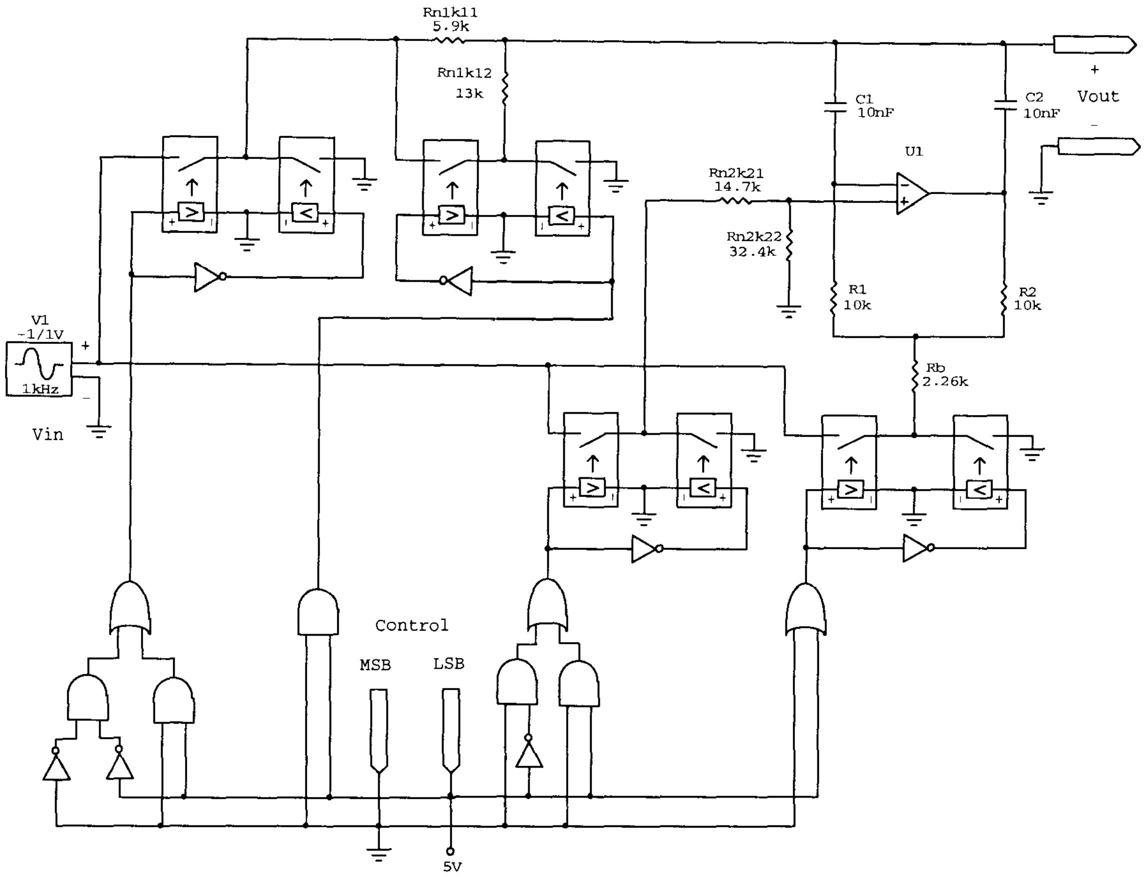

(a)

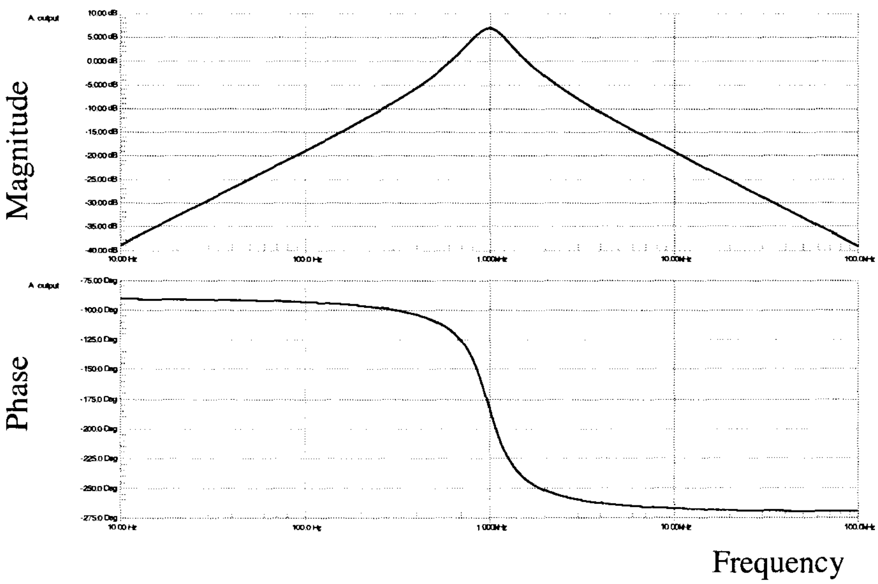

(b)

Figure 28. Universal filter set for BP1 configuration, $\omega_0 = 2\Pi \cdot 1000$ rad/sec, Q=2

(a) Schematic diagram, and (b) frequency response.

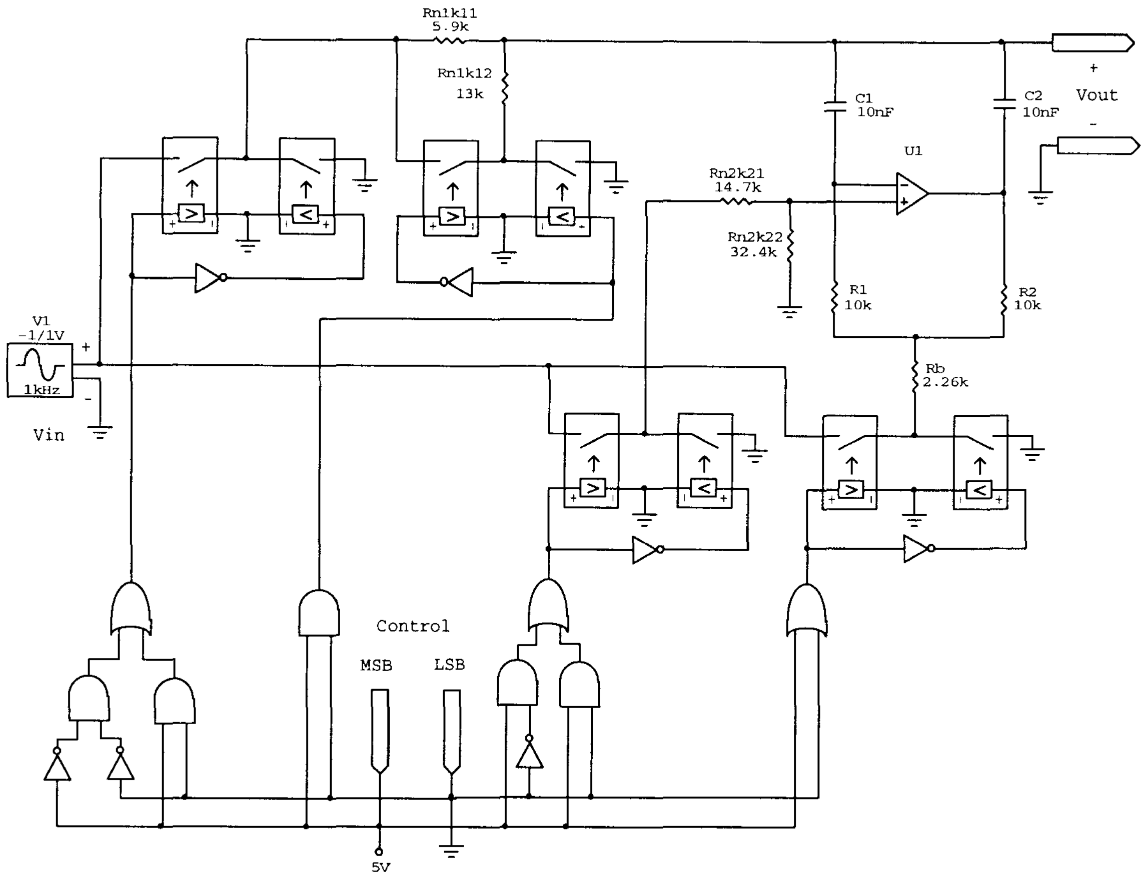

(a)

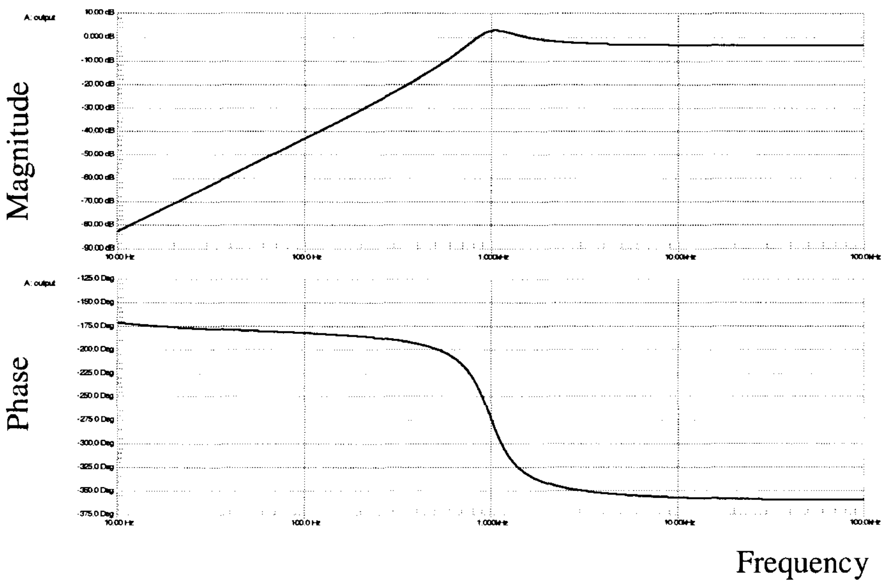

(b)

Figure 29. Universal filter set for HP1 configuration, $\omega_0 = 2\Pi \cdot 1000$ rad/sec, Q=2

(a) Schematic diagram, and (b) frequency response.

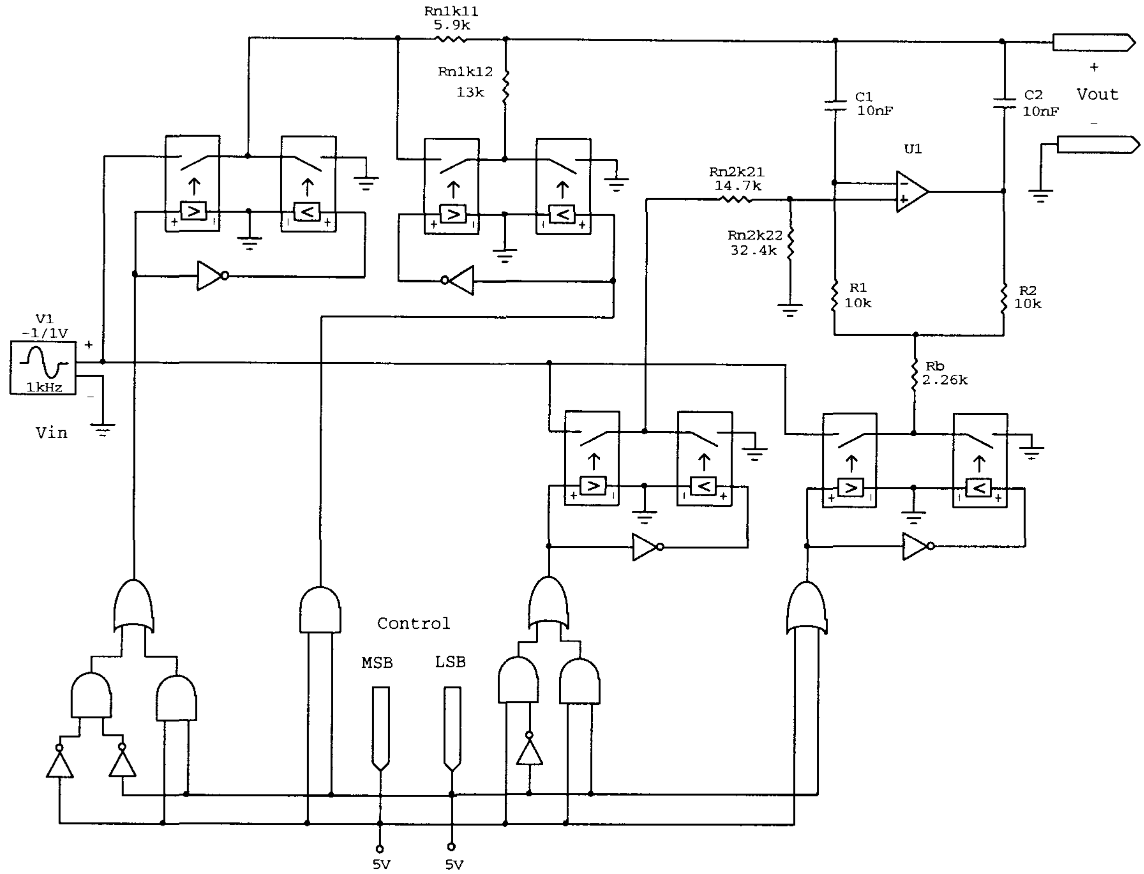

(a)

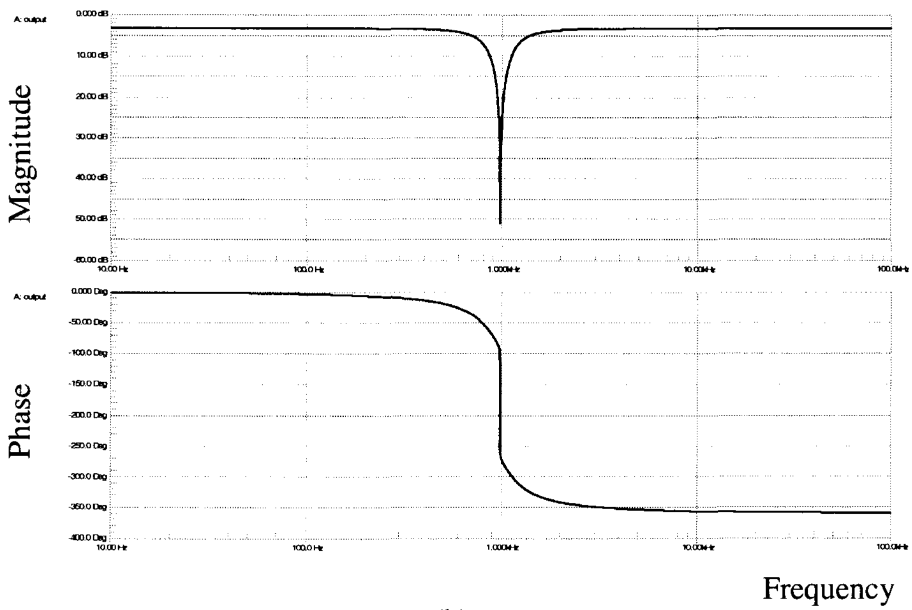

(b)

Figure 30. Universal filter set for BS1 configuration, $\omega_0 = 2\Pi \cdot 1000$ rad/sec, Q=2

(a) Schematic diagram, and (b) frequency response.

For each filter configuration the schematic diagram is shown together with resulting Bode plot.

Simulated magnitude and phase responses for each filter configuration of programmable universal second order filter are coincident to respective magnitude and phase responses of individual filter sections, shown in Figs. 6, 7, 9, and 11. More specifically:

(a) The universal filter set for the LP function shown in Figure 27 yields an equivalent response as the LP filter section shown in Fig 6.

(b) The universal filter set for the BP function shown in Figure 28 yields an equivalent response as the BP1 filter section shown in Figure 9.

(c) The universal filter set for the HP function shown in Figure 29 yields an equivalent response as the HP1 filter section shown in Figure 7.

(d) The universal filter set for the BS function shown in Figure 30 yields an equivalent response as the BS1 filter section shown in Figure 11.

CHAPTER XII

HIGHER ORDER FILTERS

The discussion so far has been primarily focused on the design and the analysis of the second order filters using a single op-amp. The given filter configuration can be cascaded with other common RC op-amp filter configurations in order to achieve higher order filters. A general transfer function of the original circuit configuration shown in Figure 2 is developed and analyzed in order to understand the feasibility of cascading multiple filter stages to achieve higher order filters. The general transfer function of the original second order circuit configuration is given below:

$$
\begin{aligned}
V_O(s) &= V_A \frac{k_1}{s^2 R_A R_K C_2 C_1 + sR_A(C_1 + C_2) + 1} \\
&- V_B \frac{sR_A C_2 \beta}{s^2 R_A R_K C_2 C_1 + sR_A(C_1 + C_2) + 1} \\
&+ V_C \frac{G_2(s)[s^2 R_A R_K C_1 C_2 + sR_A(C_1 + C_2 k_0)]}{s^2 R_A R_K C_2 C_1 + sR_A(C_1 + C_2) + 1}
\end{aligned} \tag{82}
$$

where the signal sources are defined as the V_A, V_B, and V_C; k_1 is the transfer function of purely resistive network n_1, and $G_2(s)$ is the transfer function of network n_2. The remaining variables and components were previously defined and discussed. The denominator expression is recognized as a form of characteristic second order polynomial defined in (35) as:

$$D(s) = s^2 R_A R_K C_2 C_1 + sR_A(C_1 + C_2) + 1 \tag{83}$$

Thus the general transfer function simplifies to:

$$V_O(s) = V_A \frac{k_1}{D(s)} - V_B \frac{sR_A C_2 \beta}{D(s)} + V_C \frac{G_2(s)[s^2 R_A R_K C_1 C_2 + sR_A(C_1 + C_2 k_0)]}{D(s)} \quad (84)$$

Figure 31 shows the original circuit configuration with labeled filter expansion nodes. Note that the BP-EXP node is identified as an optimum band pass filter expansion node, while the HP-EXP node is identified as an optimum high pass filter expansion node. Three design goals are followed:

(1) Maintain the circuit simplicity by using the smallest number of passive components and operational amplifiers,

(2) Minimize the "loading effect" between multiple filter stages, and

(3) Retain the benefit of not having undesired DC offset signals present at the filter's output.

The first design requirement is satisfied by applying well-known and developed filter configurations, such as Sallen and Key filter configurations. They enable an implementation of the second order filters requiring only one op-amp and a simple RC network.

The second design requirement arises as a consequence of cascading multiple filter stages, where the challenge resides in minimizing the loading effect between the stages. Each filter stage must be able to drive the subsequent filter stage without the signal loss caused by input impedance of the driven stage "loading" the output node of the driving stage. Minimizing this "loading effect" is achieved by ensuring that each filter stage has its input impedance as high as possible and its output impedance as low as possible. The application of Sallen and Key filter configurations is desirable in this case

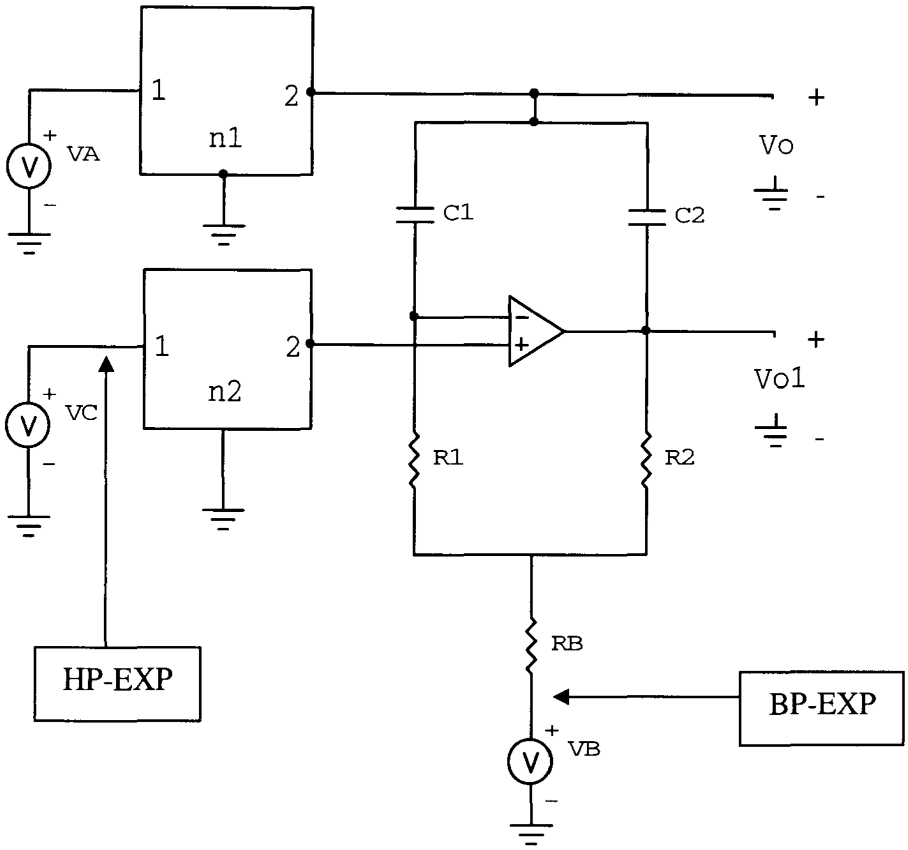

Figure 31. Optimum expansion nodes for BP and HP expansion

as well, since the output node of each Sallen and Key filter configuration is coincident with the op-amp output node used in respective design. This ensures low output impedance and high driving capability of Sallen and Key filter configurations.

The third design requirement is achieved by retaining the original second order filter configuration as the last stage in proposed cascaded configuration for higher order filters. Since the output node of the original second order filter configuration is capacitively coupled to the output node of the op-amp used in the design, undesired DC offset signals are blocked and do not appear at the filter's output. A major advantage of the original second order filter configuration is thus preserved.

A. BP Filter Expansion

The BP-EXP node is identified as the optimum node for the BP filter expansion, as shown in Figure 31. To achieve the BP1 filter expansion from second order to higher order:

(1) Design the original BP1 second order filter circuit according to set specifications.

(2) Design an additional BP filter section (or sections) according to set specifications.

(3) Identify the BP-EXP node on the original BP1 filter configuration.

(4) Temporarily disconnect input signal source V_{in} from the original BP1 filter circuit.

(5) Connect an additional BP filter section(s) to the original BP1 filter circuit such that the output of added BP section(s) is connected at the BP-EXP node of the original BP1 filter circuit, as shown in Figure 32.

(6) Re-connect input signal source V_{in} at input node of added BP filter section(s).

(7) The BP filtered signal of higher order appears at the output of the original BP1 filter circuit.

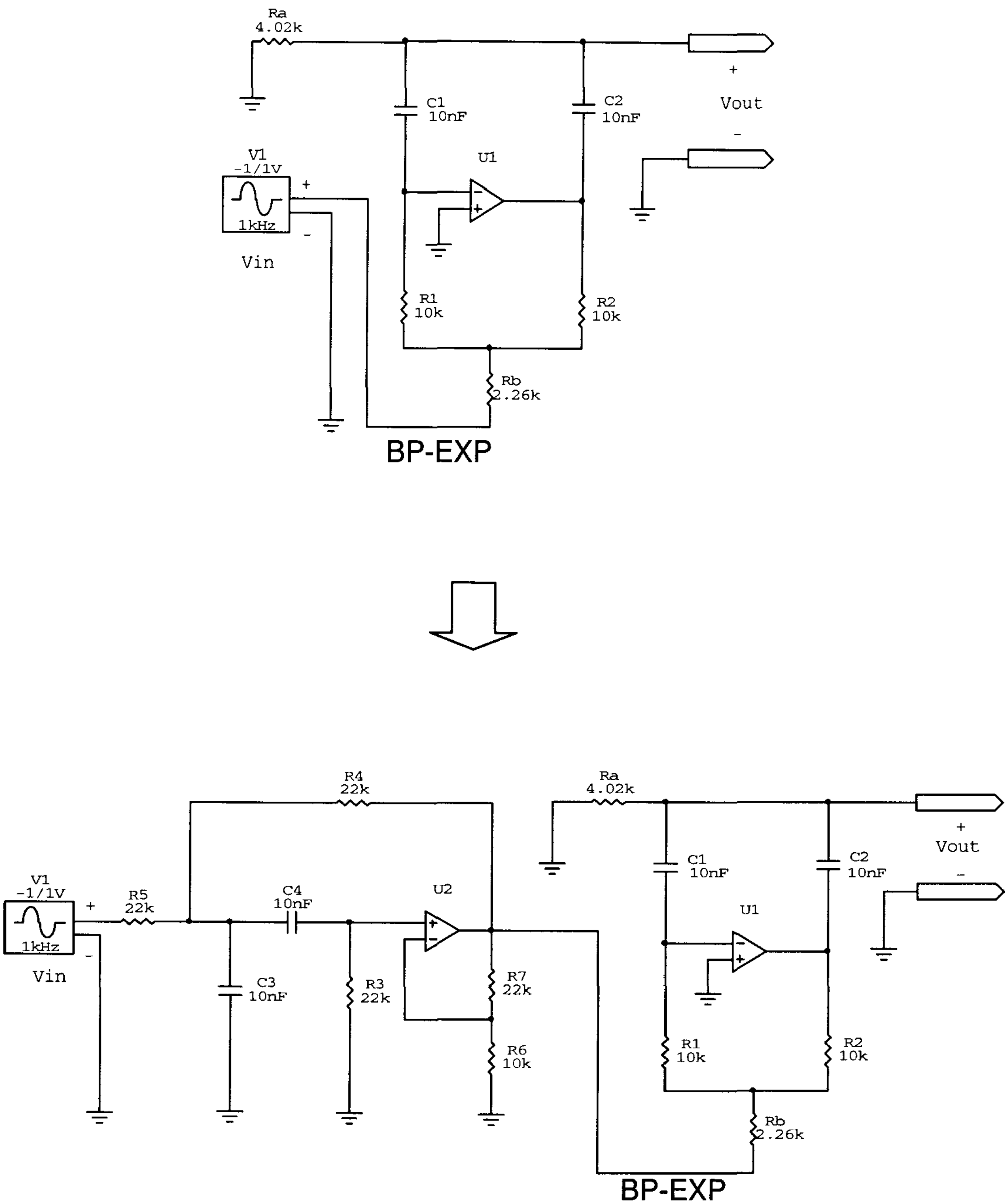

Figure 32. BP1 filter expansion from second order to fourth order BP filter

For example, designing a fourth order BP filter involves an addition of a second order BP filter stage to the original second order BP1 filter circuit as described above. The characteristic transfer function of such fourth order BP filter is given below:

$$\frac{V_{out}}{V_{in}} = \frac{H\left(\frac{\omega_{01}}{Q_1}\right)\left(\frac{\omega_{02}}{Q_2}\right)s^2}{\left[s^2 + \left(\frac{\omega_{01}}{Q_1}\right)s + \omega_{01}^2\right]\cdot\left[s^2 + \left(\frac{\omega_{02}}{Q_2}\right)s + \omega_{02}^2\right]} \tag{85}$$

An example circuit of the fourth order BP filter with its frequency response is shown in Figure 33. The designed fourth order BP filter consists of the original second order BP1 filter circuit and the second order Sallen and Key BP filter. Both filter sections are designed with undamped natural frequency $\omega_0 = 2\cdot\Pi\cdot 1000$ rad/sec and quality factor Q=2, yielding superimposing pole locations. The output node of added second order Sallen and Key BP section is connected to the BP-EXP node of the original second order BP1 filter circuit. Since input impedance of the BP1 circuit at node BP-EXP is not very high, it is imperative that the added expansion stage has very low output impedance and high driving capability; a requirement satisfied by Sallen and Key BP filter section. Input signal is applied at the input of added Sallen and Key BP section; filtered signal is taken at V_{out} node of the original second order BP1 filter circuit. The resulting cascaded circuit has a fourth order BP filter response, as shown in Figure 33.

A fourth order BP filter yields different magnitude and phase response, as compared to a second order BP filter. The rate of gain increase and decrease in magnitude response, as well as the overall value of phase shift are twice as large for the fourth order BP filter as compared to the second order BP filter. From low frequency to undamped natural frequency ω_0 the gain increases at the rate of 40 dB/dec. Beyond

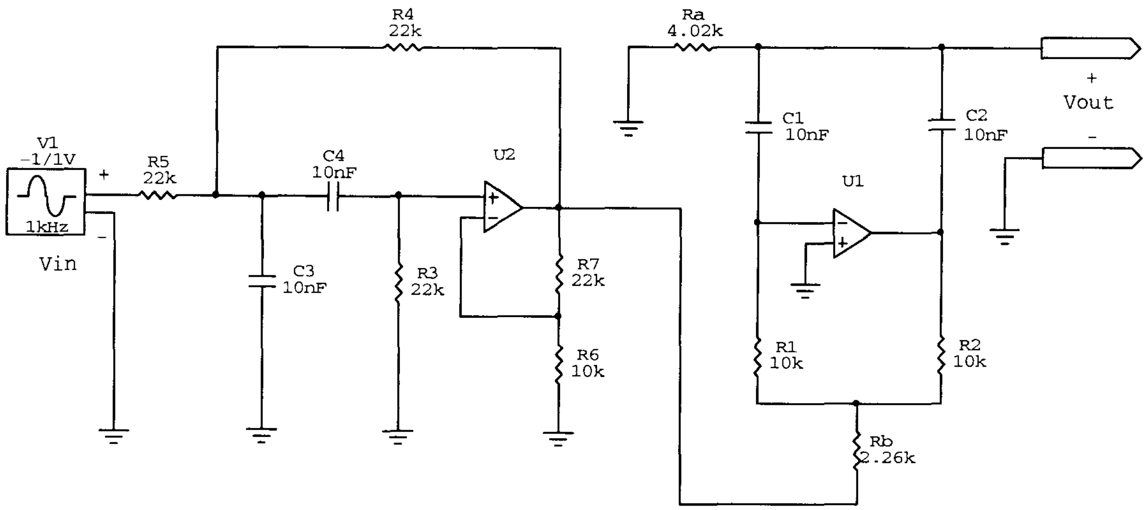

(a)

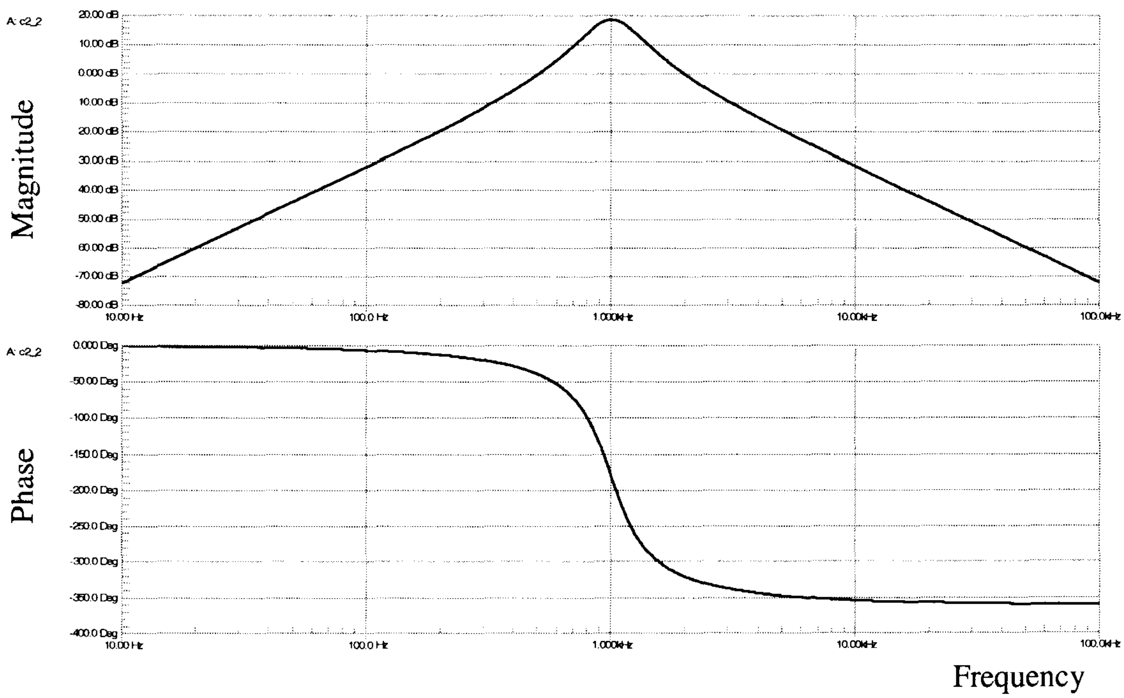

(b)

Figure 33. Fourth order BP filter, $\omega_0 = 2\Pi \cdot 1000$ rad/sec

(a) Schematic diagram, and (b) frequency response.

undamped natural frequency ω_0 the gain decreases at the rate of 40 dB/dec. The resulting phase shift of the fourth order BP filter throughout the spectrum of interest varies from 0 to -360 degrees.

B. HP Filter Expansion

The HP-EXP node is identified as the optimum node for the HP filter expansion, as shown in Figure 31. To achieve the HP2 filter expansion from second order to higher order:

(1) Design the original HP2 second order filter circuit according to set specifications.

(2) Design an additional HP filter section (or sections) according to set specifications.

(3) Identify the HP-EXP node on the original HP2 filter circuit.

(4) Temporarily disconnect input signal source V_{in} from the original HP2 filter circuit.

(5) Connect an additional HP filter section(s) to the original HP2 filter circuit such that the output of added HP section(s) is connected at the HP-EXP node of the original HP2 filter circuit, as shown in Figure 34.

(6) Re-connect input signal source V_{in} at the input node of added HP filter section(s).

(7) The HP filtered signal of higher order appears at the output of the original HP2 filter circuit.

For example, achieving a fourth order HP filter involves an addition of a second order HP filter stage to the original second order HP2 filter circuit as described above. The characteristic transfer function of such fourth order HP filter is given below:

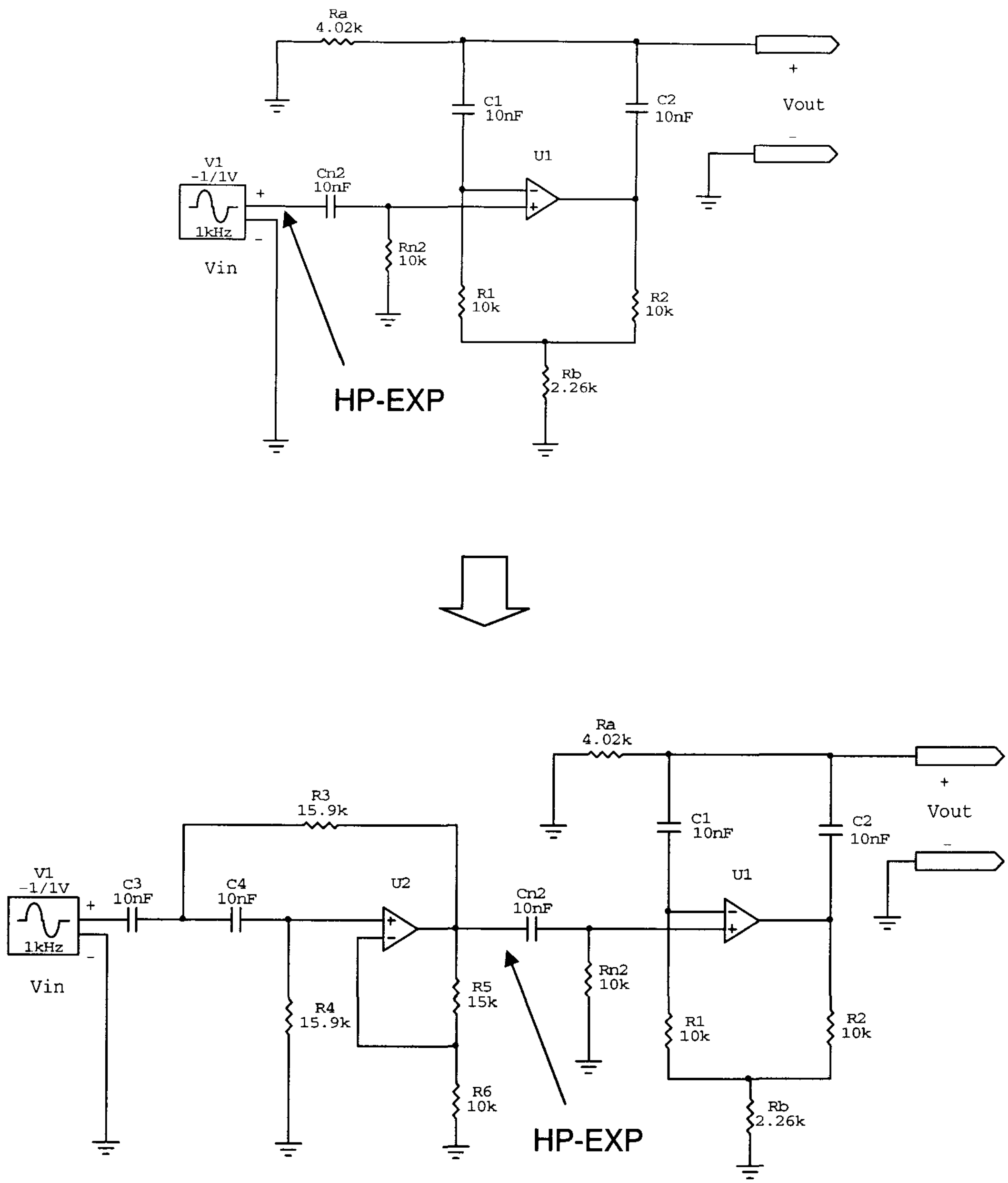

Figure 34. HP2 filter expansion from second order to fourth order HP filter

$$\frac{V_{out}}{V_{in}} = \frac{Hs^4}{\left[s^2 + \left(\frac{\omega_{01}}{Q_1}\right)s + \omega_{01}^2\right]\cdot\left[s^2 + \left(\frac{\omega_{02}}{Q_2}\right)s + \omega_{02}^2\right]} \tag{86}$$

An example circuit of the fourth order HP filter with its frequency response is shown in Figure 35. Designed fourth order HP filter consists of the original second order HP2 filter circuit and the second order Sallen and Key HP filter. Both second order sections are designed with undamped natural frequency $\omega_0 = 2 \cdot \Pi \cdot 1000$ rad/sec and quality factor Q=2, yielding superimposing pole locations. The output node of added second order Sallen and Key HP section is connected to the HP-EXP node of the original second order HP2 filter circuit. Since input impedance of the HP2 circuit at node HP-EXP is not very high, it is imperative that added expansion stage has very low output impedance and high driving capability (a requirement satisfied by Sallen and Key HP filter section). The input signal is applied at the input of added Sallen and Key HP section; the filtered signal is taken at V_{out} node of the original second order HP2 filter circuit. The resulting cascaded circuit has a fourth order HP filter response, as shown in Figure 35.

A fourth order HP filter yields different magnitude and phase response, as compared to a second order HP filter. The rate of gain increase inside the stop band as well as the overall value of phase shift are twice as large for the fourth order HP filter as compared to the second order HP filter. From low frequency to the undamped natural frequency ω_0 the gain increases at the rate of 80 dB/dec. Beyond undamped natural frequency ω_0 the gain remains relatively unchanged for smaller values of equivalent Q

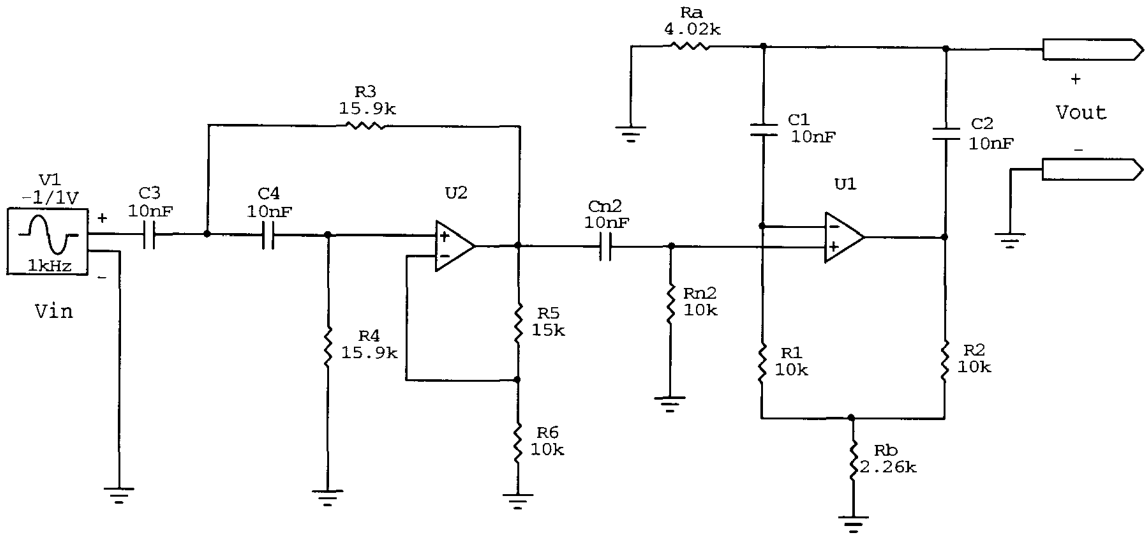

(a)

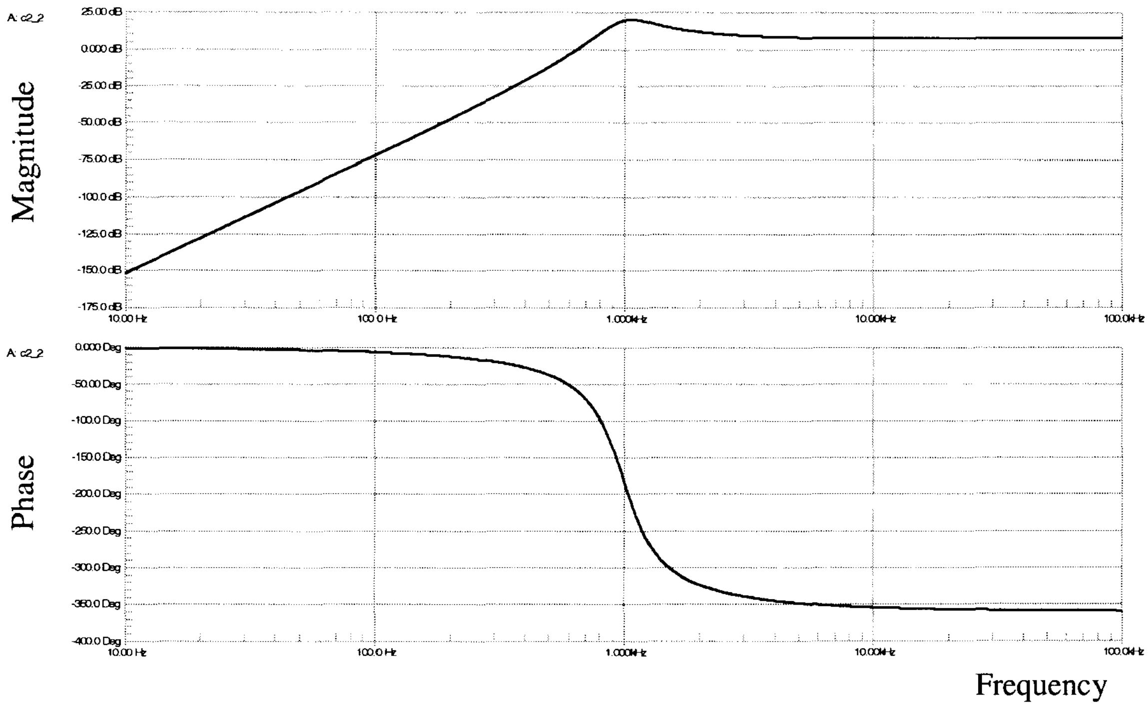

(b)

Figure 35. Fourth order HP filter, $\omega_0 = 2\Pi \cdot 1000$ rad/sec

(a) Schematic diagram, and (b) frequency response.

factor. The resulting phase shift of the fourth order HP filter throughout the spectrum of interest varies from +360 to 0 degrees.

CHAPTER XIII

SUMMARY AND CONCLUSIONS

A class of RC active filters is presented in which the DC offset of the operational amplifier (op-amp) is completely absent from the filter output. The low pass, band pass, high pass, band stop, and all pass filtering functions are defined and characterized in nine unique circuit configurations. The effects of finite gain bandwidth on the filter responses are discussed and quantified. Respective filter dynamic ranges are defined via maximum magnitude and noise analysis. Sensitivity analysis results are presented, demonstrating circuit's low ω_0 and Q sensitivities.

Step-by-step design procedures are given for all second order filter configurations. Sample filters are designed based on chosen values for critical frequency $\omega_0 = 2\Pi \cdot 1000$ rad/sec and filter quality factor Q=2. Designed filters are captured and simulated using Circuit Maker 2000 PSPICE simulation software. Sample LP, BP1, HP1, BS1, and AP1 filters are built on the breadboard and their frequency responses are characterized via the network analyzer. Obtained simulation and empirical results are in agreement with expected and anticipated filter responses.

Extension to higher order filters by addition of first and second order filter sections is discussed and demonstrated. The high pass and band pass filters can be extended into higher orders while retaining the advantage of DC offset absence at the filter output.

REFERENCES

[1] G. E. Erb, "Scanning Thermocouple Thermometry," *Sensors*, Vol. 2, No. 3, p. 41, 1985.

[2] P. R. Gray, and R. G. Meyer, *Analysis and Design of Analog Integrated Circuits*, 2nd ed., John Wiley & Sons, Inc., New York, pp. 681-686, 1984.

[3] R. Gayakwad, *Op-Amps and Linear Integrated Circuits*, 3rd edition, Regents/Prentice Hall, Inc., 1993.

[4] W. J. Kerwin, L. P. Huelsman, and R. W. Newcomb, "State-Variable Synthesis for Insensitive Integrated Circuit Transfer Functions," *IEEE Journal on Solid State Circuits*, vol. SC-2, pp. 87-92, 1967.

[5] J. Tow, "Design Formulas for Active RC Filters Using Operational-Amplifier Biquad," *Electronic Letters*, vol. 5, pp. 339-341, 1969.

[6] L. C. Thomas, "The Biquad: Part I – Some Practical Design Considerations," *IEEE Transactions on Circuit Theory*, vol. CT-18, pp. 350-357, 1971.

[7] J. J. Friend, C. A. Harris, and D. Hilberman, "STAR: An Active Biquadratic Section," *IEEE Transactions on Circuits and Systems*, vol. CAS-22, pp. 115-121, 1975.

[8] J. E. Lafser, *Active-RC Filter Design*, Meng Thesis, University of Louisville, 1989.

[9] G. Erdi, "Amplifier Techniques for Combining Low Noise, Precision, and High Speed Performance," *IEEE Journal of Solid State Circuits*, vol. SC-16, no. 5, pp. 653-661, 1981.

[10] S. Natarajan, *Theory and Design of Linear Active Networks*, Macmillan, Inc., 1987.

[11] S. Franco, *Design with Operational Amplifiers and Analog Integrated Circuits*, 3rd ed., McGraw-Hill, Inc., New York, 2002.

[12] H. W. Bode, *Network Analysis and Feedback Amplifier Design*, D. Van Nostrand Company, Inc., Princeton, N.J., p. 52, 1945.

[13] L. P. Huelsman, *Basic Circuit Theory*, 3rd ed., Prentice Hall, Inc., Englewood Cliffs, N.J., 1991.

[14] W. Stanley, *Network Analysis with Applications*, Prentice Hall, Inc., 1985.

[15] J. Nilsson, and S. Riedel, *Electric Circuits*, 7th edition, Pearson Prentice Hall, 2005.

[16] A. Budak, *Passive and Active Network Analysis and Synthesis*, Houghton Mifflin Co., Boston, 1974. Reissued by Waveland Press, Inc., Prospect Heights, IL, 1991.

[17] L. P. Huelsman, *Active & Passive Analog Filter Design*, McGraw-Hill, Inc., New York, 1980.

[18] A. S. Sedra, and P. O. Brachett, *Filter Theory and Design: Active and Passive*, Matrix Publishers, 1978.

[19] W. K. Chen, *Passive and Active Filters – Theory and Implementation*, John Wiley & Sons, New York, 1986.

[20] L. T. Burton, *RC-Active Circuits, Theory and Design*, Prentice Hall, 1980.

[21] A. S. Sedra, "Generation and Classification of Single Amplifier Filters," *IEEE Transactions on Circuit Theory and Applications*, vol. 2, pp. 51-67, 1974.

[22] K. Soundararjan, and K. Ramakrishna, "Characteristics of nonideal operational amplifiers," *IEEE Transactions on Circuits and Systems*, CAS-21, pp. 69-75, 1974.

[23] A. Budak, and D. M. Petrela, "Frequency Limitations of Active Filters Using Operational Amplifiers," *IEEE Transactions on Circuit Theory*, vol. CT-19, no. 4, pp. 322-328, 1972.

[24] A. Davis, " Predistortion design of multiple amplifier active filters," *Proceedings of the IEEE International Symposium on Circuits and Systems*, April 28-30, Houston, Texas, 1980.

[25] K. Goodman, and J. Zurada, "A Predistortion Technique for RC-Active Biquadratic Filters," *IEEE Transactions on Circuit Theory and Applications*, vol. 11, pp.289-302, 1983.

[26] J. Zurada, "Predistorted Design of 2nd Order Filters," *IEEE Southeast Conference Proceedings*, pp. 246-250, 1984.

[27] J. Gruneisen, *Computer-Aided Predistortion Design for Finite Gain Bandwidth Amplifiers*, Meng Thesis, University of Louisville, 1986.

[28] A. Oksasoglu, and L. P. Huelsman, "Effects and Compensation of Gain Bandwidth in the State-Variable Filter," *Proceedings of the Midwest Symposium on Circuits and Systems*, 1991.

[29] P. O. Brachett, and A. S. Sedra, "Active Compensation for High Frequency Effects in Op Amp Circuits with Applications to Active RC Filters," *IEEE Transactions on Circuits and Systems*, vol. CAS-23, no. 2, pp. 68-72, 1976.

[30] J. E. Lafser, and P. B. Aronhime, "Extension of a Third Order Active Filter," *Proceedings of the 31st Midwest Symposium on Circuits and Systems*, Vol. 31, 1988.

[31] L. P. Huelsman, "An Equal-Valued-Capacitor Active RC Network Realization of a Third-Order Low-Pass Butterworth Characteristics," *Electronic Letters*, vol. 7, no. 10, pp. 271-272, 1971.

[32] W. W. Mumford, and E. H. Scheibe, *Noise Performance Factors in Communication Systems*, Horizon House-Microwave, Inc., 1968.

[33] C. D. Motchenbacher, and F. C. Fitchen, *Low Noise Electronic Design*, John Wiley & Sons, Inc., 1973.

[34] F. N. Trofimenikoff, D. H. Treleaven, and L. T. Burton, "Noise Performance of RC-Active Quadratic Filter Sections," *IEEE Transactions on Circuit Theory*, vol. CT-20, no. 5, pp. 524-532, 1973.

[35] L. T. Burton, F. N. Trofimenkoff, and D. H. Treleaven, "Noise Performance of Low Sensitivity Active Filters," *Journal of Solid State Circuits*, vol. SC-8, no. 1, pp. 85-91, 1973.

[36] H. W. Ott, *Noise Reduction Techniques in Electronic Systems*, John Wiley & Sons, Inc., 1976.

[37] D. Soderquist, and J. Wong, "Minimization of Noise in Operational Amplifiers Applications," Application Note AN-15, *Linear and Conversion Applications Handbook*, Precision Monolithics, 1986.

[38] M. A. Soderstrand, and S. K. Mitra, "Sensitivity Analysis of Third-Order Filters," *International Journal of Electronics*, vol. 30, no 3, pp. 265-272, 1971.

[39] K. Blake, "Low-Sensitivity, Lowpass Filter Design," *Comlinear Application Note*, OA-27, 1996.

[40] M. H. Nichols, and L. L. Rauch, *Radio Telemetry*, John Wiley & Sons, Inc., New York, pp. 137-138, 1956.

[41] R. Schaumann, M. Ghausi, and K. Laker, *Design of Analog Filters: Passive, Active RC, and Switched Capacitor*, Prentice Hall, 1990.

[42] M. E. Van Valkenburg, *Analog Filter Design*, Holt, Rinehart and Winston, 1982.

[43] A. B. Williams, *Electronic Filter Design Handbook*, McGraw-Hill, Inc., 1981.

[44] A. Zverev, *Handbook of Filter Synthesis*, John Wiley & Sons, Inc., 1967.

[45] A. Williams, and F. Taylor, *Electronic Filter Design Handbook*, McGraw-Hill, Inc., 1995.

[46] R. P. Sallen, and E. L. Key, "A Practical Method of Designing RC Active Filters," *IRE Transactions on Circuit Theory*, vol. CT-2, pp. 74-85, 1955.

[47] H. J. Orchard, "Inductorless Filters," *Electronic Letters*, vol. 2, no. 6, pp. 224-225, 1966.

[48] M. A. Soderstrand, and J. Szczupak, "A simple filter design procedure using compensated operational amplifiers," *International Journal of Electronics*, 46, pp. 19-32, 1979.

[49] P. R. Geffe, "Exact synthesis with real amplifiers," *IEEE Transactions on Circuits and Systems*, CAS-21, pp. 369-376, 1974.

[50] S. Butterworth, "On the Theory of Filter Amplifiers," *Wireless Engineering*, vol. 7, pp. 536-541, 1930.

[51] M. E. Van Valkenburg, *Introduction to Modern Network Synthesis*, John Wiley & Sons, Inc., New York, 1964.

[52] W. E. Thomson, "Delay Networks Having Maximally Flat Frequency Characteristics," *Proceedings IEE*, part 3, vol. 96, pp. 487-490, 1949.

[53] N. Nise, *Control System Engineering*, 4th edition, John Wiley & Sons, Inc., 2004.

CURRICULUM VITAE

NAME: Kresimir Odorcic

ADDRESS: 6644 Calm River Way
Louisville, KY 40299

DOB: Zagreb, Republic of Croatia – May 03, 1973

EDUCATION
& TRAINING

B.S., Electrical Engineering (Applied Option)
California University of Pennsylvania
1992-95

M.S., Electrical Engineering
University of Louisville
2001-02

AWARDS: Presidential Scholar
1993, 1994

Electrical Engineering Excellence Award
1996

Industry and Technology Excellence Award
1996

PATENTS: US 6,703,591 – Methods and Apparatus for Shabbos/Yom Tow Appliance Control.

US 6,744,616 – Methods and Apparatus for Controlling an Electronic Control.

US 6,787,738 – Carbon Monoxide Sensed Oven Cleaning Apparatus and Method.

US 7,113,075 – Power Supply Methods and Apparatus.